Life-history evolution and uninvadable mortality schedules with and without intergenerational energy transfers

Piret Avila[1,*]

Laurent Lehmann[2]

[1]Faculty of Biological and Environmental Sciences, University of Helsinki, 00014 Helsinki, Finland

[2]Department of Ecology and Evolution, University of Lausanne, 1015 Lausanne, Switzerland

[*]Correspondence: piret.avila@gmail.com

Abstract

Intergenerational energy transfers are widespread in nature, yet most life history theory assumes that organisms balance energy production and consumption at each age, leaving the evolutionary consequences of transfers underexplored. We develop a life history model under two energy budget constraints: (i) no transfers, where production equals consumption at each age, and (ii) transfers, where energy is balanced over the lifetime. Using optimal control theory, we derive the necessary conditions for uninvadable life histories in age-structured populations with development, yielding several general results. In particular, at any age in the uninvadable life history, current fitness gains (from current reproduction, somatic investments, and transfers) are exactly offset by the loss in the value of life due to mortality, where this marginal value reflects future fitness contributions from reproduction and energy transfers. We show that the resulting uninvadable mortality schedule is not necessarily senescent and how transfers lower it even after reproduction ceases, enabling longer lifespans and a post-reproductive phase. We apply our results to human life history evolution by extending the model of Kaplan and Robson (2009) to compare scenarios with and without transfers. We find that the shift to transfers extends the juvenile growth phase, characterised by substantial early-life energy deficits, which are compensated by enhanced lifetime productivity through somatic capital accumulation and longer lifespans. Post-reproductive survival emerges when declining reproductive efficiency makes resource transfers to younger individuals optimal. Our findings show that transitioning from individual energy balance to intergenerational transfers is sufficient to account for several major hallmarks of human life history.

Keywords: life history evolution, optimal control theory, intergenerational transfers, mortality schedule, senescence, reproductive value, human life history evolution

1 Introduction

Life history theory seeks to understand how organisms allocate limited resources between the competing functions of survival, development, and reproduction throughout their lifespan (Stearns, 1992). Most life history evolution

models assume that organisms must be self-sufficient in balancing energy production and consumption at each moment in time, treating resource allocation as an individual-level optimisation problem (e.g., León, 1976; Schaffer, 1983; Stearns, 1992; Kozłowski, 1992; Perrin and Sibly, 1993; Cichoń and Kozłowski, 2000; Day and Taylor, 2000; Metz et al., 2016; González-Forero et al., 2017). However, in nature, individuals routinely share resources across age classes. Examples include (allo)parental provisioning common in birds and mammals, to bidirectional transfers in cooperative breeders, and extensive intergenerational resource flows in human societies (Clutton-Brock, 1991; Kaplan, 1994). The human case represents an evolutionary extreme as hunter-gatherer children consume more resources than they produce for nearly two decades, whereas post-reproductive individuals continue to transfer substantial resources long after stopping reproduction themselves (Kaplan, 1994; Gurven et al., 2006; Lee, 2020).

Energy budget constraints are fundamental to life history evolution because they determine not only current resource allocation but also affect the entire life course of an individual. This is because life history decisions are inherently intertemporal, creating path dependencies that constrain future energy allocation based on current ones. For example, receiving parental energy transfers early in life can accelerate growth, building somatic capital that enhances both reproductive capacity and survival later in life. The dynamic nature of resource allocation makes life history evolution a problem of dynamic optimal control. Thus, optimal control theory approaches based on Pontryagin's maximum principle (e.g. León, 1976; Iwasa and Roughgarden, 1984; Perrin, 1992; Perrin and Sibly, 1993; Day and Taylor, 2000) and dynamic programming (e.g., Houston and McNamara, 1999; Mangel and Clark, 1988; Ewald et al., 2007; Nakamura and Ohtsuki, 2016) have been fruitful for modelling and understanding life-history evolution.

The bulk of life history evolution models, however, focus on situations where resources between individuals cannot be shared, and thus energy production must equal assimilation at every age. Although several models with intergenerational transfers have been developed (e.g., Kaplan and Robson, 2002; Lee, 2003; Chu and Lee, 2006; Kaplan and Robson, 2009), this research line has mainly focused on understanding mortality patterns in humans. Related approaches have examined how kin interactions modify selection on age-specific vital rates in age-structured populations (Roper et al., 2023), though without explicit modelling resource transfers. As a result, life history evolution models with and without intergenerational transfers have remained largely disconnected in the literature. There is a lack of cohesive theoretical work that examines both budget constraints within a single and same evolutionary framework. This leaves unanswered interesting questions, such as which specific life history characteristics emerge from relaxing individual budget constraints by allowing transfers to occur?

Developing a life-history evolution model that encompasses both budget constraints would allow one to explicitly compare evolutionary outcomes and better identify which life-history features emerge specifically from relaxing individual energy budget constraints. The aim of this paper is to do just that by formalising natural selection on life history evolution under the two budget constraints of (i) no energy transfers between individuals (intratemporal budget constraint) and (ii) intergenerational transfers between individuals (intertemporal budget constraint). We employ Pontryagin's maximum principle to derive necessary conditions for uninvadable life histories under these two scenarios, which in turn allows us to characterise selection pressures on traits affecting life-history evolution.

We then apply our results to understand specifically certain hallmark features of human life histories. The human lineage exhibits a distinctive suite of life history traits that differentiate us from our closest relatives, the

great apes: exceptionally prolonged juvenile dependency lasting nearly two decades, extended post-reproductive lifespan, and elevated lifetime energy production coupled with high metabolic rates (e.g., Kaplan et al., 2000; Mace, 2000; Robson et al., 2006; van Schaik, 2016; Gurven, 2024). Evolutionary anthropologists have long been puzzled about what mechanisms have driven all these changes (e.g., Gurven, 2024 for a recent review). Building on the seminal model of Kaplan and Robson (2009) and extending their transfer-only analysis to include the case without transfer, we characterise the uninvadable life history under both scenarios and compare them. This reveals how intergenerational transfers can, by themselves, generate uniquely human life history characteristics as an uninvadable life history strategy.

The rest of the paper is organised as follows. Section 2 presents the life history model, incorporating the two energy budget constraints. Section 3 derives the maximum principle for life history evolution and the uninvadable mortality schedule. Section 4 applies the general model to human life history evolution, building on and extending Kaplan and Robson (2009). Section 5 discusses the implications for both life history theory and human evolution, the limitations of our model and relevant extensions.

2 The model

Consider an age-structured population in continuous time where individuals reproduce asexually by collecting energy from their surroundings (the assumption of asexual reproduction is standard in life-history evolution and assessed in the Discussion). These individuals can also exchange energy in an intergenerational way (detailed below). Each individual in this population is characterised by two phenotypic attributes at each age $t \in \mathcal{T} = [0, \infty)$ of its lifespan (see table 1 for a list of key symbols). First, a multidimensional quantitative physiological or functional state variable $\mathbf{x}(t) \in \mathbb{R}^{n_\mathrm{x}}$ consisting of a finite number n_x of dimensions, e.g., size, amount of fat reserve, brain volume, shell thickness, skill, etc., whose defining characteristic is that it requires energy for growth and maintenance (state variable can thus be interpreted as embodied capital *sensu* Kaplan et al., 2001). Second, a phenotypic trait $\mathbf{u}(t) \in \mathcal{U} \subseteq \mathbb{R}^{n_\mathrm{u}}$ consisting of a finite number n_u of dimensions, which is assumed to be genetically evolving and to affect the time dynamics of the state variables, as well as reproduction and survival. This evolving trait can be thought of as an open-loop control variable (as per the literature on control theory, e.g. Kamien and Schwartz, 2012; Athans and Falb, 2007; Weber, 2011), and has been in standard use in the life history evolution literature (e.g. León, 1976; Perrin and Sibly, 1993; Day and Taylor, 2000; Avila et al., 2021).

These phenotypes are assumed to affect the birth rate $b_i(t)$, death rate $\mu_i(t)$, and the rate of change $\mathrm{d}\mathbf{x}_i(t)/\,\mathrm{d}t = \boldsymbol{g}_i(t)$ of the physiological state variable of an individual i with trait $\mathbf{u}_i(t)$ and internal state $\mathbf{x}_i(t)$ at age t. Collectively, we refer to these as vital rates. Here, we focus on how natural selection affects the trait schedule or path $\mathbf{u} = \{\mathbf{u}(t)\}_{t\in\mathcal{T}}$ (formally $\mathbf{u} : \mathcal{T} \to \mathbb{R}^{n_\mathrm{u}}$) once definite assumptions are made on the dynamics of the state variables. Since the trait $\mathbf{u}$ is infinite dimensional, the model is complicated, and here we restrict ourselves to an evolutionary invasion analysis (e.g., Eshel and Feldman, 1984; Lessard, 1990; Metz et al., 1992; Charlesworth, 1994; Rand et al., 1994; Ferrière and Gatto, 1995; Eshel et al., 1998; Rousset, 2004; Metz, 2011; Lehmann et al., 2016; Avila and Mullon, 2023). Our aim then is to characterize for the two different types of energy budget constraints introduced above (and to be detailed below), the necessary conditions for a trait schedule $\mathbf{u}^* \in \boldsymbol{\mathcal{U}}[\mathcal{T},\mathcal{U}]$ which, once established

in the population, is resistant to invasion by any mutant trait schedule taken from the same trait space $\boldsymbol{\mathcal{U}}[\mathcal{T},\mathcal{U}]$. Here, $\boldsymbol{\mathcal{U}}[\mathcal{T},\mathcal{U}]$ is the set of all bounded piecewise continuous functions with domain $\mathcal{T}$ and range $\mathcal{U}$.

2.1 Invasion analysis

Let us now first characterise the invasion process of a mutant type. For this, we endorse the standard invasion analysis assumptions that the population is large enough, so that we can neglect the effects of genetic drift (the population is ideally infinite). An individual with a mutant trait schedule $\mathbf{u}_{\mathrm{m}} = \{\mathbf{u}_{\mathrm{m}}(t)\}_{t\in\mathcal{T}}$ is then introduced as a single copy in a population monomorphic for the resident schedule $\mathbf{u}_{\mathrm{r}} = \{\mathbf{u}_{\mathrm{r}}(t)\}_{t\in\mathcal{T}}$ that is at its demographic equilibrium. Then, it follows from our demographic assumptions and standard results on age-dependent branching processes (Crump and Mode, 1968, Corollary 5.1 and example 8.2, Mode, 1971) that the lineage of mutants with trait $\mathbf{u}_{\mathrm{m}}$ descending from the ancestor introduced as a single copy into a monomorphic resident population with individuals expressing trait $\mathbf{u}_{\mathrm{r}}$ goes extinct with probability one if and only if

$$R(\mathbf{u}_{\mathrm{m}}, \mathbf{u}_{\mathrm{r}}) \leq 1, \tag{1}$$

where

$$R(\mathbf{u}_{\mathrm{m}}, \mathbf{u}_{\mathrm{r}}) = \int_0^\infty l_{\mathrm{m}}(t) b\left(\mathbf{u}_{\mathrm{m}}(t), \mathbf{x}_{\mathrm{m}}(t), \mathbf{u}_{\mathrm{r}}\right) \mathrm{d}t \tag{2}$$

is the basic reproductive number of the mutant in the resident population; namely, the effective number of offspring produced by the mutant over its whole lifespan. Therein, $b\left(\mathbf{u}_{\mathrm{m}}(t), \mathbf{x}_{\mathrm{m}}(t), \mathbf{u}_{\mathrm{r}}\right)$ is the birth rate (or effective fecundity) of an individual at age t expressing trait $\mathbf{u}_{\mathrm{m}}(t)$ and the internal state $\mathbf{x}_{\mathrm{m}}(t)$. This birth rate depends on the resident population schedule $\mathbf{u}_{\mathrm{r}}$, which captures the fact that an individual may interact with its environment (e.g., fecundity may depend on the behaviour of other individuals, on the density of conspecifics or predators, etc.). This form of dependence assumes that the resident population is at a demographic equilibrium and that the interactions of an individual with its surroundings at each age is mediated by its internal state (thus age does not need to enter as an extra variable in the mortality). The probability of surviving to age t, $l_{\mathrm{m}}(t)$, satisfies

$$\frac{\mathrm{d}l_{\mathrm{m}}(t)}{\mathrm{d}t} = -\mu\left(\mathbf{u}_{\mathrm{m}}(t), \mathbf{x}_{\mathrm{m}}(t), \mathbf{u}_{\mathrm{r}}\right) l_{\mathrm{m}}(t) \quad \text{with i.c.} \quad l_{\mathrm{m}}(0) = 1, \tag{3}$$

where $\mu\left(\mathbf{u}_{\mathrm{m}}(t), \mathbf{x}_{\mathrm{m}}(t), \mathbf{u}_{\mathrm{r}}\right)$ is the death rate of the mutant individual at age t (and "i.c." means initial condition). Both the birth and death rates depend on the state $\mathbf{x}_{\mathrm{m}}(t)$ of the mutant, whose dynamics are given by

$$\frac{\mathrm{d}\mathbf{x}_{\mathrm{m}}(t)}{\mathrm{d}t} = \boldsymbol{g}(\mathbf{u}_{\mathrm{m}}(t), \mathbf{x}_{\mathrm{m}}(t), \mathbf{u}_{\mathrm{r}}) \quad \text{with i.c.} \quad \mathbf{x}_{\mathrm{m}}(0) = \mathbf{x}_0. \tag{4}$$

Note that the dependence of the different quantities on the resident control schedule $\mathbf{u}_{\mathrm{r}}$ entails that each quantity

may depend on the resident state schedules $l_\mathrm{r} = \{l_\mathrm{r}(t)\}_{t\in\mathcal{T}}$ and $\mathbf{x}_\mathrm{r} = \{\mathbf{x}_\mathrm{r}(t)\}_{t\in\mathcal{T}}$, where the latter functions satisfy

$$\frac{\mathrm{d}l_\mathrm{r}(t)}{\mathrm{d}t} = -\mu\left(\mathbf{u}_\mathrm{r}(t), \mathbf{x}_\mathrm{r}(t), \mathbf{u}_\mathrm{r}\right) l_\mathrm{r}(t) \qquad \text{with i.c.} \qquad l_\mathrm{m}(0) = 1. \tag{5}$$

$$\frac{\mathrm{d}\mathbf{x}_\mathrm{r}(t)}{\mathrm{d}t} = \boldsymbol{g}(\mathbf{u}_\mathrm{r}(t), \mathbf{x}_\mathrm{r}(t), \mathbf{u}_\mathrm{r}) \qquad \text{with i.c.} \qquad \mathbf{x}_\mathrm{m}(0) = \mathbf{x}_0. \tag{6}$$

While it is not necessary for various applications of the model to explicitly detail how the resident properties feedback on mutant vital rates, the general consistency assumption of such feedback is that, in a monomorphic resident population, the basic reproductive number must be one (that is, $R(\mathbf{u}_\mathrm{r}, \mathbf{u}_\mathrm{r}) = 1$ for all $\mathbf{u}_\mathrm{r} \in \boldsymbol{\mathcal{U}}[\mathcal{T},\mathcal{U}]$. This is the standard assumption for life history evolution in a regulated population, e.g., (Michod, 1979).

Together, eqs. (2)–(6) allow us to compute all quantities necessary to evaluate the basic reproductive number. We next turn to specify the model from the energetic point of view, which puts further constraints on the dynamics of the state variables.

2.2 Budget constraints

We now detail the two alternative budget constraints that we consider and for which we need to introduce three additional concepts. First, let $P(\mathbf{u}_\mathrm{m}(t), \mathbf{x}_\mathrm{m}(t), \mathbf{u}_\mathrm{r})$ stand for the gross rate of total energy produced or collected by an individual of age t with phenotype $(\mathbf{u}_\mathrm{m}(t), \mathbf{x}_\mathrm{m}(t))$ (i.e., "power" measured in Watts), and which can depend on the resident population. Second, let $A(\mathbf{u}_\mathrm{m}(t), \mathbf{x}_\mathrm{m}(t))$ be the assimilation rate of an individual of age t with the phenotype $(\mathbf{u}_\mathrm{m}(t), \mathbf{x}_\mathrm{m}(t))$. This is the rate at which energy is consumed by the different activities and physiological structures of the individual. It is assumed to be independent of the environment determined by $\mathbf{u}_\mathrm{r}$, since assimilation refers to the energy used specifically by the organism itself. We partition energy assimilation into different activities and/or structures as

$$A(\mathbf{u}_\mathrm{m}(t), \mathbf{x}_\mathrm{m}(t)) = E_\mathrm{b}(\mathbf{u}_\mathrm{m}(t), \mathbf{x}_\mathrm{m}(t)) + E_\mu(\mathbf{u}_\mathrm{m}(t), \mathbf{x}_\mathrm{m}(t)) + E_\mathrm{x}(\mathbf{u}_\mathrm{m}(t), \mathbf{x}_\mathrm{m}(t)) + E_\mathrm{M}(\mathbf{u}_\mathrm{m}(t), \mathbf{x}_\mathrm{m}(t)). \tag{7}$$

Here, E_i refers to the energy used in activity or vital rate $i \in \{\mathrm{b}, \mu, \mathrm{x}, \mathrm{M}\}$, which on the right-hand side of eq. (7), stands, respectively, for the rate of energy used in reproduction, survival, state variables, and finally maintenance. The energy $E_i(\mathbf{u}_\mathrm{m}(t), \mathbf{x}_\mathrm{m}(t))$ allocated to activity i can depend on both evolving traits and the state variables (e.g., the energetic cost of maintenance depends on the size).

Since vital rates depend on energy allocation, this dependence can be emphasised by writing the vital rates determining the basic reproductive number (recall eq. (2)) as

$$b(\mathbf{u}_\mathrm{m}(t), \mathbf{x}_\mathrm{m}(t), \mathbf{u}_\mathrm{r}) = \tilde{b}(E_\mathrm{b}(\mathbf{u}_\mathrm{m}(t), \mathbf{x}_\mathrm{m}(t)), \mathbf{x}_\mathrm{m}(t), \mathbf{u}_\mathrm{r}) \tag{8}$$

$$\mu(\mathbf{u}_\mathrm{m}(t), \mathbf{x}_\mathrm{m}(t), \mathbf{u}_\mathrm{r}) = \tilde{\mu}(E_\mu(\mathbf{u}_\mathrm{m}(t), \mathbf{x}_\mathrm{m}(t)), \mathbf{x}_\mathrm{m}(t), \mathbf{u}_\mathrm{r}) \tag{9}$$

$$\boldsymbol{g}(\mathbf{u}_\mathrm{m}(t), \mathbf{x}_\mathrm{m}(t), \mathbf{u}_\mathrm{r}) = \tilde{\boldsymbol{g}}(E_\mathrm{x}(\mathbf{u}_\mathrm{m}(t), \mathbf{x}_\mathrm{m}(t)), \mathbf{x}_\mathrm{m}(t), \mathbf{u}_\mathrm{r})\,. \tag{10}$$

On the right-hand side, the vital rates are written as functions of energies. This shows upfront that the effects of traits on the vital rates come through energy allocation, since vital rates are functions of energy consumption. The

formulation of eqs. (7)–(10) is based on the seminal life history evolution model of León (1976). One can often adopt a simpler formulation in which the allocated energy is taken to be directly proportional to the evolving traits and independent of state variables $\mathbf{x}_{\mathrm{m}}(t)$. For example, one could write $E_i(\mathbf{u}_{\mathrm{m}}(t)) = u_{\mathrm{m},i}(t)$ where $u_{\mathrm{m},i}(t)$ is the control variable for the total resources allocated to activity $i \in \{\mathrm{b}, \mu, \mathrm{x}, \mathrm{M}\}$ (for example, León, 1976). A whole class of classical life history evolution models even simplify things a step further by expressing the controls in terms of proportional allocations, such that the allocation traits are defined by $u_{\mathrm{m},i}(t) = E_i(\mathbf{u}_{\mathrm{m}}(t))/P(\mathbf{u}_{\mathrm{m}}(t), \mathbf{x}_{\mathrm{m}}(t), \mathbf{u}_{\mathrm{r}})$ and satisfy $\sum_{i\in\{\mathrm{b},\mu,\mathrm{x},\mathrm{M}\}} u_{\mathrm{m},i}(t) = 1$ (e.g., Perrin and Sibly, 1993 for a review), and where "x" may itself be a multi-index if we wish to differentiate the allocation to the n_{x} physiological subsystems. However, in the literature on intergenerational energy transfers (e.g. Kaplan and Robson, 2009; Chu et al., 2008), energy expenditure may depend non-linearly on controls. In order to cover such models, we do not make any specific assumptions about the relationship between traits and energy allocation at this stage.

Finally, let us define the net energy transfer rate at time t as

$$T(\mathbf{u}_{\mathrm{m}}(t), \mathbf{x}_{\mathrm{m}}(t), \mathbf{u}_{\mathrm{r}}) = P(\mathbf{u}_{\mathrm{m}}(t), \mathbf{x}_{\mathrm{m}}(t), \mathbf{u}_{\mathrm{r}}) - A(\mathbf{u}_{\mathrm{m}}(t), \mathbf{x}_{\mathrm{m}}(t), \mathbf{u}_{\mathrm{r}}), \tag{11}$$

which is the difference between the energy production rate and the energy assimilation rate. When $T > 0$, the organism generates an energy surplus, producing more than it consumes. Conversely, when $T < 0$, the organism operates in an energy deficit, assimilating more energy than it produces.

We are now ready to specify two distinct budget constraints that govern the relationship between an individual's gross energy production rate and the gross energy assimilation rate at time t. The first budget constraint enforces strict individual temporal balance, requiring that production and assimilation rates match exactly at each age t, i.e. there are no energy transfers between individuals:

$$T(\mathbf{u}_{\mathrm{m}}(t), \mathbf{x}_{\mathrm{m}}(t), \mathbf{u}_{\mathrm{r}}) = 0. \tag{12}$$

This constraint represents an intratemporal budget balance, in which energy cannot be transferred between generations. Classical life history evolution models endorse this assumption (e.g., León, 1976; Stearns, 1992; Perrin, 1992; Perrin and Sibly, 1993) and we will refer to this as the model without transfers. The second budget constraint allows for flexible energy allocation across time, requiring only that lifetime energy production matches lifetime consumption:

$$\int_0^\infty l_{\mathrm{m}}(t) T(\mathbf{u}_{\mathrm{m}}(t), \mathbf{x}_{\mathrm{m}}(t), \mathbf{u}_{\mathrm{r}})\, \mathrm{d}t = 0. \tag{13}$$

Eq. (13) implies that each individual respects an intertemporal energy budget balance, in which the expected total energy produced over its lifespan balances its energy expenditure. It is as if an individual can exchange energy with copies of itself living in different generations, i.e. with other lineage members, so that total energy produced and consumed by an individual throughout their lifespan balances out. This amounts to a standard assumption in life history evolution models for intergenerational transfers (e.g., Kaplan and Robson, 2002; Lee, 2003; Chu and Lee, 2006; Kaplan and Robson, 2009).

Note that no mutant growth rate weighing appears in eq. (13), which is different from previous formulations of

these budget constraints (Chu and Lee, 2006, eq. 6, Chu et al., 2008, eq. 4', and Kaplan and Robson, 2009, eq. 4.2 for comparison). This is because our measure of fitness, eq. (2), is the basic reproductive number of an individual, and so all accounting is done at the individual, instead of being done at the lineage level. The basic reproductive number is an appropriate fitness proxy for the mutant's growth rate (e.g., Mode, 1971; Karlin and Taylor, 1981; Caswell, 2000; Metz et al., 2008 and no mutant growth rate weighing appears in eq. (2) either).

2.3 Uninvadability

Our model, with the fitness formulation and the dynamic constraints given by eqs. (2)–(6) and the budget constraints eqs. (12)–(13), then encapsulates two classes of previous evolutionary models. First, the standard life-history evolution models with allocation of resources to different functions without any transfers (e.g., León, 1976; Oster and Wilson, 1977; Schaffer, 1982; Iwasa and Roughgarden, 1984; Stearns, 1992; Perrin, 1992; Kozłowski, 1992; Perrin and Sibly, 1993; Bulmer, 1994; Irie and Iwasa, 2005). Second, life-history models involving intergenerational transfers of energy (e.g., Kaplan and Robson, 2002; Lee, 2003; Kaplan and Robson, 2009; Chu et al., 2008). In most of these analyses, the goal is usually to identify the necessary conditions for a trait value $\mathbf{u}^*$ taken from the state space $\boldsymbol{\mathcal{U}}[\mathcal{T},\mathcal{U}]$ to be uninvadable, i.e., resistant to invasion. An uninvadable control $\mathbf{u}^*$ must be a maximiser of the basic reproductive number holding the resident population at this trait value and thus must satisfy

$$\mathbf{u}^* \in \arg \max_{\mathbf{u}\in\boldsymbol{\mathcal{U}}[\mathcal{T},\mathcal{U}]} R(\mathbf{u},\mathbf{u}^*) \tag{14}$$

subject to the mutant dynamic constraints eqs. (3)–(4) and the energy budget constraints; namely, eq. (12) under intratemporal balance and eq. (13) under intertemporal balance. This constitutes a constrained maximisation problem, for which we derive necessary conditions for uninvadability using optimal control theory, specifically Pontryagin's maximum principle (e.g., Bryson and Ho, 1975; Athans and Falb, 2007; Liberzon, 2011; Weber, 2011 for useful textbooks). Formally, the case with transfers corresponds to an optimal control problem with mixed equality constraints (see e.g., Bryson and Ho, 1975, p. 99–100 and Hartl et al., 1995, p. 186–187), while the case without transfers corresponds to an isoperimetric optimal control problem (see e.g., Bryson and Ho, 1975, p. 90–91).

3 Natural selection on life-histories

3.1 Necessary conditions for uninvadability

3.1.1 The maximum principle

In order to apply optimal control theory to our two budget balance scenarios, let us now introduce the Hamiltonian function

$$H(\mathbf{u}_{\mathrm{m}}(t),\mathbf{y}_{\mathrm{m}}(t),\boldsymbol{\lambda}(t),\mathbf{u}_{\mathrm{r}}) = l_{\mathrm{m}}(t)\Big[b\left(\mathbf{u}_{\mathrm{m}}(t),\mathbf{x}_{\mathrm{m}}(t),\mathbf{u}_{\mathrm{r}}\right) - \lambda_{\mathrm{l}}(t)\mu\left(\mathbf{u}_{\mathrm{m}}(t),\mathbf{x}_{\mathrm{m}}(t),\mathbf{u}_{\mathrm{r}}\right)\Big] + \boldsymbol{\lambda}_{\mathrm{x}}(t)\cdot\boldsymbol{g}(\mathbf{u}_{\mathrm{m}}(t),\mathbf{x}_{\mathrm{m}}(t),\mathbf{u}_{\mathrm{r}}) + \eta(t)T(\mathbf{u}_{\mathrm{m}}(t),\mathbf{x}_{\mathrm{m}}(t),\mathbf{u}_{\mathrm{r}}), \tag{15}$$

where $\mathbf{y}_{\mathrm{m}}(t) = (l_{\mathrm{m}}(t), \mathbf{x}_{\mathrm{m}}(t))$ collects all mutant state variables and $\boldsymbol{\lambda}(t) = (\lambda_{\mathrm{l}}(t), \boldsymbol{\lambda}_{\mathrm{x}}(t), \eta(t))$ collects all costates variables–also called "shadow values"– associated with state variables $\mathbf{y}_{\mathrm{m}}(t)$ and energy transfers $T(t)$, respectively. The interpretation of the costates $\lambda_{\mathrm{l}}(t)$ and $\boldsymbol{\lambda}_{\mathrm{x}}(t)$ are as the marginal effects of an increase in the corresponding state variable on expected reproduction starting at age t, i.e. the marginal effects of survival $l_{\mathrm{m}}(t)$ and physiological state $\mathbf{x}_{\mathrm{m}}(t)$ on remaining expected fitness $\int_t^\infty l(t)b(t)\,\mathrm{d}t$ (for more information on costate variables, Dorfman, 1969; Caputo, 2005; Sydsaeter et al., 2008; Weber, 2011 and Appendix A). The shadow value of the energy $\eta(t)$ takes different forms under the two budget constraints:

$$\eta(t) = \begin{cases} \eta_{\mathrm{C}}(t) & \text{no transfers} \\ \eta_{\mathrm{T}}\, l_{\mathrm{m}}(t) & \text{with transfers.} \end{cases} \tag{16}$$

Here, the subscript "C" in $\eta_{\mathrm{C}}(t)$ refers to the "classic" life history scenario without transfers. This shadow value gives the marginal effect on its remaining fitness at age t of an individual transferring a unit of energy at that age (see Appendix A.2 for more details). Namely, the change in fitness if the intra-temporal budget constraint (11) were released at t and the individual would make a positive transfer. In the presence of transfers, the interpretation of η_{T} is the marginal effect on remaining fitness at time t of increasing the cumulative transfers obtained at age t (see Appendix A.1 for more details). The constancy of η_{T} reflects the ability to freely exchange energy across the lifespan, such that the future reproductive value of past transferred energy remains age-invariant. The weighting by the survival probability in $\eta(t) = \eta_{\mathrm{T}}\, l_{\mathrm{m}}(t)$ occurs because energy transfers can only take place when an individual is alive to participate in the exchange. Intuitively, one expects $\eta_{\mathrm{C}}(t) < 0$ for all ages t, since it is always costly to make a positive transfer (lose energy), as there is no expectation of return when transfers are not allowed. In contrast, one expects $\eta_{\mathrm{T}} > 0$, as the positive value indicates that this intertemporal exchange is beneficial overall.

The Hamiltonian can be interpreted as the rate of fitness gain either directly through reproduction or indirectly through survival, growth, and maintenance. These four life history functions are weighed according to their contribution to fitness gains. The weights are measured against the effective fecundity rate (the first term in eq. (15)), which has a fitness value of "1", which is the reproductive value of a newborn. Decreasing mortality rate (i.e. increasing survival, the second term) has the fitness value $\lambda_{\mathrm{l}}(t)$, which we refer to as the value of life. Investing in the soma (physiological structures) has the fitness value of $\boldsymbol{\lambda}_{\mathrm{x}}(t)$, which we refer to as the value of the soma. Finally, transferring energy $T(t)$ has the fitness value of $\eta(t)$.

In order to apply the Hamiltonian eq. (15) to characterise uninvadability, we introduce a final piece of notation, which is the state-dependent control region:

$$\Omega(\mathbf{x}(t), \mathbf{u}_{\mathrm{r}}) = \{\mathbf{u}(t) \in \mathcal{U} : T(\mathbf{u}(t), \mathbf{x}(t), \mathbf{u}_{\mathrm{r}}) = 0\}. \tag{17}$$

This is the set of feasible controls under the intratemporal budget constraint (eq. 12). In terms of the Hamiltonian eq. (15), and applying standard optimal control theory results (e.g. Caputo, 2005 for a comprehensive text), we show in Appendix A that an uninvadable life history schedule needs to satisfy the following properties.

The maximum principle for life history evolution. *Suppose that the control* $\mathbf{u}^* = \{\mathbf{u}^*(t)\}_{t\in\mathcal{T}}$ *with associated*

state schedule $\mathbf{y}^* = (l^*, \mathbf{x}^*)$ *is uninvadable. Then, it is necessary that the control function maximises the Hamiltonian for all* $t \in \mathcal{T}$*:*

$$\mathbf{u}^*(t) \in \arg \max_{\mathbf{u}_\mathrm{m}(t) \in \Omega(t)} H(\mathbf{u}_\mathrm{m}(t), \mathbf{y}^*(t), \boldsymbol{\lambda}(t), \mathbf{u}^*), \tag{18}$$

where the control region is scenario-specific:

$$\Omega(t) = \begin{cases} \Omega(\mathbf{x}^*(t), \mathbf{u}^*) & \textit{without transfers} \\ \mathcal{U} & \textit{with tranfers.} \end{cases} \tag{19}$$

Regardless of the scenario, and except at points of discontinuities, the costates satisfy

$$-\frac{\mathrm{d}\lambda_\mathrm{l}(t)}{\mathrm{d}t} = \frac{\partial H(\mathbf{u}^*(t), \mathbf{y}_\mathrm{m}(t), \boldsymbol{\lambda}(t), \mathbf{u}^*)}{\partial l_\mathrm{m}(t)}\Big|_* \tag{20}$$

$$-\frac{\mathrm{d}\boldsymbol{\lambda}_\mathrm{x}(t)}{\mathrm{d}t} = \frac{\partial H(\mathbf{u}^*(t), \mathbf{y}_\mathrm{m}(t), \boldsymbol{\lambda}(t), \mathbf{u}^*)}{\partial \mathbf{x}_\mathrm{m}(t)}\Big|_*. \tag{21}$$

The notation means that the derivative (the vector of derivatives of the shadow values of the soma) is evaluated with all variables held at their uninvadable values. The state variables satisfy

$$\frac{\mathrm{d}l^*(t)}{\mathrm{d}t} = -\mu\left(\mathbf{u}^*(t), \mathbf{y}^*(t), \mathbf{u}^*\right) l^*(t) \quad \textit{with i.c. } l^*(0) = 1 \tag{22}$$

$$\frac{\mathrm{d}\mathbf{x}^*(t)}{\mathrm{d}t} = \boldsymbol{g}(\mathbf{u}^*(t), \mathbf{y}^*(t), \mathbf{u}^*) \quad \textit{with i.c. } \mathbf{x}^*(0) = \mathbf{x}_0, \tag{23}$$

and

$$\begin{cases} T(\mathbf{u}^*(t), \mathbf{x}^*(t), \mathbf{u}^*) = 0 \textit{ for all } t & \textit{without transfers} \\ \int_0^\infty l^*(t) T(\mathbf{u}^*(t), \mathbf{x}^*(t), \mathbf{u}^*)\, \mathrm{d}t = 0 & \textit{with tranfers.} \end{cases} \tag{24}$$

Moreover, the maximized Hamiltonian $\mathcal{H}(\mathbf{u}^*(t), \mathbf{y}^*(t), \boldsymbol{\lambda}(t), \mathbf{u}^*) = \max_{\mathbf{u}_\mathrm{m}(t) \in \Omega(t)} H(\mathbf{u}_\mathrm{m}(t), \mathbf{y}^*(t), \boldsymbol{\lambda}(t), \mathbf{u}^*)$ *is zero for all* $t \in \mathcal{T}$*:*

$$\mathcal{H}(\mathbf{u}^*(t), \mathbf{y}^*(t), \boldsymbol{\lambda}(t), \mathbf{u}^*) = 0. \tag{25}$$

Suppose further that the resident schedule does not affect mortality, $\mu(\mathbf{u}_\mathrm{m}(t), \mathbf{x}_\mathrm{m}(t), \mathbf{u}_\mathrm{r}) = \hat{\mu}(\mathbf{u}_\mathrm{m}(t), \mathbf{x}_\mathrm{m}(t))$*, soma dynamics,* $\boldsymbol{g}(\mathbf{u}_\mathrm{m}(t), \mathbf{x}_\mathrm{m}(t), \mathbf{u}_\mathrm{r}) = \boldsymbol{g}(\mathbf{u}_\mathrm{m}(t), \mathbf{x}_\mathrm{m}(t))$*, the rate of transfers,* $T(\mathbf{u}_\mathrm{m}(t), \mathbf{x}_\mathrm{m}(t), \mathbf{u}_\mathrm{r}) = T(\mathbf{u}_\mathrm{m}(t), \mathbf{x}_\mathrm{m}(t))$*, and that resident effects on fertility are multiplicatively separable* $b\left(\mathbf{u}_\mathrm{m}(t), \mathbf{x}_\mathrm{m}(t), \mathbf{u}_\mathrm{r}\right) = \hat{b}\left(\mathbf{u}_\mathrm{m}(t), \mathbf{x}_\mathrm{m}(t)\right) g_\mathrm{b}(\mathbf{u}_\mathrm{r})$ *for some* $g_\mathrm{b}(\mathbf{u}_\mathrm{r}) \in \mathbb{R}$ *capturing density-dependent population regulation. Then, the previous results hold by setting* $g_\mathrm{b}(\mathbf{u}_\mathrm{r}) = 1$ *and the maximum principle becomes fully independent of resident properties. Namely, characterising uninvadability becomes an optimisation problem that can be characterised using a Hamiltonian* $H(\mathbf{u}_\mathrm{m}(t), \mathbf{y}_\mathrm{m}(t), \boldsymbol{\lambda}(t))$ *independent of* $\mathbf{u}_\mathrm{r}$*.*

An uninvadable schedule thus maximises the Hamiltonian throughout the lifespan. At each moment in time, the uninvadable life-history thus balances the trade-off between (i) present reproduction, (ii) staying alive to acquire future reproduction, (iii) transferring resources, and (iv) investing in the soma (or more generally embodied capital).

It follows from the maximum principle that the value of life changes according to

$$\frac{\mathrm{d}\lambda_{\mathrm{l}}(t)}{\mathrm{d}t} = -\Big[b\left(\mathbf{u}^*(t),\mathbf{x}^*(t),\mathbf{u}^*\right) + \eta_{\mathrm{T}} T(\mathbf{u}^*(t),\mathbf{x}^*(t),\mathbf{u}^*)\Big] + \mu^*(\mathbf{u}^*(t),\mathbf{x}^*(t),\mathbf{u}^*)\lambda_{\mathrm{l}}(t), \tag{26}$$

where the second term in the brackets is nil without transfers. Hence, the value of life decreases with forgone reproduction, increases with forgone death proportionally to its value, and increases with transfers given away. Setting the value of life of a newborn to one, $\lambda_{\mathrm{l}}(0) = 1$, we find in Appendix B.2 that

$$\lambda_{\mathrm{l}}(t) = v_{\mathrm{F}}(t) + \eta_{\mathrm{T}} v_{\mathrm{T}}(t), \tag{27}$$

where

$$v_{\mathrm{F}}(t) = \frac{1}{l^*(t)} \int_t^\infty l^*(\tau) b\left(\mathbf{u}^*(\tau),\mathbf{x}^*(\tau),\mathbf{u}^*\right) \mathrm{d}\tau \tag{28}$$

is Fishers' reproductive value at age t (Fisher, 1930), and

$$v_{\mathrm{T}}(t) = \frac{1}{l^*(t)} \int_t^\infty l^*(\tau) T(\mathbf{u}^*(\tau),\mathbf{x}^*(\tau),\mathbf{u}^*) \mathrm{d}\tau \tag{29}$$

is the "transfer value" of an individual. This is the remaining net energy balance at age t, given that the individual is alive at age t (note that when an individual is born, then $v_{\mathrm{T}}(0) = 0$). Thus, in the absence of intergenerational transfers, the value of life reduces to Fisher's reproductive value $v_{\mathrm{F}}(t)$, as it should (Perrin, 1992). With transfers, the value of life can be positive even when an individual has ceased to reproduce, as long as it transfers resources (as noted earlier by Kaplan and Robson, 2009, p. 1841 where $V(t)$ in their model corresponds to our $v_{\mathrm{T}}(t)$). If an individual at age t has received a substantial amount of transfers earlier in life, then the transfer value $v_{\mathrm{T}}(t)$ of that individual is positive, as everything received by transfers must eventually be repaid due to the budget balance constraint (13).

The maximum principle also shows that the value of the soma $\boldsymbol{\lambda}_{\mathrm{x}}(t)$ satisfies the dynamics

$$\begin{aligned}\frac{\mathrm{d}\boldsymbol{\lambda}_{\mathrm{x}}(t)}{\mathrm{d}t} = l^*(t) \Bigg[&-\frac{\partial b\left(\mathbf{u}^*(t),\mathbf{x}_{\mathrm{m}}(t),\mathbf{u}^*\right)}{\partial \mathbf{x}_{\mathrm{m}}(t)} + \lambda_{\mathrm{l}}(t) \frac{\partial \mu\left(\mathbf{u}^*(t),\mathbf{x}_{\mathrm{m}}(t),\mathbf{u}^*\right)}{\partial \mathbf{x}_{\mathrm{m}}(t)} \Bigg]_* \\ &- \boldsymbol{\lambda}_{\mathrm{x}}(t) \cdot \frac{\partial \boldsymbol{g}(\mathbf{u}^*(t),\mathbf{x}_{\mathrm{m}}(t),\mathbf{u}^*)}{\partial \mathbf{x}_{\mathrm{m}}(t)} \Bigg|_* - \eta(t) \frac{\partial T\left(\mathbf{u}^*(t),\mathbf{x}_{\mathrm{m}}(t),\mathbf{u}^*\right)}{\partial \mathbf{x}_{\mathrm{m}}(t)} \Bigg|_*, \end{aligned} \tag{30}$$

which is driven by four forces. First, when the marginal increase in a given state variable $x_{\mathrm{m},i}(t) \in \mathbf{x}_{\mathrm{m}}(t)$ enhances current reproduction ($\partial b(t)/\partial x_{\mathrm{m},i}(t) > 0$), then the corresponding shadow value decreases as these reproductive benefits are realised immediately, depleting the remaining potential fitness gains available from that state variable. Second, when a marginal increase in the state variable reduces mortality ($\partial \mu(t)/\partial x_{\mathrm{m},i}(t) < 0$), the shadow value decreases because it is depleting the remaining potential for that state variable to contribute to future fitness by increasing survival. Third, when a marginal increase in the state variable increases its own growth rate ($\partial g_i(t)/\partial x_{\mathrm{m},i} > 0$), the shadow value decreases. This reflects a compound interest effect, whereby initial investments into the state are more valuable. Finally, for the case of transfers, when a marginal increase in the state variable enhances energy production available to make transfers ($\partial T/\partial x_{\mathrm{m},i} > 0$), the shadow value decreases as

these resources are allocated to lineage members, depleting remaining fitness benefits analogously to how current reproduction depletes individual fitness potential. In the absence of transfers, the marginal effects of state variables are constrained by the requirement that production equals assimilation at each age. Owing to the fact that eq. (30) defines a multidimensional linear dynamical system with varying coefficients, no general explicit representation of $\boldsymbol{\lambda}_{\mathrm{x}}(t)$ can be obtained (see Appendix B.1). Although typically the shadow value of the soma decreases over the lifespan, stationary values are possible when the competing forces remain balanced, as may occur in steady-state life histories. Finally, note that there are no dynamical equations associated with the variable $\eta(t)$. In the transfer case, η_{T} is a constant determined by the integral constraint (recall the second line of eq. (24)). In the case without transfers, $\eta_C(t)$ is a Lagrange multiplier function implicitly determined by enforcing $T(t) = 0$ at each age (first line of eq. (24)). The constraints given by eq. (24) provide the additional relationships needed to determine η_T or $\eta_C(t)$.

3.1.2 Transversality conditions

As is usual for infinite-horizon optimal control problems, the maximum principle as stated above does not yet contain in itself enough information to single out one or a few candidates for uninvadability. This is because no boundary conditions are given for the costate variables in the statement of the maximum principle. This is the well-known problem of identifying the correct transversality conditions for infinite-horizon optimal control problems (Caputo, 2005; Sydsaeter et al., 2008; Weber, 2011). This problem is often sidelined in life history evolution models by working with the assumption of a finite horizon (e.g. the review by Perrin and Sibly, 1993). But this problem needs to be confronted in the infinite-horizon case, which allows us to model an unknown time of death and this is of biological relevance.

In order to identify the transversality conditions for our model, we make the following observations. First, the value of life (the righ-hand-side of eq. (27)) should remain bounded at all times, since infinite reproductive value does not appear to be biologically meaningful. This in turn entails that the value of life of a newborn must be one, which provides a transversality condition for the costate $\lambda_{\mathrm{l}}(t)$ and leads to its general solution given by eq. (27) (see Appendix B.2 for details). To obtain a boundary condition for the value of the soma $\boldsymbol{\lambda}_{\mathrm{x}}(t)$, we note that eq. (25) provides the transversality condition $\lim_{t\to\infty} \mathcal{H}(\mathbf{u}^*(t), \mathbf{y}^*(t), \boldsymbol{\lambda}(t), \mathbf{u}_{\mathrm{r}}) = 0$. In force of eq. (15) and owing to the fact that $\lim_{t\to\infty} l^*(t) = 0$, this transversality condition then implies that $\lim_{t\to\infty} \boldsymbol{\lambda}_{\mathrm{x}}(t) = 0$. This then provides a final condition to eq. (21). Thus, the maximum principle for life history evolution with boundary conditions $\lambda_{\mathrm{l}}(0) = 1$ and $\lim_{t\to\infty} l^*(t) = 0$ to eqs. (20)–(21) provides enough information to solve for all dynamic equations and single out one or a few candidates for uninvadability. Sufficient conditions for uninvadability can, as is usual, be established using the Mangasarian or Arrow conditions (Sydsaeter et al., 2008, Theorem 10.3.2, p. 372, Caputo, 2005, Theorem 14.4, p. 388), but we do not delve into such conditions here.

We close this section by clarifying that the maximum principle for life history evolution presented above generalizes previous versions of optimal control models found in the life-history evolution literature (e.g., León, 1976; Schaffer, 1982; Iwasa and Roughgarden, 1984; Perrin, 1992; Perrin and Sibly, 1993; Day and Taylor, 2000; Kaplan and Robson, 2009) by simultaneously incorporating (i) both intratemporal and intertemporal energy budget constraints within a single model, (ii) ecological embedding through resident-dependent vital rates, and (iii) allowing for an infinite horizon. Further, it brings upfront the role of the shadow value of the energy $\eta(t)$, which does generally

not appear in previous versions of the maximum principle for life history owing to more specific assumptions made on the controls (e.g., comments below eq. 10).

3.2 Selection pressures and characteristics of uninvadable life-histories

3.2.1 The selection pressures

According to the maximum principle, the necessary first-order condition for the i-th component $u_i^*(t)$ of the trait $\mathbf{u}^*(t)$ to be uninvadable is

$$\begin{aligned}
&\text{if } u_i^*(t) = \underline{\omega}_i(t) && \text{then} && \frac{\partial H(\mathbf{u}_{\mathrm{m}}(t), \mathbf{y}^*(t), \boldsymbol{\lambda}(t), \mathbf{u}^*)}{\partial u_{\mathrm{m},i}(t)}\bigg|_* \leq 0, \\
&\text{if } \underline{\omega}_i(t) < u_i^*(t) < \overline{\omega}_i(t) && \text{then} && \frac{\partial H(\mathbf{u}_{\mathrm{m}}(t), \mathbf{y}^*(t), \boldsymbol{\lambda}(t), \mathbf{u}^*)}{\partial u_{\mathrm{m},i}(t)}\bigg|_* = 0, \\
&\text{if } u_i^*(t) = \overline{\omega}_i(t) && \text{then} && \frac{\partial H(\mathbf{u}_{\mathrm{m}}(t), \mathbf{y}^*(t), \boldsymbol{\lambda}(t), \mathbf{u}^*)}{\partial u_{\mathrm{m},i}(t)}\bigg|_* \geq 0,
\end{aligned} \tag{31}$$

where $\underline{\omega}_i(t)$ and $\overline{\omega}_i(t)$ are the lower and upper values the i-th component of the trait can take at time t. Setting $\mathcal{U} = \prod_{i=1}^{n_u}[\underline{u}_i, \overline{u}_i]$, we have $\underline{\omega}_i(t) = \underline{u}_i$ and $\overline{\omega}_i(t) = \overline{u}_i$ for the case with transfers and thus $u_i^*(t) \in [\underline{u}_i, \overline{u}_i]$. For the case without transfers, $u_i^*(t) \in [\underline{\omega}_i(t), \overline{\omega}_i(t)] = \{u_i \in [\underline{u}_i, \overline{u}_i] : T(\mathbf{u}^*(t), \mathbf{x}^*(t), \mathbf{u}^*) = 0\}$ (recall eq. (19)). The derivative in eq. (31) can be unpacked as follows

$$\begin{aligned}
\frac{\partial H(\mathbf{u}_{\mathrm{m}}(t), \mathbf{y}^*(t), \boldsymbol{\lambda}(t), \mathbf{u}^*)}{\partial u_{\mathrm{m},i}(t)}\bigg|_* = l^*(t) \Bigg[&\frac{\partial b\left(\mathbf{u}_{\mathrm{m}}(t), \mathbf{x}^*(t), \mathbf{u}^*\right)}{\partial u_{\mathrm{m},i}(t)} - \lambda_{\mathrm{l}}(t) \frac{\partial \mu\left(\mathbf{u}_{\mathrm{m}}(t), \mathbf{x}^*(t), \mathbf{u}^*\right)}{\partial u_{\mathrm{m},i}(t)} \Bigg]_* \\
&+ \boldsymbol{\lambda}_{\mathrm{x}}(t) \cdot \frac{\partial \boldsymbol{g}(\mathbf{u}_{\mathrm{m}}(t), \mathbf{x}^*(t), \mathbf{u}^*)}{\partial u_{\mathrm{m},i}(t)}\bigg|_* + \eta(t) \frac{\partial T\left(\mathbf{u}_{\mathrm{m}}(t), \mathbf{x}^*(t), \mathbf{u}^*\right)}{\partial u_{\mathrm{m},i}(t)}\bigg|_*.
\end{aligned} \tag{32}$$

This represents the age-specific force of selection, or the selection pressure (the i-th component of the selection gradient). It consists of the marginal effect of the trait value on all vital rates, including the transfers, weighted by the costates. Because both $l^*(t)$ and $\boldsymbol{\lambda}_{\mathrm{x}}(t)$ approach asymptotically zero, we see that the force of selection generally decreases as time passes by.

A special yet important case in practice is when the Hamiltonian is linear in the control $u_i^*(t) \in [\underline{\omega}_i(t), \overline{\omega}_i(t)]$. In this case, a non-zero selection pressure becomes sufficient to determine boundary control values and one has

$$\begin{aligned}
&\text{if } \frac{\partial H(\mathbf{u}_{\mathrm{m}}(t), \mathbf{y}^*(t), \boldsymbol{\lambda}(t), \mathbf{u}^*)}{\partial u_{\mathrm{m},i}(t)}\bigg|_* < 0 \quad \text{then} && u_i^*(t) = \underline{\omega}_i(t), \\
&\text{if } \frac{\partial H(\mathbf{u}_{\mathrm{m}}(t), \mathbf{y}^*(t), \boldsymbol{\lambda}(t), \mathbf{u}^*)}{\partial u_{\mathrm{m},i}(t)}\bigg|_* = 0 \quad \text{then} && \underline{\omega}_i(t) \leq u_i^*(t) \leq \overline{\omega}_i(t), \\
&\text{if } \frac{\partial H(\mathbf{u}_{\mathrm{m}}(t), \mathbf{y}^*(t), \boldsymbol{\lambda}(t), \mathbf{u}^*)}{\partial u_{\mathrm{m},i}(t)}\bigg|_* > 0 \quad \text{then} && u_i^*(t) = \overline{\omega}_i(t)
\end{aligned} \tag{33}$$

(Caputo, 2005, p. 135). This allows for a so-called bang-bang solution in which the control can switch between boundary values, except when the selection pressure vanishes. When the selection pressure vanishes, the control may take an interior value $\underline{\omega}_i(t) < u_i^*(t) < \overline{\omega}_i(t)$, which can hold for some time interval resulting in a so-called singular arc. The control in this case can be determined by repeatedly differentiating $\partial H/\partial u_{m,i}(t)|* = 0$ with

respect to time:

$$\left(\frac{\mathrm{d}}{\mathrm{d}t}\right)^{i}\left(\frac{\partial H(t)}{\partial u_{\mathrm{m},i}(t)}\Big|_{*}\right)=0 \qquad \forall i\in\{1,2,...\}, \tag{34}$$

until the control $u_{m,i}(t)$ appears explicitly in the equation (e.g., Kopp and Moyer, 1965). Obtaining a singular arc, however, requires specific restrictions on the functional form of the model and tends to be more common in models with high-dimensional state spaces (Rebhuhn, 1978, yet see Iwasa and Roughgarden, 1984; Perrin et al., 1993 for examples in the context of life-history evolution).

3.2.2 The uninvadable mortality schedule

The vanishing Hamiltonian $\mathcal{H}(t)=0$ (eq. (25), see also Appendix A.3) provides a useful optimality principle; namely, an uninvadable life history must allocate resources such that the immediate fitness gains from current activities are perfectly balanced against their effects on future fitness opportunities, ensuring that no reallocation of resources at any age can improve lifetime fitness. This condition can be used to reveal the mortality schedule on an uninvadable path by substituting eq. (15) into eq. (25) and solving for mortality. This yields

$$\mu\left(\mathbf{u}^{*}(t),\mathbf{x}^{*}(t),\mathbf{u}^{*}\right)=\frac{f_{\mathrm{c}}\left(\mathbf{u}^{*}(t),\mathbf{x}^{*}(t),\mathbf{u}^{*}\right)}{\lambda_{\mathrm{l}}(t)}=\frac{f_{\mathrm{c}}\left(\mathbf{u}^{*}(t),\mathbf{x}^{*}(t),\mathbf{u}^{*}\right)}{v_{\mathrm{F}}(t)+\eta_{\mathrm{T}}v_{\mathrm{T}}(t)}, \tag{35}$$

where

$$f_{\mathrm{c}}\left(\mathbf{u}^{*}(t),\mathbf{x}^{*}(t),\mathbf{u}^{*}\right)=b\left(\mathbf{u}^{*}(t),\mathbf{x}^{*}(t),\mathbf{u}^{*}\right)+\boldsymbol{\lambda}_{\mathrm{x}}^{\mathrm{c}}(t)\cdot\boldsymbol{g}(\mathbf{u}^{*}(t),\mathbf{x}^{*}(t),\mathbf{u}^{*})+\eta^{\mathrm{c}}(t)T\left(\mathbf{u}^{*}(t),\mathbf{x}^{*}(t),\mathbf{u}^{*}\right) \tag{36}$$

is the fitness gain from current activities (reproduction, changes in the state of the soma, and transfers). Here, $\boldsymbol{\lambda}_{\mathrm{x}}^{\mathrm{c}}(t)=\boldsymbol{\lambda}_{\mathrm{x}}(t)/l^{*}(t)$ and $\eta^{\mathrm{c}}(t)=\eta(t)/l^{*}(t)$ are the current values of the soma and the energy (marginal values conditional on survival) and in force of eq. (30), we get

$$\begin{aligned}\frac{\mathrm{d}\boldsymbol{\lambda}_{\mathrm{x}}^{\mathrm{c}}(t)}{\mathrm{d}t}=&\left[\mu(\mathbf{u}^{*}(t),\mathbf{x}^{*}(t),\mathbf{u}^{*})-\frac{\partial\boldsymbol{g}(\mathbf{u}^{*}(t),\mathbf{x}_{\mathrm{m}}(t),\mathbf{u}^{*})}{\partial\mathbf{x}_{\mathrm{m}}(t)}\right]_{*}\boldsymbol{\lambda}_{\mathrm{x}}^{\mathrm{c}}(t)\\&+\left[-\frac{\partial b\left(\mathbf{u}^{*}(t),\mathbf{x}_{\mathrm{m}}(t),\mathbf{u}^{*}\right)}{\partial\mathbf{x}_{\mathrm{m}}(t)}+\lambda_{\mathrm{l}}(t)\frac{\partial\mu\left(\mathbf{u}^{*}(t),\mathbf{x}_{\mathrm{m}}(t),\mathbf{u}^{*}\right)}{\partial\mathbf{x}_{\mathrm{m}}(t)}-\eta^{\mathrm{c}}(t)\frac{\partial T\left(\mathbf{u}^{*}(t),\mathbf{x}_{\mathrm{m}}(t),\mathbf{u}^{*}\right)}{\partial\mathbf{x}_{\mathrm{m}}(t)}\right]_{*}.\end{aligned} \tag{37}$$

Eq. (35) reveals five insights about life-history evolution. First, mortality increases when current activities rise relative to future fitness potential, showing that the mortality rate represents a direct trade-off between current reproduction, growth, and transfers and future reproduction and transfers. Second, it generalises Fisher's (1930) observation that mortality varies inversely with reproductive value to incorporate intergenerational transfers. Third, because $v_{\mathrm{T}}(t)>0$ increases the denominator of eq. (35), transfers reduce the uninvadable mortality rate and thereby extend lifespan, all else being equal. Fourth, without transfers, mortality becomes unbounded ($\mu^{*}(t)\to\infty$), when reproductive value vanishes ($v_{\mathrm{F}}(t)\to 0$), and thus selection would not favour survival after reproduction has ceased. However, with transfers, the value of life remains positive, with $\eta_{\mathrm{T}}v_{\mathrm{T}}(t)>0$ even after reproduction ceases, showing that a post-reproductive lifespan can be favoured under transfers.

Finally, $\boldsymbol{\lambda}_{\mathrm{x}}^{\mathrm{c}}(t)$ may reach a stationary value (its dynamic, eq. 37, is not weighed by $l^{*}(t)$, compare to eq. 30). Hence, all life history component may reach a steady state (that is, $\lim_{t\to\infty}\mathbf{u}^{*}(t)=\hat{\mathbf{u}}^{*}$, $\lim_{t\to\infty}\mathbf{x}^{*}(t)=\hat{\mathbf{x}}^{*}$, $\lim_{t\to\infty}\lambda_{\mathrm{l}}(t)=\hat{\lambda}_{\mathrm{l}}$, $\lim_{t\to\infty}\boldsymbol{\lambda}_{\mathrm{x}}^{\mathrm{c}}(t)=\hat{\boldsymbol{\lambda}}_{\mathrm{x}}^{\mathrm{c}}$, and $\lim_{t\to\infty}\eta^{\mathrm{c}}(t)=\hat{\eta}^{\mathrm{c}}$). The uninvadable mortality rate in this case is given

by

$$\mu\left(\hat{\mathbf{u}}^{*},\hat{\mathbf{x}}^{*},\mathbf{u}^{*}\right)=\frac{1}{\hat{\lambda}_{\mathrm{l}}}\Big[b\left(\hat{\mathbf{u}}^{*},\hat{\mathbf{x}}^{*},\mathbf{u}^{*}\right)+\hat{\boldsymbol{\lambda}}_{\mathrm{x}}^{\mathrm{c}}\cdot\boldsymbol{g}(\hat{\mathbf{u}}^{*},\hat{\mathbf{x}}^{*},\mathbf{u}^{*})+\hat{\eta}^{\mathrm{c}}\,T\left(\hat{\mathbf{u}}^{*},\hat{\mathbf{x}}^{*},\mathbf{u}^{*}\right)\Big],\tag{38}$$

which is stationary. Although schedules leading to stationary life history have not been much investigated in evolutionary biology, their prevalence in economic problems concerned with intertemporal allocations (e.g. Dorfman, 1969; Caputo, 2005; Sydsaeter et al., 2008; Weber, 2011) suggests that they are possible outcomes of evolution. In other words, a life history in which mortality decreases early in life and then increases later in life is not a necessary outcome of evolution.

Given that the uninvadable mortality rate does not necessarily have to increase with age, why did Kaplan and Robson (2009) conclude that senescence (increase in mortality rate with age) is inevitable? Their conclusion stems from a specific assumption of their model and the parameter space they considered, which can be examined using eq. (35). In their model, mortality is directly a control variable, and thus an evolving trait, written now as $\mu\left(\mathbf{u}^{*}(t),\mathbf{x}^{*}(t)\right)=\mu(t)$ with associated cost of resources $E_{\mu}(\mu(t))$ depending only on the trait itself. Differentiating eq. (35) with respect to mortality, and using eq. (11) and eq. (7), shows that the necessary first-order condition for the uninvadable mortality schedule satisfies $\partial E_{\mu}(\mu(t))/\partial\mu(t)\propto\lambda_{\mathrm{l}}(t)$. Using the fact that $\mu(t)=\exp[\log(\mu(t))]$ we can write $\partial E_{\mu}(\mu(t))/\partial\mu(t)=(\partial E_{\mu}(\mu(t))/\partial\log(\mu(t))/\mu(t)$, whereby

$$\mu(t)\propto\frac{1}{\lambda_{\mathrm{l}}(t)}\frac{\partial E_{\mu}(\mu(t))}{\partial\log(\mu(t))}.\tag{39}$$

Hence, mortality varies inversely with the value of life under the stated assumptions. Furthermore, Kaplan and Robson (2009) assumed that somatic maintenance costs are sufficiently high to ensure that the value of life $\lambda_{\mathrm{l}}(t)$ declines rather than reaches a steady state. However, these assumptions are unlikely to hold in general. Moreover, when mortality emerges indirectly from the allocation to multiple life history traits (rather than being directly controlled), the relationship between age and mortality becomes even more complex, allowing for diverse ageing patterns including negligible or even negative senescence (e.g, Vaupel et al., 2004). The goal of this paper, however, is not to investigate these various forms of mortality schedules, but to compare the broad features of life-history evolution with and without transfers. For this, it is useful to analyse a concrete model to which we next turn.

4 Application: life history evolution with and without transfers

4.1 Model formulation

We now apply our results to analyse life history evolution in a model that allows us to compare evolutionary outcomes with and without intergenerational energy transfers. This model builds upon that of Kaplan and Robson (2009), which considered only intertemporal budget balance (recall eq. (13)). To build the model, we first follow the biological assumptions of Kaplan and Robson (2009) and let the control schedule consist of four evolving traits $\mathbf{u}_{\mathrm{m}}(t)=(b_{\mathrm{m}}(t),\mu_{\mathrm{m}}(t),g_{\mathrm{m}}(t),z_{\mathrm{m}}(t))$. These stand, respectively, for the birth rate, the mortality rate, the somatic growth rate, and the rate of maintenance of the somatic quality (see table 2 for a list of key symbols). We further assume that both the mortality rate $\mu_{\mathrm{m}}(t)$ and the quality maintenance rate $z_{\mathrm{m}}(t)$ are unbounded from above

$(\mu_{\mathrm{m}}(t), z_{\mathrm{m}}(t) \in \mathbb{R}_+)$, reflecting that these quantities are only constrained by the budget balance condition. For the scenario without transfers, we similarly assume that $b_{\mathrm{m}}(t)$ and $g_{\mathrm{m}}(t)$ have fixed bounds from below $(b_{\mathrm{m}}(t), g_{\mathrm{m}}(t) \geq 0)$, but their maximum feasible values are determined endogenously by the intratemporal budget constraint eq. (12), which defines the feasible control region (recall eq. (17)). However, for the scenario with transfers, the intertemporal budget constraint eq. (13) is not constraining enough for $b_{\mathrm{m}}(t)$ and $g_{\mathrm{m}}(t)$. Without additional physiological constraints, this permits extremely rapid early-life growth through essentially unlimited energy borrowing, leading to biologically unrealistic somatic capital accumulation. Therefore, we impose upper limits $b_{\max}$ and $g_{\max}$ on both $b_{\mathrm{m}}(t)$ and $g_{\mathrm{m}}(t)$, which capture limits on cellular production capacity.

Given these assumptions, we write the effective fertility and mortality rates as

$$b(\mathbf{u}_{\mathrm{m}}(t), \mathbf{x}_{\mathrm{m}}(t), \mathbf{u}_{\mathrm{r}}) = g_{\mathrm{b}}(\mathbf{u}_{\mathrm{r}}) b_{\mathrm{m}}(t) \quad \text{and} \quad \mu\left(\mathbf{u}_{\mathrm{m}}(t), \mathbf{x}_{\mathrm{m}}(t), \mathbf{u}_{\mathrm{r}}\right) = \mu_{\mathrm{m}}(t) + \mu_{\mathrm{e}}, \tag{40}$$

where $g_{\mathrm{b}}(\mathbf{u}_{\mathrm{r}})$ accounts for density-dependence regulation affecting fertility and μ_{e} is the external mortality rate. The probability of survival thus satisfies

$$\frac{\mathrm{d}l_{\mathrm{m}}(t)}{\mathrm{d}t} = -(\mu_{\mathrm{m}}(t) + \mu_{\mathrm{e}}) l_{\mathrm{m}}(t) \qquad \text{with i.c. } \; l_{\mathrm{m}}(0) = 1. \tag{41}$$

The somatic state $\mathbf{x}_{\mathrm{m}}(t) = (k_{\mathrm{m}}(t), q_{\mathrm{m}}(t))$ at age t is assumed to consist of the quantity and quality of somatic capital, respectively, which satisfy

$$\frac{\mathrm{d}k_{\mathrm{m}}(t)}{\mathrm{d}t} = g_{\mathrm{m}}(t) \qquad \text{with i.c. } \; k_{\mathrm{m}}(0) = k_0 \tag{42}$$

$$\frac{\mathrm{d}q_{\mathrm{m}}(t)}{\mathrm{d}t} = z_{\mathrm{m}}(t) - \epsilon \qquad \text{with i.c. } \; q_{\mathrm{m}}(0) = q_0, \tag{43}$$

where $\epsilon > 0$ is a positive parameter describing the baseline depreciation rate of the somatic quality (in the absence of allocation of resources to maintenance).

We write the energy transfer (eq. (11) with (7)) for this model as

$$T(\mathbf{u}_{\mathrm{m}}(t), \mathbf{x}_{\mathrm{m}}(t)) = F\Big(P(k_{\mathrm{m}}(t), q_{\mathrm{m}}(t)), E_{\mathrm{b}}(b_{\mathrm{m}}(t), k_{\mathrm{m}}(t), q_{\mathrm{m}}(t))\Big) - \Big(E_\mu(\mu_{\mathrm{m}}(t)) + E_{\mathrm{k}}(g_{\mathrm{m}}(t)) + E_{\mathrm{q}}(k_{\mathrm{m}}(t), z_{\mathrm{m}}(t))\Big), \tag{44}$$

where E_i is the energy used for life history trait $i \in \{\mathrm{b}, \mu, \mathrm{k}, \mathrm{q}\}$ and

$$F\Big(P(k_{\mathrm{m}}(t), q_{\mathrm{m}}(t)), b_{\mathrm{m}}(t)\Big) = P(k_{\mathrm{m}}(t), q_{\mathrm{m}}(t)) - E_{\mathrm{b}}(b_{\mathrm{m}}(t), P(k_{\mathrm{m}}(t), q_{\mathrm{m}}(t))) \tag{45}$$

is the energy available after accounting for reproduction cost. The production rate $P(t)$ and the surplus energy $F(t)$ after reproductive cost correspond to the functions $G(t)$ and $F(t)$, respectively, in Kaplan and Robson (2009, p. 1839), and we follow their assumptions of the properties of these functions. In particular, we assume that the production rate is zero if any of its arguments is zero and is monotonically increasing in each argument $(P(0, q_{\mathrm{m}}) = P(k_{\mathrm{m}}, 0) = 0$, $\partial P(k_{\mathrm{m}}, q_{\mathrm{m}})/(\partial k_{\mathrm{m}}) > 0$ and $\partial P(k_{\mathrm{m}}, q_{\mathrm{m}})/(\partial q_{\mathrm{m}}) > 0)$, $F(P, b_{\mathrm{m}})$ be a concave function of P and a decreasing function of b_{m} such that as the gross energy increases, reproduction is cheaper at the margin

($\partial F(P,b_{\rm m})/\partial z_{\rm m}>0$, and $\partial^2 F(P,b_{\rm m})/(\partial P\partial b_{\rm m})>0$). The energies devoted to survival (reducing mortality rate), the somatic quantity, and the somatic quality are given by

$$E_\mu(\mu_{\rm m}(t))=e(\mu_{\rm m}(t)), \tag{46}$$

$$E_{\rm k}(g_{\rm m}(t))=\alpha g_{\rm m}(t), \tag{47}$$

$$E_{\rm q}(k_{\rm m}(t),z_{\rm m}(t))=d(k_{\rm m}(t),z_{\rm m}(t)), \tag{48}$$

where $e(\mu_{\rm m})$ is a decreasing convex function of the mortality rate ($\partial e(\mu_{\rm m})/\partial\mu_{\rm m}<0$ and $\partial^2 e(\mu_{\rm m})/\partial\mu_{\rm m}^2>0$). In eq. (47), α is the cost of producing one unit of somatic capital. In eq. (48), $d(k_{\rm m}(t),z_{\rm m}(t))$ is the cost function of investing in somatic quality (i.e. maintenance cost of soma) and it is a monotonically increasing in somatic capital $k_{\rm m}$ ($\partial d(k_{\rm m},z_{\rm m})/\partial k_{\rm m}(t)>0$), a convex function in somatic quality $z_{\rm m}$ ($\partial d(k_{\rm m},z_{\rm m})/\partial z_{\rm m}(t)>0$, $\partial^2 d(k_{\rm m},z_{\rm m})/\partial z_{\rm m}^2>0$), and additionally it is zero if any of its arguments is zero ($d(0,z_{\rm m})=d(k_{\rm m},0)=0$).

We now depart slightly from the original model of Kaplan and Robson (2009). They assumed that the time of onset of reproduction is determined by a switching time where allocation to growth ceases. We do not make this assumption and let the time of reproduction be determined by the allocation schedule to reproduction, which is more in line with classical life-history evolution models in the absence of transfer (e.g., Perrin and Sibly, 1993). To that end, we assume that

$$E_{\rm b}(b_{\rm m}(t),P(k_{\rm m}(t),q_{\rm m}(t)))=b_{\rm m}(t)G(P(k_{\rm m}(t),q_{\rm m}(t))) \tag{49}$$

for some monotonically decreasing function $G(P)$ of P. Here, $G(P)$ can be interpreted as the marginal cost of reproduction and is assumed to be high when individuals are less productive (low P).

4.2 The optimal life-history with transfers

We first analyse the model with transfers because it turns out to be simpler and can also be read as a sanity check of the formulation of our model, since we need to recover the main results of Kaplan and Robson (2009) who used a different approach; namely, dynamic programming, to derive their results. Let then $\boldsymbol{\lambda}_{\rm x}(t)=(\lambda_{\rm k}(t),\lambda_{\rm q}(t))$ stand for the physiological costate variables associated with $k_{\rm m}(t)$ and $q_{\rm m}(t)$, respectively. In force of the assumptions of section 4.1 and the last statement (ii) of the maximum principle, we can write the Hamiltonian for the model in the presence of transfers as

$$\begin{aligned}H(\mathbf{u}_{\rm m}(t),\mathbf{y}_{\rm m}(t),\boldsymbol{\lambda}(t))&=l_{\rm m}(t)\Big[b_{\rm m}(t)-\lambda_{\rm l}(t)(\mu_{\rm m}(t)+\mu_{\rm e})\Big]+\lambda_{\rm k}(t)g_{\rm m}(t)+\lambda_{\rm q}(t)(z_{\rm m}(t)-\epsilon)\\&+\eta_{\rm T}l_{\rm m}(t)\Big[F\Big(P(k_{\rm m}(t),q_{\rm m}(t)),E_{\rm b}(b_{\rm m}(t),k_{\rm m}(t),q_{\rm m}(t))\Big)-\alpha g_{\rm m}(t)-d(k_{\rm m}(t),z_{\rm m}(t))-e(\mu_{\rm m}(t))\Big].\end{aligned} \tag{50}$$

Applying eq. (32), we get the selection pressures on the evolving traits as

$$\frac{\partial H(t)}{\partial b_{\mathrm{m}}(t)}\Big|_{*} = l^{*}(t)\left[1-\eta_{\mathrm{T}}G(P(t))\right], \tag{51}$$

$$\frac{\partial H(t)}{\partial \mu_{\mathrm{m}}(t)}\Big|_{*} = l^{*}(t)\left[-\lambda_{\mathrm{l}}(t)-\eta_{\mathrm{T}}\frac{\partial e(t)}{\partial \mu^{*}(t)}\right], \tag{52}$$

$$\frac{\partial H(t)}{\partial g_{\mathrm{m}}(t)}\Big|_{*} = \lambda_{\mathrm{k}}(t)-\eta_{\mathrm{T}}l^{*}(t)\alpha, \tag{53}$$

$$\frac{\partial H(t)}{\partial z_{\mathrm{m}}(t)}\Big|_{*} = \lambda_{\mathrm{q}}(t)-\eta_{\mathrm{T}}l^{*}(t)\frac{\partial d(t)}{\partial z^{*}(t)}, \tag{54}$$

where we used shorthand notations, writing e.g., $P(t) = P(k^{*}(t), q^{*}(t))$, thus suppressing the explicit dependence on state variables while retaining time dependence, and similarly for other functions of various variables. The first and second terms on the right-hand sides of eqs. (51)–(54) are the marginal benefits and costs, respectively, of increasing the corresponding trait values. From the maximum principle, the costates satisfy

$$\frac{\mathrm{d}\lambda_{\mathrm{l}}(t)}{\mathrm{d}t} = -\frac{\partial H(t)}{\partial l_{\mathrm{m}}(t)}\Big|_{*} = \lambda_{\mathrm{l}}(t)(\mu^{*}(t)+\mu_{\mathrm{e}})-b^{*}(t)-\eta_{\mathrm{T}}T(t), \tag{55}$$

$$\frac{\mathrm{d}\lambda_{\mathrm{k}}(t)}{\mathrm{d}t} = -\frac{\partial H(t)}{\partial k_{\mathrm{m}}(t)}\Big|_{*} = -\eta_{\mathrm{T}}l^{*}(t)\left(\frac{\partial F(t)}{\partial k^{*}(t)}-\frac{\partial d(t)}{\partial k^{*}(t)}\right), \tag{56}$$

$$\frac{\mathrm{d}\lambda_{\mathrm{q}}(t)}{\mathrm{d}t} = -\frac{\partial H(t)}{\partial q_{\mathrm{m}}(t)}\Big|_{*} = -\eta_{\mathrm{T}}l^{*}(t)\frac{\partial F(t)}{\partial q^{*}(t)}. \tag{57}$$

Applying eq. (B.6) along eq. (B.10), we get that the costate can be written as

$$\lambda_{\mathrm{l}}(t) = \frac{1}{l^{*}(t)}\int_{t}^{\infty} l^{*}(\tau)\Big[b^{*}(\tau)+\eta_{\mathrm{T}}T(\tau)\Big]\,\mathrm{d}\tau, \tag{58}$$

$$\lambda_{\mathrm{k}}(t) = \eta_{\mathrm{T}}\int_{t}^{\infty} l^{*}(\tau)\left(\frac{\partial F(\tau)}{\partial k^{*}(\tau)}-\frac{\partial d(\tau)}{\partial k^{*}(\tau)}\right)\mathrm{d}\tau, \tag{59}$$

$$\lambda_{\mathrm{q}}(t) = \eta_{\mathrm{T}}\int_{t}^{\infty} l^{*}(\tau)\frac{\partial F(\tau)}{\partial q^{*}(\tau)}\,\mathrm{d}\tau. \tag{60}$$

Let us now identify the general properties of a candidate uninvadable allocation schedule and let us first consider selection pressures on survival and quality, given by eq. (52) and eq. (54). Because the cost functions for maintenance $d(t) = d(k^{*}(t), z^{*}(t))$ and survival $e(t) = e(\mu^{*}(t))$ are convex, with respect to the rates of maintenance $z^{*}(t)$ and mortality $\mu^{*}(t)$, respectively. Thus, an interior solution satisfied by both $\mu^{*}(t)$ and $z^{*}(t)$ for all t exists and is characterised by

$$\frac{\partial d(t)}{\partial z^{*}(t)} = \frac{\lambda_{\mathrm{q}}^{\mathrm{c}}(t)}{\eta_{\mathrm{T}}} = \frac{1}{l^{*}(t)}\int_{t}^{\infty} l^{*}(\tau)\frac{\partial F(\tau)}{\partial q^{*}(\tau)}\,\mathrm{d}\tau, \tag{61}$$

$$-\frac{\partial e(t)}{\partial \mu^{*}(t)} = \frac{\lambda_{\mathrm{l}}(t)}{\eta_{\mathrm{T}}} = \frac{1}{l^{*}(t)}\int_{t}^{\infty} l^{*}(\tau)\Big[\frac{b^{*}(\tau)}{\eta_{\mathrm{T}}}+T(\tau)\Big]\,\mathrm{d}\tau. \tag{62}$$

Both shadow values, $\lambda_{\mathrm{q}}^{\mathrm{c}}(t)$ and $\lambda_{\mathrm{l}}(t)$, can be nonmonotonic functions of time. For example, if the value of life $\lambda_{\mathrm{l}}(t)$ is dome-shaped, then the schedule of $\mu^{*}(t)$ is therefore expected to be U-shaped (due to the negative sign on the left-hand side in eq. (62)). Similarly, if the value of quality $\lambda_{\mathrm{q}}^{\mathrm{c}}(t)$ is dome-shaped, then the somatic quality schedule $z^{*}(t)$ would be dome-shaped.

Let us now turn to the selection pressures on reproduction and growth, focusing first on growth. Since the growth rate $g^*(t)$ enters the Hamiltonian (50) linearly, the selection pressure given by eq. (53) does not explicitly depend on growth rate $g^*(t)$. For this case, we know from eq. (33) that when the selection pressure (53) is strictly positive, the uninvadable growth rate takes its maximal value $g^*(t) = g_{\max}$, and when strictly negative, no growth occurs ($g^*(t) = 0$). Thus, it follows from eq. (53) that when the marginal benefit exceeds the marginal cost $\lambda_{\mathrm{k}}(t) > \eta_{\mathrm{T}} l^*(t)\alpha$, growth occurs at its maximal rate $g_{\max}$. From eq. (59) it follows that $\lambda_{\mathrm{k}}(t)$ is high early in life and decreases with age. Thus, early in life, condition $\lambda_{\mathrm{k}}(t) > \eta_{\mathrm{T}} l^*(t)\alpha$ is expected to occur, which yields that growth occurs at its maximal rate $g_{\max}$ early in life. As $\lambda_{\mathrm{k}}(t)$ decreases with age, the growth can eventually cease when the marginal benefit becomes less than the cost $\lambda_{\mathrm{k}}(t) < l^*(t)\eta_{\mathrm{T}}\alpha$. If this is the case, the age at which growth ceases t^*_{g} is given by requiring that the marginal benefit is equal to the marginal cost

$$\lambda_{\mathrm{k}}(t^*_{\mathrm{g}}) = l^*(t^*_{\mathrm{g}})\eta_{\mathrm{T}}\alpha. \tag{63}$$

It is theoretically possible that after reaching age t^*_{g}, the condition (63) holds over a period of time, yielding a singular arc, where $0 < g^*(t) < u_{\max}$ for some period of time, but we were unable to find illuminating analytical results about candidate singular arcs and do not investigate this further here (in section (4.4) we fully solve the model numerically and do not detect singular arcs).

Now, let us consider reproduction. Like the growth rate $g^*(t)$, the birth rate $b^*(t)$ also enters the Hamiltonian (50) linearly, so the selection pressure (51) does not explicitly depend on birth rate $b^*(t)$. Thus, when the selection pressure (51) is strictly positive, reproduction occurs at its maximal rate $b^*(t) = b_{\max}$, and when strictly negative, no reproduction occurs ($b^*(t) = 0$). From the expression of the selection pressure (51) we observe that the benefit of reproduction is constant, while the cost $\eta_{\mathrm{T}} G(P(t))$ is a decreasing function of productivity $P(t)$ (recall the assumption after eq. (49)). Thus, we expect that reproduction is initially suppressed early in life, $b^*(t) = 0$, due to low production (consistent with the assumption below eq. (45) that production increases with soma size). As production $P(t)$ increases with age, the cost of reproduction $\eta_{\mathrm{T}} G(P(t))$ decreases. Eventually, at some time t^*_{b}, the benefit of reproduction becomes equal to the cost:

$$1 = \eta_{\mathrm{T}} G(P(t^*_{\mathrm{b}})), \tag{64}$$

which determines the start of reproduction. It is again possible that this condition holds over a period of time, yielding a singular arc with intermediate value for reproductive investment ($0 < b_{\mathrm{m}}(t) < b_{\max}$), but this requires that production $P(t)$ remains constant and appears here unrealistic. If production $P(t)$ further increases after the start of reproduction (e.g., due to continued growth), then we can have $1 > \eta_{\mathrm{T}} G(P(t^*_{\mathrm{b}}))$, which means that reproduction should be set at its maximum rate $b^*(t) = b_{\max}$. Production $P(t)$ can also decline if quality $q^*(t)$ declines with age, and this decline can cause reproduction to eventually stop, as the cost of reproduction increases with decreasing $P(t)$. Thus, if $1 = \eta_{\mathrm{T}} G(P(t^*_{\mathrm{m}}))$ at some age $t^*_{\mathrm{m}} > t^*_{\mathrm{b}}$, then age t^*_{m} can be interpreted as the onset of post-reproductive age, which is caused by quality decline making reproduction more expensive at the margin. Note also that determining $b^*(t)$ requires estimating η_T, as it appears in eq. (64). To obtain η_{T}, we can use the constraints

that the transfer $T^*(t) = T(b^*(t), \mu^*(t), g^*(t), z^*(t), k^*(t), q^*(t))$ given by eq. (44) must satisfy the budget balance $\int_0^\infty l^*(t)T^*(t)(t)\,\mathrm{d}t = 0$. In practice, such calculations are complicated, and we will resort to numerical calculations to illustrate solutions for the optimal life history schedule in section 4.4.

In summary, from the analytical analysis above, we outline some general properties of the candidate allocation schedule favoured by selection. Allocation of survival and maintenance occurs throughout the lifespan, with $\mu^*(t) > 0$ and $z^*(t) > 0$ for all $t \in \mathcal{T}$. Growth is expected to be positive early in life and is given by the maximum growth rate $g_{\max}$. Allocation to reproduction begins when production is high enough (once a sufficient somatic size is reached) and should, in general, be given by its maximal value $b_{\max}$, when growth continues after reproduction has started, as this causes the cost of reproduction to grow. Somatic quality decline can cause reproduction later in life, giving rise to a post-reproductive period. We also discussed how we cannot formally exclude the possibility of growth and reproduction to take some intermediate values, i.e. $0 < g^*(t) < g_{\max}$ and $0 < b^*(t) < b_{\max}$ for some periods, but there are restrictions for such singular arcs to be optimal.

These results are broadly consistent with those of Kaplan and Robson (2009, pp. 1840-1841) and eqs. (61)–(62) recover exactly their first-order conditions, as it should. Kaplan and Robson (2009) further proved that the function $\mu^*(t)$ is U-shaped, while $z^*(t)$ is dome-shaped under the assumption that reproduction does not occur during growth ($b^*(t) = 0$ for $t \in [0, t^*_{\mathrm{g}}]$). However, we do not make such an assumption here and, thus, we do not exclude the possibility of continued growth after reproduction has started. Kaplan and Robson (2009) also left the parameter η_{T} (which corresponds to their $1/\eta$) undetermined as they were concerned only with the general shape of the optimal trait schedules. In Section (4.4), we numerically investigate the above model in more detail and demonstrate that different qualitative results are possible. Before presenting these results, we analyse the qualitative results for the model without transfers.

4.3 The optimal life-history without transfers

To analyse the model without resource transfer, we assume the intra-temporal budget balance eq. (12). On substituting eqs. (45)–(49) into eqs. (11)-(12), the budget balance constraint can be written as

$$F(P(k_{\mathrm{m}}(t), q_{\mathrm{m}}(t)), b_{\mathrm{m}}(t))) - [\alpha g_{\mathrm{m}}(t) + d(k_{\mathrm{m}}(t), z_{\mathrm{m}}(t)) + e(\mu_{\mathrm{m}}(t))] = 0. \tag{65}$$

Thereby, the Hamiltonian in the absence of transfers can be expressed as

$$\begin{aligned} H(\mathbf{u}_{\mathrm{m}}(t), \mathbf{y}_{\mathrm{m}}(t), \boldsymbol{\lambda}(t)) = l_{\mathrm{m}}(t)\Big[b_{\mathrm{m}}(t) - \lambda_{\mathrm{l}}(t)(\mu_{\mathrm{m}}(t) + \mu_{\mathrm{e}}))\Big] + \lambda_{\mathrm{k}}(t) g_{\mathrm{m}}(t) + \lambda_{\mathrm{q}}(t)(z_{\mathrm{m}}(t) - \epsilon) \\ + \eta_{\mathrm{C}}(t)\Big(F(P(k_{\mathrm{m}}(t), q_{\mathrm{m}}(t)), b_{\mathrm{m}}(t)) - [\alpha g_{\mathrm{m}}(t) + d(k_{\mathrm{m}}(t), z_{\mathrm{m}}(t)) + e(\mu_{\mathrm{m}}(t))]\Big). \end{aligned} \tag{66}$$

Applying eq. (32), the selection pressures are

$$\frac{\partial H(t)}{\partial b_{\mathrm{m}}(t)}\Big|_{*} = l^{*}(t)\Big(1 - \frac{\eta_{\mathrm{C}}(t)}{l^{*}(t)}G(P(t))\Big), \tag{67}$$

$$\frac{\partial H(t)}{\partial \mu_{\mathrm{m}}(t)}\Big|_{*} = -l^{*}(t)\lambda_{\mathrm{l}}(t) - \eta_{\mathrm{C}}(t)\frac{\partial e(t)}{\partial \mu^{*}(t)}, \tag{68}$$

$$\frac{\partial H(t)}{\partial g_{\mathrm{m}}(t)}\Big|_{*} = \lambda_{\mathrm{k}}(t) - \eta_{\mathrm{C}}(t)\alpha, \tag{69}$$

$$\frac{\partial H(t)}{\partial z_{\mathrm{m}}(t)}\Big|_{*} = \lambda_{\mathrm{q}}(t) - \eta_{\mathrm{C}}(t)\frac{\partial d(t)}{\partial z^{*}(t)}. \tag{70}$$

The difference between these selection pressures and the corresponding ones for the case with transfers (given by eq. (51)–(54)) is that in the second summand of each term, the weight $\eta_{\mathrm{T}}l^{*}(t)$ has been replaced by $\eta_{\mathrm{C}}(t)$. In turn, the costates satisfy

$$\frac{\mathrm{d}\lambda_{\mathrm{l}}(t)}{\mathrm{d}t} = -\frac{\partial H(t)}{\partial l_{\mathrm{m}}(t)}\Big|_{*} = \lambda_{\mathrm{l}}(t)(\mu^{*}(t) + \mu_{\mathrm{e}})) - b^{*}(t), \tag{71}$$

$$\frac{\mathrm{d}\lambda_{\mathrm{k}}(t)}{\mathrm{d}t} = -\frac{\partial H(t)}{\partial k_{\mathrm{m}}(t)}\Big|_{*} = -\eta_{\mathrm{C}}(t)\left(\frac{\partial F(t)}{\partial k^{*}(t)} - \frac{\partial d(t)}{\partial k^{*}(t)}\right), \tag{72}$$

$$\frac{\mathrm{d}\lambda_{\mathrm{q}}(t)}{\mathrm{d}t} = -\frac{\partial H(t)}{\partial q_{\mathrm{m}}(t)}\Big|_{*} = -\eta_{\mathrm{C}}(t)\frac{\partial F(t)}{\partial q^{*}(t)}, \tag{73}$$

where the value of life no longer has a transfer component and the weight $\eta_{\mathrm{T}}l^{*}(t)$ has been replaced by $\eta_{\mathrm{C}}(t)$. The application of eq. (B.6) along eq. (B.10) now leads to

$$\lambda_{\mathrm{l}}(t) = \frac{1}{l^{*}(t)}\int_{t}^{\infty} l^{*}(\tau)b^{*}(\tau)\,\mathrm{d}\tau, \tag{74}$$

$$\lambda_{\mathrm{k}}(t) = \int_{t}^{\infty} \eta_{\mathrm{C}}(\tau)\left(\frac{\partial F(\tau)}{\partial k^{*}(\tau)} - \frac{\partial d(\tau)}{\partial k^{*}(\tau)}\right)\mathrm{d}\tau, \tag{75}$$

$$\lambda_{\mathrm{q}}(t) = \int_{t}^{\infty} \eta_{\mathrm{C}}(\tau)\frac{\partial F(\tau)}{\partial q^{*}(\tau)}\,\mathrm{d}\tau. \tag{76}$$

As in the case with transfers, let us identify the candidate uninvadable allocation schedule and consider again first selection on survival and quality, given by eq. (68) and eq. (70), which are both explicit functions of the controls. Since the cost of each allocation are convex functions of the corresponding allocation, an interior solution satisfied by both $\mu^{*}(t)$ and $z^{*}(t)$ for all t has to exist and is characterized by

$$\frac{\partial d(t)}{\partial z_{\mathrm{m}}(t)} = \frac{\lambda_{\mathrm{q}}(t)}{\eta_{\mathrm{C}}(t)}, \tag{77}$$

$$-\frac{\partial e(\mu_{\mathrm{m}}(t))}{\partial \mu_{\mathrm{m}}(t)} = \frac{l^{*}(t)\lambda_{\mathrm{l}}(t)}{\eta_{\mathrm{C}}(t)}, \tag{78}$$

which is obtained by setting the derivativers in eq. (68) and eq. (70) to zero. Similarly to the case with transfers, we expect the mortality schedule $\mu_{\mathrm{m}}(t)$ to be the inverse of the value of life $\lambda_{\mathrm{l}}(t)$, which here is given by Fisher's reproductive value (recall eq. (27)). The maintenance shedule $z_{\mathrm{m}}(t)$ is proportional to $\lambda_{\mathrm{q}}(t)/\eta_{\mathrm{C}}(t)$.

Since reproduction and growth schedule enter linearly in the Hamiltonian (66), these controls generally switch between their boundary values (recall section 3.2.1), and here the upper bounds are endogenously determined from

the budget balance condition (65). Let us then first consider the growth allocation schedule. From eq. (69), we can expect growth to occur early in life, because the marginal benefit of growth is expected to be greater than the cost ($\lambda_{\mathrm{k}}(t) > \eta_{\mathrm{C}}(t)\alpha$). In contrast to the case without transfers, where growth was given by the maximal rate $g_{\max}$, here the growth rate is constrained by the budget balance condition eq. (65) (e.g. Appendix D for a worked-out example). Growth will eventually stop when the cost of further growth exceeds its benefit ($\lambda_{\mathrm{k}}(t) < \eta_{\mathrm{C}}(t)\alpha$). Age t^*_{g} at which growth stops is given by the condition when the marginal benefit is equal to the cost

$$\lambda_{\mathrm{k}}(t^*_{\mathrm{g}}) = \eta_{\mathrm{C}}(t^*_{\mathrm{g}})\alpha. \tag{79}$$

This condition differs from the case with transfers (see eq. (63)) in that it explicitly depends on the shadow value of energy $\eta_{\mathrm{C}}(t)$ at a given age. Similarly to the case with transfers, eq. (79) may hold over a period of time, yielding a singular arc, which we do not investigate further analytically (we did not detect singular arcs numerically, see section (4.4)) Let us thus turn to the reproduction allocation schedule. From eq. (67), we observe that, for similar reasons as for the case of transfers, reproduction due to low productivity $P(t)$ early in life causes the cost of reproduction to be high compared to the benefit [i.e., $G(P(t)) > l^*(t)/\eta_{\mathrm{C}}(t)$], whereby $b^*(t) = 0$. As productivity increases, eventually a time t^*_{b} is reached when the marginal benefit of reproduction becomes equal to the cost:

$$1 = \frac{\eta_{\mathrm{C}}(t^*_{\mathrm{b}})}{l^*(t^*_{\mathrm{b}})} G(P(t^*_{\mathrm{b}})), \tag{80}$$

which determines the switch to reproduction. Compared to the case with transfers (recall eq. (64)), instead of the constant multiplier η_{T}, the condition here depends additionally on survival $l^*(t)$ and the shadow value of energy $\eta_{\mathrm{C}}(t)$ (note that again, we cannot exclude the possibility of singular arcs).

In summary, we find that the candidate resource allocation schedule favoured by selection has the following qualitative characteristics. The allocation of survival and maintenance occurs throughout the lifespan, i.e. $\mu^*(t) > 0$ and $z^*(t) > 0$ for all $t \in \mathcal{T}$, whereby the mortality rate $\mu^*(t)$ is proportional to the inverse of Fisher's reproductive value. Allocation to growth occurs early in life until a switching time t^*_{g} is reached; namely $g^*(t) > 0$ for all $t \in [0, t^*_{\mathrm{g}}]$. The allocation to reproduction is nil early in life and necessarily occurs after a switching time t^*_{b} has been reached. As in the case of transfers, we cannot formally exclude the possibility of growth and reproduction to have intermediate values, i.e. $0 < g^*(t) < g_{\max}$ and $0 < b^*(t) < b_{\max}$ for some periods, but there are many restrictions for such a life history to be optimal. The rates of $g^*(t)$ and $b^*(t)$ are here constrained by the intratemporal budget balance condition eq. (65) which also causes a direct linear trade-off between growth and reproduction, and in the absence of singular arcs, growth and reproduction are expected to be sequential $t^*_{\mathrm{g}} = t^*_{\mathrm{g}}$ as is the case of standard bang-bang solutions. This allocation schedule is qualitatively similar to that obtained under classical life history evolution models (e.g.,Perrin, 1992; Perrin and Sibly, 1993; Cichoń and Kozłowski, 2000).

4.4 Worked-out example: evolution with and without intergenerational transfers

We now present a complete implementation of the model given by eqs. (40)–(49), which will allow for a detailed comparison of the evolutionary outcomes under both energy budget scenarios. To that end, we assume that the

production function is given by

$$P(k_{\mathrm{m}}(t), q_{\mathrm{m}}(t)) = a[k_{\mathrm{m}}(t)]^{c} q_{\mathrm{m}}(t), \tag{81}$$

where $a > 0$ and $0 < c < 1$. This entails a standard power-law assumption between energy acquisition and body size (e.g. Day and Taylor, 1997), and here we also assume that production is proportional to somatic quality. The energy cost of reproduction is assumed to be

$$G(P(k_{\mathrm{m}}(t), q_{\mathrm{m}}(t))) = \alpha_{\mathrm{b}} \exp(-r_{\mathrm{b}} P(k_{\mathrm{m}}(t), q_{\mathrm{m}}(t))), \tag{82}$$

where $\alpha_{\mathrm{b}} > 0$ is the efficiency of the conversion of resources to reproduction and $r_{\mathrm{b}} > 0$ determines the rate at which reproductive costs decline with increasing productivity. The exponential decline reflects economies of scale, where organisms near peak capacity become more efficient through metabolic reallocation, achieving lower per-offspring costs paralleling how production costs decrease with scale in economics (e.g., Pontzer, 2015, section 1.2 in Tirole, 1988). The energy cost of survival is assumed to be

$$e(\mu_{\mathrm{m}}(t)) = \frac{\alpha_{\mu}}{\mu_{\mathrm{m}}(t) - \mu_0}, \tag{83}$$

where μ_0 represents the lower bound of mortality achievable when allocating infinite energy to survival (in the absence of external mortality), $\alpha_{\mu} > 0$ and $\zeta > 0$ are parameters for the energy conversion to survival. Finally, the energy cost of maintenance is taken to be

$$d(k_{\mathrm{m}}(t), z_{\mathrm{m}}(t)) = \alpha_{\mathrm{q}} [z_{\mathrm{m}}(t)]^{\kappa} k_{\mathrm{m}}(t), \tag{84}$$

where $\alpha_{\mathrm{q}} > 0$ determines the conversion of energy to quality, and $\kappa > 0$ is an exponents that govern the cost of investment in quality, which is assumed to scale with body size.

With these specifications, the life history model described by eqs. (40)–(49) is closed. Because the model is complicated, we did not further explore the analytical results and used the optimal control software GPOPS-II (Patterson and Rao, 2014) to explicitly solve the model numerically for the two energy budget scenarios described by eq. (12) and eq. (13). We verified that the numerical results, shown in Figs. **1** and **3**, satisfy the necessary conditions for the maximum principle, which by the same token allows to confirm the results of sections 4.2–4.3 (see Appendix section D for additional details on the consistency between numerical results and analytical findings). Next, we summarise the key findings from the numerical analysis illustrated in Figs. **1**–**3**.

4.4.1 Transfers lead to higher investment into somatic capital and energetic productivity

Comparing life history evolution under the two energy budget scenarios reveals that allowing for transfers leads to an overall energetically more productive life history, namely a higher $P^*_{\mathrm{T}} = \int_0^{\infty} l^*(t) P^*(t)\, \mathrm{d}t$. This energy productivity is achieved through an increased investment in early life growth. With transfers, juveniles sustain maximum growth rates, $g^*(t) = g_{\max}$, throughout an extended period (see Fig. **1** panels (a) and (b)). In contrast, without transfers, the growth period is significantly shorter and is restricted by juvenile production capacity, as juveniles must rely

only on the energy they can produce themselves. Thus, somatic capital $k^*(t)$ accumulates to a higher level in the case of transfers (Fig. **3** panel (b)). This yields substantial returns through the elevated lifetime energy production (Fig. **3** panels (b)-(d)). Furthermore, higher productivity creates a positive feedback loop: more resources can be allocated to maintain somatic quality and higher survival, which in turn sustains high productivity levels over an extended period of life (Fig. **3** panels (a) and (c)). Thus, transfers allow for running energy deficits early in life, while increasing somatic investments that generate compound returns through enhanced productivity later in life.

4.4.2 Transfers lead to continued growth after reproduction and a post-reproductive phase

The life course without transfers follows the typical two-phase life-history (see Fig. **2** panel (a)): (i) a juvenile growth phase $[0, t^*_{\mathrm{g}}]$, where growth occurs, somatic quality declines and mortality rate decreases, and (ii) an *adult reproductive phase* $[t^*_{\mathrm{b}}, \infty]$, where reproduction occurs and mortality rate starts to increase. We find that growth and reproduction are sequential ($t^*_{\mathrm{g}} = t^*_{\mathrm{b}}$) because the intratemporal budget constraint $T^*(t) = 0$ creates a direct trade-off between energy allocated to growth and reproduction. This is consistent with our analytical results because the Hamiltonian is linear in both control variables and thus selection favours bang-bang solutions. But we did not observe any singular arc for growth or reproduction across different parameter values in either budget-constraint scenario.

When transfers are allowed, four distinct life history phases are observed (see Fig. **2** panel (b)): (i) a *juvenile growth phase* $[0, t^*_{\mathrm{b}}]$, during which the individual grows and is a net energy consumer ($T^*(t) < 0$) and the quality does not degrade and the mortality rate decreases; (ii) a *transitional mixed growth and reproduction phase* $[t^*_{\mathrm{b}}, t^*_{\mathrm{g}}]$ during which individuals simultaneously grow and reproduce and reach peak energy deficit, with quality beginning to decline and mortality rate continues to decrease; (iii) an *adult reproductive phase* $[t^*_{\mathrm{g}}, t^*_{\mathrm{m}}]$ during which reproduction continues and individual becomes net energy producer ($T^*(t) > 0$), somatic quality continues to degrade, while mortality rate begins to increase; and (iv) an *adult post-reproductive producer phase* $[t^*_{\mathrm{m}}, t^*_{\mathrm{L}}]$ during which reproduction has ceased, but individuals keep on investing substantially to survival and maintenance, while majority of resources are transferred. The emergence of continued growth after reproduction is due to a much less restrictive assumption of the intertemporal balance condition ($\int_0^\infty l^*(t)T^*(t)\,\mathrm{d}t = 0$), which allows organisms to run large energy deficits when reproduction and growth overlap. The post-reproductive phase emerges because the decline in somatic quality raises the marginal cost of reproduction (recall eqs. (49) and (82)), leading to a transfer of resources to younger, more fitness enhancing individuals.

4.4.3 Transfers lead to longevity and increased investment in maintenance

Mortality rates exhibit U-shaped curves under both scenarios, with the lowest point occurring at the end of the growth phase, as expected from life history theory (compare Fig. **1** panels (a) and (c)). Consistent with eq. (35), mortality varies inversely with the value of life in both scenarios (compare Fig. **3** panel (f)). However, under intergenerational transfers, mortality rates are consistently lower throughout life compared to the no-transfer scenario (compare Fig. **1** panels (a) and (c)), because more resources are available under the transfer scenario and the value of life is higher under transfers even after reproduction ceases. Thus, intergenerational transfers facilitate significantly longer lifespans as organisms can allocate more energy to survival throughout life (Fig. **3** panel (a)). We observe

that the somatic quality degrades under both scenarios, but more slowly under the case of transfers (see Fig. **1** panels (a) and (c)). Since somatic capital is much higher and the cost of maintenance increases nonlinearly with somatic capital under the case of transfers, investing resources into somatic capital is substantially higher under the case of transfers (see Fig. **1** panels (b) and (d)).

4.4.4 Shadow value of energy

The magnitude $|\eta(t)|$ of the shadow value of energy decreases monotonically with age in both scenarios, indicating that energy investments in younger individuals yield the highest fitness returns (Fig. **3** panel (h)). The shadow value of the energy is particularly high at young ages in the no-transfer scenario due to severe resource constraints: young individuals have minimal somatic capital and must rely entirely on their limited self-produced energy, making any additional received energy yield substantial fitness gains. In contrast, with intergenerational transfers, the shadow value $\eta(t) = \eta_{\mathrm{T}} l^*(t)$ reflects the equilibrium value η_{T} of energy exchanges throughout the lineage, weighted by survival probability $l^*(t)$.

4.5 Robustness analysis of the worked-out example

We now assess the robustness of our main findings from section 4.4 through two complementary analyses. First, we examine whether our results hold under a more biologically realistic constraint on energy assimilation that scales with body size (section 4.5.1). Second, we explore how variation in key model parameters affects the qualitative and quantitative differences between transfer and non-transfer scenarios (section 4.5.2).

4.5.1 Age-dependent metabolic capacity on energy assimilation under transfers

For the scenario with intergenerational transfers, we imposed upper bounds $b(t) \leq b_{\max}$ and $g(t) \leq g_{\max}$ on reproduction and growth rates (and where $b_{\max}$ and $g_{\max}$ were taken to the the maximum values of $b(t)$ and $g(t)$ obtained in the scenario without transfers, e.g.,4.1). This entails that total assimilated energy $A(t)$ at age t is not constrained by age. A more biologically grounded assumption is that assimilation is constrained, taking, for instance, the form

$$A(t) \leq A_{\max}(k_{\mathrm{m}}(t), q_{\mathrm{m}}(t)) = a_{\max} k_{\mathrm{m}}(t)^c q_{\mathrm{m}}(t), \tag{85}$$

where $A_{\max}(k_{\mathrm{m}}(t), q_{\mathrm{m}}(t))$ is the maximal metabolic capacity at age t. Here, this capacity is assumed to scale with somatic quantity following Kleiber's law (West et al., 1997) as well as with somatic quality, such that $A_{\max}(t)$ has the same functional form as the production function $P(t)$ (recall eq. (81)). The parameter $a_{\max}$ is a metabolic capacity coefficient, and if $a_{\max} > a$ an individual can metabolise more energy than it produces, a necessary condition for intergenerational transfers to occur (when $a_{\max} = a$, one recovers exactly the case without transfers). While the metabolic constraint $A(t) \leq A_{\max}(k_{\mathrm{m}}(t), q_{\mathrm{m}}(t))$ is more biologically grounded, it complicates the formal analysis by introducing an additional inequality constraint to the life-history evolution problem (eq. (14)), which will have an associated shadow value $\eta_A(t)$, measuring the fitness benefit an organism would gain from increased metabolic capacity at age t (see Appendix C for details). When $\eta_A(t) > 0$ the organism is constrained by its metabolic

capacity and would benefit from being able to process energy faster. When $\eta_A(t) = 0$ the organism is assimilating below its metabolic limit.

In Figures **4**–**6**, we compare the results of endorsing the constratins eq. (85) under a tight metabolic constraint ($a_{\max} = 1.1$, allowing only 10% more assimilation than production since $a = 1$) and a more relaxed constraint ($a_{\max} = 1.3$, permitting 30% excess assimilation). Broadly, with this more realistic model, we recover our main findings: intergenerational transfers lead to longer growth phases, greater somatic capital accumulation, higher lifetime productivity, extended lifespans, and a post-reproductive phase. The key qualitative difference is the absence of a mixed growth-and-reproduction phase. This occurs because the metabolic constraint caps total energy assimilation at each age, preventing the large simultaneous investments in both growth and reproduction that characterise this phase in the baseline model for transfers (as presented in section 4.2), where growth and reproduction are capped separately and thus do not directly trade off with each other. Notably, $\eta_A(t) > 0$ throughout the growth phase, indicating that juveniles are operating at their metabolic limit and would benefit from higher metabolic capacity. Once growth ceases, $\eta_A(t)$ drops to zero, indicating that organisms no longer fully utilise their metabolic capacity. Thus, while we recover the main qualitative results from intergenerational transfers observed in the baseline model, the extent to which transfers alter life history outcomes relative to the case without transfers depends critically on the metabolic capacity coefficient $a_{\max}$.

4.5.2 Parameter variation analysis

To further assess the robustness of our numerical results in Figs. **1**–**3** and to explore their ecological relevance, we examine how key parameters affect life history evolution under both scenarios (see S.I. for detailed results). While an exhaustive parameter analysis is infeasible given the high dimensionality of the parameter space, we focus on biologically meaningful variations that illuminate the conditions under which transfers most strongly influence life history evolution. This analysis reveals the following results. First, ageing is not an inevitable outcome of natural selection in our version of the model of Kaplan and Robson (2009). When the cost of quality maintenance is reduced (from $\alpha_{\mathrm{q}} = 40$ to $\alpha_{\mathrm{q}} = 30$), mortality decreases early in life and then remains constant throughout the evolutionarily relevant lifespan (during the lifespan when natural selection can act, defined as the age range where survival probability remains high enough for natural selection to meaningfully shape trait evolution (i.e., where changes in age-specific traits can affect R_0; see Fig. **S4**, where we have shown results for $l^*(t) < 0.001$). We observe that for this parameter combination, the quantitative advantages of transfers largely disappear, with both transfer and non-transfer scenarios achieving nearly identical somatic capital accumulation, production levels, and lifespans. Second, increasing external mortality (from $m_{\mathrm{e}} = 0.01$ to $m_{\mathrm{e}} = 0.04$) produces shorter growth phases, earlier onset of reproduction, reduced somatic investment, and steeper declines in the shadow value of energy. Here we chose a dramatic increase in external mortality to better illustrate the classic result that external mortality drives "live fast, die young" strategies, when density-dependence acts on fecundity (e.g. Charlesworth, 1994; André and Rousset, 2020). Finally, a reduction in the baseline quality depreciation rate (from $\epsilon = 0.1$ to $\epsilon = 0.09$) delays the onset of somatic quality degradation, extends growth periods, and enhances the quantitative differences between transfer and non-transfer scenarios. Lower depreciation rates enable greater somatic capital accumulation and longer periods before quality decline becomes the dominant factor driving mortality increases.

5 Discussion

Applying optimal control theory, we derived necessary conditions for uninvadable life histories under two types of energy budget constraints: (i) no transfers between individuals and (ii) intergenerational transfers between individuals. Our main theoretical result is the (Pontryagin's) maximum principle for life history evolution that encompasses both budget-constraint scenarios and yields an age-specific selection gradient on genetic traits affecting vital rates, regardless of the mechanistic details of development (e.g., eq. (32)). Our contribution lies in unifying the two types of energy budget constraints within a single modelling framework. Previous applications of optimal control theory to life history theory have typically treated them separately with different underlying assumptions, often more restrictive, and have not explicitly compared their evolutionary implications. By enabling such comparisons, we can clarify how resource transfers shape life history evolution. We first discuss some general theoretical results that emerge from the maximum principle for life history evolution, and then discuss results from the worked-out example that explicitly contrast the two transfer scenarios.

5.1 Natural selection on life-histories

The maximum principle for life history evolution entails that the optimal (uninvadable) life history strategy has to maximise at each point in time the Hamiltonian function, which quantifies how age-specific trait expression affects current and future fitness gains including those through transfers (eq. (15)). While this qualitative feature is well established in evolutionary models without transfers (e.g., Perrin and Sibly, 1993; Day and Taylor, 2000), it is usually left implicit in models with transfers (e.g., Chu et al., 2008; Kaplan et al., 2009). We showed that the maximised Hamiltonian with and without transfers vanishes at all ages (eq. (25)). This yields that, at uninvadability, fitness gains $f_c^*(t)$ from current activities (reproduction, somatic investments and transfers) are exactly balanced by the loss of future fitness due to mortality ($\lambda_1(t)\mu^*(t)$). This ensures that no further fitness can be gained by reallocating resources among the different life history functions of reproduction, survival, somatic investments, and transfers. Although the vanishing maximised Hamiltonian is standard in autonomous optimal control problems with infinite horizon (e.g. Caputo, 2005, Theorem 14.9), we are not aware that it has been previously applied in the life history theory evolution literature.

The vanishing maximised Hamiltonian result yields an explicit expression for the uninvadabe mortality schedule ($\mu^*(t) = f_c^*(t)/\lambda_1(t)$), which is the ratio of current fitness gains $f_c^*(t)$ to future fitness gains– the value of life $\lambda_1(t)$ (eq. (27)). This result yields several relevant insights. First, mortality increases when current fitness gains rise relative to future fitness potential, revealing that the uninvadable mortality rate reflects a direct trade-off between present and future fitness gains. Second, senescence is not an inevitable outcome of selection on life history, since steady-state life-histories are plausible evolutionary outcomes (i.e., eq. (39)). Third, without transfers, we recover Fisher's (1930) prediction that mortality varies inversely with reproductive value. Fourth, transfers reduce mortality and thereby extend lifespan, all else being equal. Fifth, a post-reproductive period can emerge with transfers, but not without, all else being equal.

The maximum principle for life history evolution also provides insight into the marginal fitness value of receiving

energy transfers. For the case without transfers, our analysis quantifies the shadow value of energy $\eta(t)$, the fitness benefit of transferring a unit energy at age t, which is a marginal value typically absent from classical life history models (León, 1976; Stearns, 1992; Perrin and Sibly, 1993; Cichoń and Kozłowski, 2000). Without transfers, $\eta(t)$ is strongly negative throughout life, with the largest magnitude at birth, declining with age. This reveals that juveniles would benefit most from additional energy, providing a conceptual explanation for why young organisms across taxa have evolved powerful resource extraction mechanisms, from begging displays in birds to manipulation tactics in mammals (Clutton-Brock, 1991; Hrdy, 2009). Juveniles are expected to be net energy consumers because somatic investment early in life yields high future fitness returns, while older individuals can become post-reproductive producers because their accumulated somatic capital enables efficient resource acquisition even as reproductive efficiency declines. Together, these results establish that the marginal value of receiving energy is highest in juveniles, explaining formally the widespread pattern of resource flows from older to younger individuals across taxa with parental care and intergenerational transfers.

5.2 Life history with and without transfers: implications from the example

As an application, we extended the seminal baseline model of Kaplan et al. (2009) to cover the case without transfers in order to be able to explicitly compare evolutionary outcomes under the two energy budget constraints. The model is involved, and so the analytical analysis (section 4.2–4.3) needs to be complemented by a numerical one (section 4.4). This enabled us to explicitly solve the model for all control and state variables under both scenarios with and without transfers, thereby highlighting qualitatively and quantitatively the role of transfers in life history evolution.

In the absence of transfers, the uninvadable life history consists of two phases: juvenile growth and adult reproduction, throughout which energy production equals consumption ($P^*(t) = A^*(t)$), constraining individuals to energetic self-sufficiency (Fig. **2**, panel (a)). This is qualitatively in line with standard results (e.g., Perrin and Sibly, 1993). In contrast, transfers, $T^*(t) = P^*(t) - A^*(t) \neq 0$, cause a temporal decoupling of resource production $P^*(t)$ and assimilation $A^*(t)$ (Fig. **2**) that enable four distinct phases, defined by both the life history phases and net energy status (Fig. **2**, panel (b)): (i) juvenile dependency, where individuals are net consumers ($T^*(t) < 0$) and invest maximally in growth; (ii) mixed growth and reproduction, where peak consumption occurs while individuals remain net consumers ($T^*(t) < 0$); (iii) reproductive production, where individuals become net producers ($T^*(t) > 0$), transferring surplus energy to repay earlier deficits; and (iv) post-reproductive production, where reproduction ceases but substantial energy production and transfers continue ($T^*(t) > 0$).

The decoupling of consumption from production enables significantly higher lifetime energy productivity, as early-life energy deficits facilitate the accelerated accumulation of somatic capital. This generates compound returns through an elevated productivity rate and allows for longer lifetimes by making more resources available for maintenance and survival. Post-reproductive production emerges as older individuals are less efficient at reproduction due to somatic quality declines, and thus transferring resources to younger adults yields higher fitness returns. Kaplan and Robson (2009) already demonstrated that intergenerational transfers can lead to a post-reproductive lifespan, thereby reducing mortality rate later in life by increasing the value of life. Our contribution here lies in explicitly comparing life history evolution with and without transfers, and thus we are able to explicitly show that intergenerational transfers trigger a cascade of life history changes, producing a unique combination of metabolically

costly future-oriented investments (high somatic investment, extended growth period, and increased investment in survival and maintenance) along with high investment in reproduction during midlife and the emergence of a postreproductive period and long lifespan (see also table 3 for details). In Table 3, we summarise results from the parameter variation analysis. Most notably, from that analysis, we observe that when the somatic maintenance cost is low enough, senescence becomes negligible under both scenarios of budget constraints (see S.I. for further details).

The results of the baseline model prove robust to alternative assumptions about physiological constraints on energy processing. When we replace fixed upper bounds on growth and reproduction with a more realistic age-dependent metabolic capacity constraint following Kleiber's law (Section 4.5.1 and Appendix C), the core findings persist. Namely, intergenerational transfers lead to longer growth phases, greater somatic capital accumulation, higher lifetime productivity, extended lifespans, and post-reproductive survival. The key qualitative difference is the absence of a mixed growth-and-reproduction phase, which is arguably more realistic. This occurs because the metabolic constraint caps total energy assimilation at each age, preventing the large simultaneous investments that characterise this phase when growth and reproduction are bounded separately. This analysis also reveals that growing organisms operate at their maximal physiological capacity and would benefit from increasing their metabolic capacity. This finding is consistent with the high metabolic rates observed in juveniles across taxa (Glazier, 2005; Hou et al., 2008). Once growth ceases, organisms no longer fully utilise their metabolic capacity (assimilation is lower than the maximal metabolic capacity).

The life history differences identified through comparing the two scenarios of budget constraints mirror the distinctive human life-history features among great apes, demonstrating how transfers enable enhanced somatic capital, prolonged development, and extended post-reproductive lifespan as observed in humans (e.g. Mace, 2000; Robson et al., 2006; van Schaik, 2016; Gurven, 2024). More precisely, the patterns that emerge when allowing for intergenerational transfers to occur in the worked-out example align with convergent empirical evidence from paleontological, ethnographic, and comparative physiological studies of human life history. First, in subsistence societies, individuals consume more than they produce until their late teens (Kaplan, 1994; Gurven et al., 2006), while older individuals produce surpluses that they transfer to younger individuals (Lee, 2020), aligning with our age-specific transfer predictions. Second, humans evolved substantially higher metabolic rates and energy expenditure than great apes (Pontzer et al., 2016; Yegian et al., 2024), consistent with the prediction of our model of enhanced lifetime energy production under transfers. Third, dietary changes and intergenerational transfers appear to have co-evolved in a mutually reinforcing manner (Wrangham, 2009; Wood and Gilby, 2017). More broadly, our result aligns with embodied capital theory, demonstrating that intergenerational transfers and somatic investment operate as mutually reinforcing mechanisms rather than independent adaptations (e.g. Kaplan et al., 2001, see also Davison and Gurven, 2022 for further empirical support using ethnographic production-consumption data). Post-reproductive survival emerges here under the transfer scenario (as well as in Kaplan and Robson, 2009) as an optimal life-history outcome when transferring resources to younger, more reproductively efficient individuals yields higher fitness returns than continued reproduction. We show that this outcome obtains only when transfers are allowed. This result formalises a key mechanism that can drive the so-called grandmother hypothesis (Hawkes et al., 1998), and is likely extends beyond humans to other taxa with extensive intergenerational transfers and

post-reproductive life, such as toothed whales (Ellis et al., 2024).

5.3 Limitations and conclusion

Our model relies on the simplifying assumption of clonal interactions. While clonal interactions are usually assumed in the literature on intergenerational transfer and life history evolution (León, 1976; Schaffer, 1983; Perrin and Sibly, 1993; Cichoń and Kozłowski, 2000; Lee, 2003; Chu et al., 2008; Kaplan and Robson, 2009; Metz et al., 2016; Avila et al., 2021; Avila and Lehmann, 2023), as well as adaptive dynamics more generally (e.g., Geritz et al., 1998), that assumption does not affect the location of evolutionary equilibria by invasion analyis when gene action is additive and thus applies under sexual reproduction (Mullon and Lehmann, 2017). Our assumptions, however, overlook the additional costs of resource transfer when genetic relatedness between individuals falls below unity, which inevitably occurs under sexual reproduction, where donors and recipients are not clones. Conceptually, we anticipate that introducing sexual reproduction into our model would diminish the magnitude of transfers, but not alter our qualitative results. The effects of transfers under sexual reproduction in the population in the absence of a market for energy transfer would likely fall between the two extremes presented here: the no-transfer scenario and the clonal transfer scenario. However, if a market for resource exchange exists, then our results for the transfer scenario extend beyond the assumption of interactions occurring among fully related individuals. This is so because any Pareto-efficient allocation can be implemented through a competitive market mechanism (see e.g., Mas-Colell et al., 1995). Since the uninvadable life history derived here under the assumption of clonal interactions is Pareto efficient, a well-functioning resource transfer market can, in principle, allow to sustain the same intergenerational transfer schedule without requiring clonal interactions. Our model thus characterises transfers in the absence of transaction costs (e.g., bargaining or information costs), representing an upper bound on what markets can achieve for enhanced somatic capital and survival.

A relevant extension of our model would be to incorporate sex-specific differences in life-history traits and resource transfer patterns, which are also fundamental to human evolution. Evidence from modern horticultural and hunter-gatherer societies reveals a striking sexual division in resource production and allocation, with men typically producing significantly more caloric resources, while women focus primarily on childcare and the provision of offspring (Kaplan et al., 2010; Gurven et al., 2012). Thus, the outcomes of sex-specific differences in the division of labour (e.g., Gavrilets, 2012; Loo et al., 2020; Alger et al., 2020, 2023) on life-history evolution could be explored.

In conclusion, we derived a maximum principle for life-history evolution that unifies intratemporal budget balance (without transfers) and intertemporal budget balance (with transfers) within a single life history model. The uninvadable mortality schedule result provides a foundation for understanding how intergenerational transfers can lead to longer lifespans and post-reproductive lifespan. Application to human life history illustrates how these predictions can account for increased somatic capital, prolonged development, and an extended lifespan with a postreproductive phase.

Appendix

Appendix A: The maximum principle for life history evolution

To prove the maximum principle stated in the main text, we prove the case with and without transfer separately, and then bring together their common structure.

A.1 Maximum principle with transfers

To prove the maximum principle with transfers, let us rewrite the basic reproductive number eq. (2) subject to its dynamics constraints in the form

$$R(\mathbf{u}_{\mathrm{m}}, \mathbf{u}_{\mathrm{r}}) = \int_0^{\infty} f\left(\mathbf{u}_{\mathrm{m}}(t), \mathbf{z}_{\mathrm{m}}(t), \mathbf{u}_{\mathrm{r}}\right) \mathrm{d}t, \tag{A.1}$$

where $f\left(\mathbf{u}_{\mathrm{m}}(t), \mathbf{z}_{\mathrm{m}}(t), \mathbf{u}_{\mathrm{r}}\right) = l_{\mathrm{m}}(t) b\left(\mathbf{u}_{\mathrm{m}}(t), \mathbf{x}_{\mathrm{m}}(t), \mathbf{u}_{\mathrm{r}}\right)$ and $\mathbf{z}_{\mathrm{m}}(t) = \left(l_{\mathrm{m}}(t), \mathbf{x}_{\mathrm{m}}(t), k_{\mathrm{m}}(t)\right)$ is a vector of state variables satisfying

$$\frac{\mathrm{d}l_{\mathrm{m}}(t)}{\mathrm{d}t} = -\mu\left(\mathbf{u}_{\mathrm{m}}(t), \mathbf{x}_{\mathrm{m}}(t), \mathbf{u}_{\mathrm{r}}\right) l_{\mathrm{m}}(t) \quad \text{with i.c.} \quad l_{\mathrm{m}}(0) = 1. \tag{A.2}$$

$$\frac{\mathrm{d}\mathbf{x}_{\mathrm{m}}(t)}{\mathrm{d}t} = \boldsymbol{g}(\mathbf{u}_{\mathrm{m}}(t), \mathbf{x}_{\mathrm{m}}(t), \mathbf{u}_{\mathrm{r}}) \quad \text{with i.c.} \quad \mathbf{x}_{\mathrm{m}}(0) = \mathbf{x}_0 \tag{A.3}$$

$$\frac{\mathrm{d}k_{\mathrm{m}}(t)}{\mathrm{d}t} = l_{\mathrm{m}}(t) T(\mathbf{u}_{\mathrm{m}}(t), \mathbf{x}_{\mathrm{m}}(t), \mathbf{u}_{\mathrm{r}}) \quad \text{with i.c. } k_{\mathrm{m}}(0) = 0 \text{ and f.c. } \lim_{t\to\infty} k_{\mathrm{m}}(t) = 0. \tag{A.4}$$

To obtain eq. (A.1) we have introduced a new state variable $k_{\mathrm{m}}(t)$ that expresses the integral constraints eq. (13) as a differential equation and have made explicit through the function f that the objective function R may potentially depend directly on all state variables, although in our specific problem it depends only on the state variable $\mathbf{y}_{\mathrm{m}}(t) = \left(l_{\mathrm{m}}(t), \mathbf{x}_{\mathrm{m}}(t)\right)$, and not on $k_{\mathrm{m}}(t)$. In our application $k_{\mathrm{m}}(t)$ can be interpreted as the cumulative expected transfer until age t, since eq. (A.4) entails that $k_{\mathrm{m}}(t) = \int_0^t l_{\mathrm{m}}(\tau) T(\mathbf{u}_{\mathrm{m}}(\tau), \mathbf{x}_{\mathrm{m}}(\tau), \mathbf{u}_{\mathrm{r}})\, \mathrm{d}\tau$.

Holding $\mathbf{u}_{\mathrm{r}}$ fixed, the maximisation of eq. (A.1) with respect to the variable $\mathbf{u}_{\mathrm{m}}$ varying in $\boldsymbol{\mathcal{U}}[\mathcal{T},\mathcal{U}]$ and subject to the dynamics constraints eqs. (A.2)–(A.4) defines an infinite horizon optimal control problem with $n_{\mathrm{x}}+1$ free state variables and one asymptotically fixed state variable (e.g., problem 1 described in Sydsaeter et al., 2008, section 10.3, p. 370 and problem 1 described in Caputo, 2005, section 14 in the absence of path constraints). For such an optimal control problem with standard end constraints, it is well established that the Pontryagin maximum principle holds (e.g., Sydsaeter et al., 2008, Theorem 10.1.1 and Caputo, 2005, Theorem 14.3). In particular, suppose the schedule $\mathbf{u}^*$ is optimal with associated state path $\{\mathbf{z}^*(t)\}_{t\in\mathcal{T}} = \{(\mathbf{y}^*(t), k^*(t))\}_{t\in\mathcal{T}}$, where $\mathbf{y}^*(t) = (l^*(t), \mathbf{x}^*(t))$, and that this holds for the resident population state $\mathbf{u}_{\mathrm{r}}$ itself held at this schedule $\mathbf{u}_{\mathrm{r}} = \mathbf{u}^*$. Then, in force of Caputo (2005, Theorem 14.3), it is necessary that the control function $\mathbf{u}^*$ satisfies for all $t \in \mathcal{T}$

$$\mathbf{u}^*(t) \in \arg\max_{\mathbf{u}_{\mathrm{m}}(t)\in U} H(\mathbf{u}_{\mathrm{m}}(t), \mathbf{z}^*(t), \boldsymbol{\lambda}(t), \mathbf{u}^*), \tag{A.5}$$

where

$$H(\mathbf{u}_{\mathrm{m}}(t),\mathbf{z}(t),\tilde{\boldsymbol{\lambda}}(t),\mathbf{u}_{\mathrm{r}}) = l_{\mathrm{m}}(t)\Big[b\left(\mathbf{u}_{\mathrm{m}}(t),\mathbf{x}_{\mathrm{m}}(t),\mathbf{u}_{\mathrm{r}}\right) - \lambda_{\mathrm{l}}(t)\mu\left(\mathbf{u}_{\mathrm{m}}(t),\mathbf{x}_{\mathrm{m}}(t),\mathbf{u}_{\mathrm{r}}\right) + \lambda_{\eta}(t)\,T(\mathbf{u}_{\mathrm{m}}(t),\mathbf{x}_{\mathrm{m}}(t),\mathbf{u}_{\mathrm{r}})\Big] + \boldsymbol{\lambda}_{\mathrm{x}}(t)\cdot\boldsymbol{g}(\mathbf{u}_{\mathrm{m}}(t),\mathbf{x}_{\mathrm{m}}(t),\mathbf{u}_{\mathrm{r}})\,, \quad \text{(A.6)}$$

with $\tilde{\boldsymbol{\lambda}}(t) = (\lambda_{\mathrm{l}}(t), \boldsymbol{\lambda}_{\mathrm{x}}(t), \lambda_{\eta}(t))$ being a vector of costates variables corresponding to the state variables $l_{\mathrm{m}}(t)$, $\mathbf{x}_{\mathrm{m}}(t)$, and $k_{\mathrm{m}}(t)$, respectively. Except at points of discontinuities, the costates satisfy

$$-\frac{\mathrm{d}\lambda_{\mathrm{l}}(t)}{\mathrm{d}t} = \frac{\partial H(\mathbf{u}^*(t),\mathbf{z}(t),\tilde{\boldsymbol{\lambda}}(t),\mathbf{u}^*)}{\partial l_{\mathrm{m}}(t)}\Big|_* \quad \text{(A.7)}$$

$$-\frac{\mathrm{d}\boldsymbol{\lambda}_{\mathrm{x}}(t)}{\mathrm{d}t} = \frac{\partial H(\mathbf{u}^*(t),\mathbf{z}(t),\tilde{\boldsymbol{\lambda}}(t),\mathbf{u}^*)}{\partial \mathbf{x}_{\mathrm{m}}(t)}\Big|_* \quad \text{(A.8)}$$

$$-\frac{\mathrm{d}\lambda_{\eta}(t)}{\mathrm{d}t} = \frac{\partial H(\mathbf{u}^*(t),\mathbf{z}(t),\tilde{\boldsymbol{\lambda}}(t),\mathbf{u}^*)}{\partial k_{\mathrm{m}}(t)}\Big|_* = 0 \quad \text{(A.9)}$$

and the state variables satisfy

$$\frac{\mathrm{d}l^*(t)}{\mathrm{d}t} = \frac{\partial H(\mathbf{u}^*(t),\mathbf{z}^*(t),\tilde{\boldsymbol{\lambda}}(t),\mathbf{u}^*)}{\partial \lambda_{\mathrm{l}}(t)} \text{ with i.c. } l^*(0) = 1 \quad \text{(A.10)}$$

$$\frac{\mathrm{d}\mathbf{x}^*(t)}{\mathrm{d}t} = \frac{\partial H(\mathbf{u}^*(t),\mathbf{z}^*(t),\tilde{\boldsymbol{\lambda}}(t),\mathbf{u}^*)}{\partial \boldsymbol{\lambda}_{\mathrm{x}}(t)} \text{ with i.c. } \mathbf{x}^*(0) = \mathbf{x}_0 \quad \text{(A.11)}$$

$$\frac{\mathrm{d}k^*(t)}{\mathrm{d}t} = \frac{\partial H(\mathbf{u}^*(t),\mathbf{z}^*(t),\tilde{\boldsymbol{\lambda}}(t),\mathbf{u}^*)}{\partial \lambda_{\eta}(t)} \text{ with i.c. } k_{\mathrm{m}}(0) = 0 \text{ and f.c. } \lim_{t\to\infty} k_{\mathrm{m}}(t) = 0. \quad \text{(A.12)}$$

Eqs. (A.5)–(A.12) are standard necessary conditions for the maximum principle (e.g., Sydsaeter et al., 2008, section 10.3 and Caputo, 2005, section 14), but we need to note one specific clarification about this application to our modelling context. In our biological setting, the maximum principle provides a necessary condition for uninvadability, i.e. for $\mathbf{u}^*$ to solve $\max_{\mathbf{u}\in\boldsymbol{\mathcal{U}}[\mathcal{T},\mathcal{U}]} R(\mathbf{u},\mathbf{u}^*)$ so that $\mathbf{u}^*$ specifies a best reply to self.

Now, since $-\,\mathrm{d}\lambda_{\eta}(t)/\,\mathrm{d}t = 0$, we can set $\lambda_{\eta}(t) = \eta_{\mathrm{T}}$, a constant and the dynamics constraint eq. (A.12) can be expressed upon integration as

$$0 = \int_0^{\infty} l^*(t)T(\mathbf{u}^*(t),\mathbf{x}^*(t),\mathbf{u}^*)\,\mathrm{d}t. \quad \text{(A.13)}$$

With this and writing the Hamiltonian directly as $H(\mathbf{u}_{\mathrm{m}}(t),\mathbf{z}_{\mathrm{m}}(t),\tilde{\boldsymbol{\lambda}}(t),\mathbf{u}_{\mathrm{r}}) = H(\mathbf{u}_{\mathrm{m}}(t),\mathbf{y}_{\mathrm{m}}(t),\tilde{\boldsymbol{\lambda}}(t),\mathbf{u}_{\mathrm{r}})$ because the right-hand side of eq. (A.6) does not depend explicitly on the variable $k_{\mathrm{m}}(t)$, the maximum principle defined by eq. (A.5)—(A.12) can be expressed as in the main text by way of eqs. (15)–(25) for the case with transfers.

Costate interpretation. In order to have an interpretation for each costate variable in the vector $\tilde{\boldsymbol{\lambda}}(t) = (\lambda_{\mathrm{l}}(t), \boldsymbol{\lambda}_{\mathrm{x}}(t), \lambda_{\eta}(t))$, let us introduce

$$V^*(\mathbf{z}^*(t)) = \int_t^{\infty} f\left(\mathbf{u}^*(\tau),\mathbf{z}^*(\tau),\mathbf{u}^*\right)\mathrm{d}\tau. \quad \text{(A.14)}$$

This is the so-called value function at age t; namely, the expected remaining fitness on the uninvadable path of an individual of age t in state $\mathbf{z}^*(t)$, whereby $V^*(\mathbf{z}^*(0)) = R(\mathbf{u}^*,\mathbf{u}^*)$. This value function depends on time only through

the value of the state variable, since the optimisation problem is autonomous (i.e., f does not depend directly on time). Then, the shadow values of the state variables are the marginal changes of the remaining fitness $V^*(\mathbf{z}^*(t))$ with respect to change in the corresponding state variable of the vector $\mathbf{z}(t) = (l_{\mathrm{m}}(t), \mathbf{x}_{\mathrm{m}}(t), k_{\mathrm{m}}(t))$:

$$\tilde{\boldsymbol{\lambda}}(t) = \nabla_{\mathbf{z}^*(t)} V^*(\mathbf{z}^*(t)), \tag{A.15}$$

where $\nabla_{\mathbf{z}}$ denotes the gradient with respect to $\mathbf{z}$ (e.g. Dorfman, 1969; Caputo, 2005; Sydsaeter et al., 2008). Hence, the interpretation of $\lambda_\eta(t) = \partial V^*(\mathbf{z}^*(t))/\partial k^*(t)$ is as the marginal change of expected fitness from t onwards with respect to the cumulative expected transfer until t (recall eq. (A.4)).

A.2 Maximum principle without transfers

For the case without transfers, eqs. (A.1)–(A.3) still apply but with $\mathbf{z}_{\mathrm{m}}(t) = \mathbf{y}_{\mathrm{m}}(t) = (l_{\mathrm{m}}(t), \mathbf{x}_{\mathrm{m}}(t))$ because the variable $k_{\mathrm{m}}(t)$ no longer appears in the constraints (eq. 11). The maximisation of eq. (A.1) with respect to the variable $\mathbf{u}_{\mathrm{m}}$ varying in $\boldsymbol{\mathcal{U}}[\mathcal{T},\mathcal{U}]$ subject to the dynamic constraints eqs. (A.2)–(A.3) defines an infinite horizon optimal control problem with n_{x} free state variables and mixed equality constraints (e.g., problem 1 described in Caputo, 2005, section 14 with mixed path constraints). For such an optimal control problem, it is again well established that the Pontryagin maximum principle holds (e.g., Caputo, 2005, Theorem 14.3). Then, in force of Caputo (2005, Theorem 14.3) and recalling that the constraints for this model (eq. 11) entail that the control variable $\mathbf{u}(t)$ at time t is restricted to the feasible set $\Omega(\mathbf{x}(t), \mathbf{u}_{\mathrm{r}}) = \{\mathbf{u}(t) \in \mathcal{U} : T(\mathbf{u}(t), \mathbf{x}(t), \mathbf{u}_{\mathrm{r}}) = 0\}$ (recall eq. (17)), it is necessary that the control function $\mathbf{u}^*$ satisfies for all $t \in \mathcal{T}$

$$\mathbf{u}^*(t) \in \arg \max_{\mathbf{u}_{\mathrm{m}}(t) \in \Omega(\mathbf{y}^*(t), \mathbf{u}^*)} H(\mathbf{u}_{\mathrm{m}}(t), \mathbf{y}^*(t), \tilde{\boldsymbol{\lambda}}(t), \mathbf{u}^*). \tag{A.16}$$

Here,

$$H(\mathbf{u}_{\mathrm{m}}(t), \mathbf{y}_{\mathrm{m}}(t), \tilde{\boldsymbol{\lambda}}(t), \mathbf{u}_{\mathrm{r}}) = l_{\mathrm{m}}(t) \Big[b\left(\mathbf{u}_{\mathrm{m}}(t), \mathbf{x}_{\mathrm{m}}(t), \mathbf{u}_{\mathrm{r}}\right) - \lambda_{\mathrm{l}}(t) \mu\left(\mathbf{u}_{\mathrm{m}}(t), \mathbf{x}_{\mathrm{m}}(t), \mathbf{u}_{\mathrm{r}}\right) \Big] + \boldsymbol{\lambda}_{\mathrm{x}}(t) \cdot \boldsymbol{g}(\mathbf{u}_{\mathrm{m}}(t), \mathbf{x}_{\mathrm{m}}(t), \mathbf{u}_{\mathrm{r}}) + \eta_{\mathrm{C}}(t)\, T(\mathbf{u}_{\mathrm{m}}(t), \mathbf{x}_{\mathrm{m}}(t), \mathbf{u}_{\mathrm{r}}), \tag{A.17}$$

where $\tilde{\boldsymbol{\lambda}}(t) = (\lambda_{\mathrm{l}}(t), \boldsymbol{\lambda}_{\mathrm{x}}(t), \eta_{\mathrm{C}}(t))$ now stands for a vector of costate variables, of the states variables $l_{\mathrm{m}}(t)$, and $\mathbf{x}_{\mathrm{m}}(t)$, and of a Lagrange multiplier $\eta_{\mathrm{C}}(t)$, where the latter is associated to the equality constraint $T(\mathbf{u}_{\mathrm{m}}(t), \mathbf{x}_{\mathrm{m}}(t), \mathbf{u}_{\mathrm{r}}) = 0$. Except at points of discontinuities, the costates satisfy

$$-\frac{\mathrm{d}\lambda_{\mathrm{l}}(t)}{\mathrm{d}t} = \frac{\partial H(\mathbf{u}^*(t), \mathbf{y}_{\mathrm{m}}(t), \tilde{\boldsymbol{\lambda}}(t), \mathbf{u}^*)}{\partial l_{\mathrm{m}}(t)}\Big|_* \tag{A.18}$$

$$-\frac{\mathrm{d}\boldsymbol{\lambda}_{\mathrm{x}}(t)}{\mathrm{d}t} = \frac{\partial H(\mathbf{u}^*(t), \mathbf{y}_{\mathrm{m}}(t), \tilde{\boldsymbol{\lambda}}(t), \mathbf{u}^*)}{\partial \mathbf{x}_{\mathrm{m}}(t)}\Big|_*, \tag{A.19}$$

the state variables satisfy

$$\frac{\mathrm{d}l^*(t)}{\mathrm{d}t} = \frac{\partial H(\mathbf{u}^*(t), \mathbf{y}^*(t), \tilde{\boldsymbol{\lambda}}(t), \mathbf{u}^*)}{\partial \lambda_{\mathrm{l}}(t)} \text{ with i.c. } l^*(0) = 1 \tag{A.20}$$

$$\frac{\mathrm{d}\mathbf{x}^*(t)}{\mathrm{d}t} = \frac{\partial H(\mathbf{u}^*(t), \mathbf{y}^*(t), \tilde{\boldsymbol{\lambda}}(t), \mathbf{u}^*)}{\partial \boldsymbol{\lambda}_{\mathrm{x}}(t)} \text{ with i.c. } \mathbf{x}^*(0) = \mathbf{x}_0, \tag{A.21}$$

and the Lagrange multiplier satisfies for all t

$$\frac{\partial H(\mathbf{u}^*(t), \mathbf{y}^*(t), \tilde{\boldsymbol{\lambda}}(t), \mathbf{u}^*)}{\partial \eta_{\mathrm{C}}(t)} = T(\mathbf{u}^*(t), \mathbf{y}^*(t), \mathbf{u}^*) = 0. \tag{A.22}$$

Eqs. (A.16)–(A.22) are the standard necessary conditions for the maximum principle under mixed-path equality constraints, but we need to note two specific clarifications about this application to our model context. First, and as already noted in section A.1, the maximum principle provides a necessary condition for uninvadability, i.e. for $\mathbf{u}^*$ to solve $\max_{\mathbf{u}\in\boldsymbol{\mathcal{U}}[\mathcal{T},\mathcal{U}]} R(\mathbf{u}, \mathbf{u}^*)$ so that $\mathbf{u}^*$ specifies a best reply to self. Second, technically equation eq. (A.17) represents an extended Hamiltonian (or Lagrangian), which incorporates the constraint $T(\mathbf{u}_{\mathrm{m}}(t), \mathbf{x}_{\mathrm{m}}(t), \mathbf{u}_{\mathrm{r}}) = 0$ via the Lagrange multiplier $\eta_{\mathrm{C}}(t)$. Specifically, the extended Hamiltonian equals the regular Hamiltonian, which is the first line of eq. (A.17), plus $\eta_C(t) \times T(\mathbf{u}_{\mathrm{m}}(t), \mathbf{x}_{\mathrm{m}}(t), \mathbf{u}_{\mathrm{r}})$ (e.g., Caputo, 2005, Theorem 14.3). However, since the constraint is $T(\mathbf{u}_{\mathrm{m}}(t), \mathbf{x}_{\mathrm{m}}(t), \mathbf{u}_{\mathrm{r}}) = 0$ for all time, then this additional term consists of adding a zero term to the regular Hamiltonian. Therefore, the extended Hamiltonian reduces to the regular Hamiltonian. With this in mind, the maximum principle defined by eqs. (A.16)–(A.22) for the case of transfers can be expressed as in the main text by way of eqs. (15)–(25).

Lagrange multiplier interpretation. Since both $\lambda_{\mathrm{l}}(t)$ and $\boldsymbol{\lambda}_{\mathrm{x}}(t)$ in $\tilde{\boldsymbol{\lambda}}(t) = (\lambda_{\mathrm{l}}(t), \boldsymbol{\lambda}_{\mathrm{x}}(t), \eta_{\mathrm{C}}(t))$ are shadow values, they take their interpretation from eq. (A.15). We now provide an interpretation for the Lagrange multiplier $\eta_{\mathrm{C}}(t)$, which, it turns out, can be regarded as the marginal effect

$$\eta_{\mathrm{C}}(t) = \frac{\partial V^*(\mathbf{z}^*(t))}{\partial \epsilon(t)} \tag{A.23}$$

on the value function of releasing the budget constraints at time t; namely, obtaining some posititve transfer $\epsilon(t)$ at time t. To obtain this interpretation, we treat the deviation $\epsilon(t)$ as a parameter of the Hamiltonian (A.17) and proceed in three steps. First, according to the dynamic envelope theorem (Caputo, 2005, Theorem 14.10), we have that

$$\frac{\partial V^*(0, \mathbf{z}_0)}{\partial \epsilon(t)} = \int_0^\infty \frac{\partial H(\mathbf{u}^*(\tau), \mathbf{y}^*(\tau), \tilde{\boldsymbol{\lambda}}(\tau), \mathbf{u}^*)}{\partial \epsilon(t)} \, \mathrm{d}\tau, \tag{A.24}$$

where $\mathbf{z}_0 = (1, \mathbf{x}_0)$ is the initial condition for the state variables. Second, we clarify that $\epsilon(t)$ affects the Hamiltonian (A.17) by relaxing the budget constraint only at time t by setting

$$T(\mathbf{u}_{\mathrm{m}}(\tau), \mathbf{y}_{\mathrm{m}}(\tau), \mathbf{e}_{\mathrm{r}}(\tau)) = \begin{cases} \epsilon(t) & \text{if } \tau = t \\ 0 & \text{if } \tau \neq t. \end{cases} \tag{A.25}$$

This can be written more formally using the Dirac delta function

$$T(\mathbf{u}_{\mathrm{m}}(\tau), \mathbf{y}_{\mathrm{m}}(\tau), \mathbf{e}_{\mathrm{r}}(\tau)) = \epsilon(t)\delta(\tau - t). \tag{A.26}$$

Then, substituting into eq. (A.17) and eq. (A.24), we have

$$\begin{aligned} \frac{\partial V^*(\mathbf{z}_0)}{\partial \epsilon(t)} &= \int_0^\infty \frac{\partial H(\mathbf{u}^*(\tau), \mathbf{y}^*(\tau), \tilde{\boldsymbol{\lambda}}(\tau), \mathbf{u}^*)}{\partial \epsilon(t)} \,\mathrm{d}\tau \\ = \int_0^\infty \eta_C(\tau) \frac{\partial}{\partial \epsilon(t)} [\epsilon(t)\delta(\tau - t)] \,\mathrm{d}\tau &= \int_0^\infty \eta_C(\tau)\delta(\tau - t) \,\mathrm{d}\tau = \eta_C(t) \end{aligned} \tag{A.27}$$

Third, we note that owing to the optimality principle and because the integral is additive, we can decompose the value function, eq. (A.14), as

$$V^*(\mathbf{z}_0) = \int_0^t f\left(\mathbf{u}^*(\tau), \mathbf{z}^*(\tau), \mathbf{u}^*\right) \mathrm{d}\tau + V^*(\mathbf{z}^*(t)). \tag{A.28}$$

Because the first term on the right-hand side is unaffected by a perturbation $\eta_C(t)$ occurring at time t, since $\epsilon(t)$ can only change reproduction and survival from time t onwards, we also have that

$$\frac{\partial V^*(\mathbf{z}_0)}{\partial \epsilon(t)} = \frac{\partial V^*(\mathbf{z}^*(t))}{\partial \epsilon(t)}. \tag{A.29}$$

Eq. (A.29) together with (A.27) yields eq. (A.23) and thus we have derived the interpretation of the Lagrange multiplier $\eta_C(t)$.

A.3 Vanishing Hamiltonian

Let us now show that the maximized Hamiltonian function is nil for all $t \in \mathcal{T}$:

$$\mathcal{H}(\mathbf{u}^*(t), \mathbf{y}^*(t), \boldsymbol{\lambda}(t), \mathbf{u}^*) = \max_{\mathbf{u}_{\mathrm{m}}(t) \in \Omega(t)} H(\mathbf{u}_{\mathrm{m}}(t), \mathbf{y}^*(t), \boldsymbol{\lambda}(t), \mathbf{u}^*) = 0. \tag{A.30}$$

This is a standard infinite horizon optimal control theory result (Michel, 1982), which also holds for the case of equality constraints–thus covering the case without transfers–since then only a zero is added to the Hamiltonian. We here provide a heuristic proof of this result using the argument of Caputo (2005, Theorem 14.8); why the proof is heuristic is explained after the proof.

Let us then use again the value function and write it as

$$V^*(\mathbf{z}^*(\tau)) = \int_\tau^\infty f\left(\mathbf{u}^*(t), \mathbf{z}^*(t), \mathbf{u}^*\right) \mathrm{d}t = \max_{\mathbf{u}_{\mathrm{m}} \in \boldsymbol{\mathcal{U}}[\mathcal{T}, \mathcal{U}]} \int_\tau^\infty f\left(\mathbf{u}_{\mathrm{m}}(t), \mathbf{z}_{\mathrm{m}}(t), \mathbf{u}^*\right) \mathrm{d}t, \tag{A.31}$$

where the maximization problem over the whole schedule on the right-hand side is subject to the dynamical constraints

$$\frac{\mathrm{d}\mathbf{z}_{\mathrm{m}}(t)}{\mathrm{d}t} = h(\mathbf{u}_{\mathrm{m}}(t), \mathbf{z}_{\mathrm{m}}(t), \mathbf{u}^*) \text{ with b.c. } \mathbf{z}_{\mathrm{m}}(\tau) = \mathbf{z}_\tau \tag{A.32}$$

and some mixed path constraints

$$c(\mathbf{u}_{\mathrm{m}}(t), \mathbf{z}_{\mathrm{m}}(t)) = 0 \quad \text{for all } t \in [\tau, \infty). \tag{A.33}$$

This value function accommodates free end as well as fixed end constraints, and path constraints, and thus covers the scenario with and without transfers. Now owing to the optimality principle and because the integral is additive, and thus repeating the argument underlying eq. (A.28), we can write

$$V^*(\mathbf{z}_0) = \int_0^\tau f\left(\mathbf{u}^*(t), \mathbf{z}^*(t), \mathbf{u}^*\right) \mathrm{d}t + V^*(\mathbf{z}^*(\tau)). \tag{A.34}$$

Differentiating with respect to τ yields

$$0 = f\left(\mathbf{u}^*(\tau), \mathbf{z}^*(\tau), \mathbf{u}^*\right) + \nabla_{\mathbf{z}^*(\tau)} V^*(\mathbf{z}^*(\tau)) \cdot \frac{\mathrm{d}\mathbf{z}^*(\tau)}{\mathrm{d}\tau}, \tag{A.35}$$

where $\nabla_{\mathbf{z}}$ denotes the gradient with respect to $\mathbf{z}$. Adding the equality constraints, we can also write

$$0 = f\left(\mathbf{u}^*(\tau), \mathbf{z}^*(\tau), \mathbf{u}^*\right) + \nabla_{\mathbf{z}^*(\tau)} V^*(\mathbf{z}^*(\tau)) \cdot \frac{\mathrm{d}\mathbf{z}^*(\tau)}{\mathrm{d}\tau} + \eta_{\mathrm{C}}(\tau) c(\mathbf{u}^*(\tau), \mathbf{z}^*(\tau)), \tag{A.36}$$

for some Lagrange multiplier $\eta_{\mathrm{C}}(\tau)$. Now, since $\nabla_{\mathbf{z}^*(\tau)} V^*(\mathbf{z}^*(\tau)) = \tilde{\boldsymbol{\lambda}}(\tau)$ are the costate on the optimal path associated to the state dynamics (recall eq. (A.15)), we can recognize the right-hand side of eq. (A.36) as being the (extended) Hamiltonian for our model. This produces the desired result eq. (A.30) of vanishing Hamiltonian for the case with transfers, where the maximised Hamiltonian is obtained from eqs. (A.5)–(A.6), as well as for the case without transfer, where the maximised Hamiltonian is obtained from eqs. (A.16)–(A.17).

We mentioned that the above proof is heuristic. This is so because we have not made sure that the partial derivatives of the optimal value function exist, and it can happen that the value function is not differentiable even if the f, h and c functions are (Liberzon, 2011). Yet it is customary in the control literature to apply proofs under the assumption that the value function is differentiable (e.g., Dockner et al., 2000; Caputo, 2005; Sydsaeter et al., 2008; Kamien and Schwartz, 2012), since such results often hold more generally, and a rigorous proof of the vanishing Hamiltonian can be found in Michel (1982).

A.4 Optimisation versus best-reply

Let us now prove the last statement in the maximum principle of the main text. Suppose, $\boldsymbol{g}(\mathbf{u}_{\mathrm{m}}(t), \mathbf{x}_{\mathrm{m}}(t), \mathbf{u}_{\mathrm{r}}) = \boldsymbol{g}(\mathbf{u}_{\mathrm{m}}(t), \mathbf{x}_{\mathrm{m}}(t))$, $\mu(\mathbf{u}_{\mathrm{m}}(t), \mathbf{x}_{\mathrm{m}}(t), \mathbf{u}_{\mathrm{r}}) = \hat{\mu}(\mathbf{u}_{\mathrm{m}}(t), \mathbf{x}_{\mathrm{m}}(t))$,$T(\mathbf{u}_{\mathrm{m}}(t), \mathbf{x}_{\mathrm{m}}(t), \mathbf{u}_{\mathrm{r}}) = T(\mathbf{u}_{\mathrm{m}}(t), \mathbf{x}_{\mathrm{m}}(t))$, and substitute into eq. (2) along $b\left(\mathbf{u}_{\mathrm{m}}(t), \mathbf{x}_{\mathrm{m}}(t), \mathbf{u}_{\mathrm{r}}\right) = \hat{b}\left(\mathbf{u}_{\mathrm{m}}(t), \mathbf{x}_{\mathrm{m}}(t)\right) g_{\mathrm{b}}(\mathbf{u}_{\mathrm{r}})$. Then, we can write

$$R(\mathbf{u}_{\mathrm{m}}, \mathbf{u}_{\mathrm{r}}) = \hat{R}(\mathbf{u}_{\mathrm{m}}) g_{\mathrm{b}}(\mathbf{u}_{\mathrm{r}}), \tag{A.37}$$

where

$$\hat{R}(\mathbf{u}_{\mathrm{m}}) = \int_0^\infty l_{\mathrm{m}}(t) \hat{b}\left(\mathbf{u}_{\mathrm{m}}(t), \mathbf{x}_{\mathrm{m}}(t)\right) \mathrm{d}t. \tag{A.38}$$

Thus, the basic reproductive number is multiplicatively separable in terms of mutant and resident properties and where $g_{\mathrm{b}}(\mathbf{u}_{\mathrm{r}})$ accounts for density-dependent regulation. Then maximizing $R(\mathbf{u}_{\mathrm{m}}, \mathbf{u}_{\mathrm{r}})$ with respect to $\mathbf{u}_{\mathrm{m}}$ is akin to maximizing $\hat{R}(\mathbf{u}_{\mathrm{m}})$. That is, solving for the uninvadable life-history becomes a pure optimisation problem, instead of computing a best-reply. It is a standard result of evolutionary theory that when the fitness function is multiplicatively separable in mutant and resident quantities, then evolution optimises (Metz et al., 2008).

Appendix B: Cauchy formula

B.1 General considerations

We here give a representation of the solution to the non-homogeneous linear system of ordinary differential equations of the form $\mathrm{d}\boldsymbol{\lambda}(t)/\,\mathrm{d}t = -\mathbf{A}(t)\boldsymbol{\lambda}(t) - \mathbf{b}(t)$ with boundary condition $\boldsymbol{\lambda}(\zeta)$ at $t = \zeta$. According to the Cauchy formula, the following solution is unique and holds for all $t \in [0, T]$:

$$\boldsymbol{\lambda}(t) = \boldsymbol{\Psi}(t,\zeta)\left[\boldsymbol{\lambda}(\zeta) - \int_{\zeta}^{t} \boldsymbol{\Psi}(\tau,\zeta)^{-1}\mathbf{b}(\tau)\,\mathrm{d}\tau\right] = \boldsymbol{\Psi}(t,\zeta)\boldsymbol{\lambda}(\zeta) - \int_{\zeta}^{t} \boldsymbol{\Psi}(t,\tau)\mathbf{b}(\tau)\,\mathrm{d}\tau, \tag{B.1}$$

where $\boldsymbol{\Psi}(t,\tau)$ is the so-called fundamental matrix satisfying

$$\frac{\mathrm{d}\boldsymbol{\Psi}(t,\tau)}{\mathrm{d}t} = -\mathbf{A}(t)\boldsymbol{\Psi}(t,\tau) \quad \text{with i.c.} \quad \boldsymbol{\Psi}(\tau,\tau) = \mathbf{I} \tag{B.2}$$

as well as

$$\boldsymbol{\Psi}(t,\tau) = \boldsymbol{\Psi}(t,\zeta)\boldsymbol{\Psi}(\zeta,\tau) = \boldsymbol{\Psi}(t,\zeta)\boldsymbol{\Psi}(\tau,\zeta)^{-1} \tag{B.3}$$

with $\mathbf{I}$ being the identity matrix (e.g., Athans and Falb, 2007, pp. 127–130, Weber, 2011, pp. 69–72, Aseev and Kryazhimskiy, 2008, eq. 15). The ith column of $\Psi(t,\tau)$ is the solution $\boldsymbol{\lambda}(t)$ of the system $\mathrm{d}\boldsymbol{\lambda}(t)/\,\mathrm{d}t = -\mathbf{A}(t)\boldsymbol{\lambda}(t)$ at time t when the initial condition $\boldsymbol{\lambda}(\tau)$ at time τ is the standard basis with unit value at entry i, zero otherwise.

For the multidimensional case, there is no analytic representation for $\boldsymbol{\Psi}(t,\tau)$ when the system has variable coefficients and various method have been developed to evaluate it $\Psi(t,\tau)$ (Weber, 2011, p. 71). But if the system is one-dimensional, namely, $\mathrm{d}\lambda(t)/\,\mathrm{d}t = -a(t)\lambda(t) - b(t)$ with b.c. $\lambda(\zeta)$ at $t = \zeta$, then the solution to eq. (B.3) is $\Psi(t,\tau) = \exp\left(-\int_{\tau}^{t} a(h)\,\mathrm{d}h\right)$ and recalling that $\int_{\tau}^{t} f(h)\,\mathrm{d}h = -\int_{t}^{\tau} f(h)\,\mathrm{d}h$, we can write the Cauchy formula as

$$\lambda(t) = \exp\left(\int_{t}^{\zeta} a(h)\,\mathrm{d}h\right)\lambda(\zeta) + \int_{t}^{\zeta} \exp\left(\int_{t}^{\tau} a(h)\,\mathrm{d}h\right) b(\tau)\,\mathrm{d}\tau. \tag{B.4}$$

This shows that regardless of the sign of $a(h)$ and its pattern, a positive increase in $b(\tau)$ for at least some τ and holding every else the same, can only increase the shadow value since $\Psi(t,\tau) \geq 0$. For the boundary condition taken at the limit $\zeta \to \infty$ when $\lambda(\zeta) = 0$, we further get

$$\lambda(t) = \int_{t}^{\infty} \exp\left(\int_{t}^{\tau} a(h)\,\mathrm{d}h\right) b(\tau)\,\mathrm{d}\tau, \tag{B.5}$$

and when $a(h) = 0$ for all h, i.e., the diffential equation reduces to $\mathrm{d}\lambda(t)/\,\mathrm{d}t = -b(t)$, we then get

$$\lambda(t) = \int_t^\infty b(\tau)\,\mathrm{d}\tau. \tag{B.6}$$

B.2 The value of life

We here focus on solving for the value of life eq. (26) written in terms of the short-hand notations $b\,(t) = b\,(\mathbf{u}^*(t), \mathbf{x}^*(t), \mathbf{u}^*)$, $T(t) = T(\mathbf{u}^*(t), \mathbf{x}^*(t), \mathbf{u}^*)$, and $\mu(t) = \mu^*(\mathbf{u}^*(t)\mathbf{x}^*(t), \mathbf{u}^*)$, which gives

$$\frac{\mathrm{d}\lambda_{\mathrm{l}}(t)}{\mathrm{d}t} = -\left[b\,(t) + \eta_{\mathrm{T}} T(t)\right] + \mu(t)\lambda_{\mathrm{l}}(t). \tag{B.7}$$

Owing to eq. (B.4), using $\zeta = 0$, and $l(t) = \exp\left(-\int_0^t \mu(h)\,\mathrm{d}h\right)$ yields

$$\begin{aligned}
\lambda_{\mathrm{l}}(t) &= \exp\left(-\int_t^0 \mu(h)\,\mathrm{d}h\right)\lambda(0) + \int_t^0 \exp\left(-\int_t^\tau \mu(h)\,\mathrm{d}h\right)\left[b(\tau) + \eta_{\mathrm{T}} T(\tau)\right]\mathrm{d}\tau \\
&= \exp\left(\int_0^t \mu(h)\,\mathrm{d}h\right)\lambda(0) - \int_0^t \exp\left(-\int_t^\tau \mu(h)\,\mathrm{d}h\right)\left[b(\tau) + \eta_{\mathrm{T}} T(\tau)\right]\mathrm{d}\tau \\
&= \frac{1}{l(t)}\left(\lambda(0) - l(t)\int_0^t \exp\left(-\int_t^\tau \mu(h)\,\mathrm{d}h\right)\left[b(\tau) + \eta_{\mathrm{T}} T(\tau)\right]\mathrm{d}\tau\right) \\
&= \frac{1}{l(t)}\left(\lambda(0) - \int_0^t \exp\left(-\left[\int_0^t \mu(h)\,\mathrm{d}h + \int_t^\tau \mu(h)\,\mathrm{d}h\right]\right)\left[b(\tau) + \eta_{\mathrm{T}} T(\tau)\right]\mathrm{d}\tau\right) \\
&= \frac{1}{l(t)}\left(\lambda(0) - \int_0^t \exp\left(-\int_0^\tau \mu(h)\,\mathrm{d}h h\right)\left[b(\tau) + \eta_{\mathrm{T}} T(\tau)\right]\mathrm{d}\tau\right) \\
&= \frac{1}{l(t)}\left(\lambda(0) - \int_0^t l(\tau)\left[b(\tau) + \eta_{\mathrm{T}} T(\tau)\right]\mathrm{d}\tau\right) \\
&= \frac{1}{l(t)}\left(\lambda(0) - 1 + 1 - \int_0^t l(\tau)\left[b(\tau) + \eta_{\mathrm{T}} T(\tau)\right]\mathrm{d}\tau\right) \\
&= \frac{1}{l(t)}\left(\lambda(0) - 1 + \int_t^\infty l(\tau)\left[b(\tau) + \eta_{\mathrm{T}} T(\tau)\right]\mathrm{d}\tau\right),
\end{aligned} \tag{B.8}$$

where the last equality follows from see that $1 = \int_0^\infty l(\tau)\left[b(\tau) + \eta_{\mathrm{T}} T(\tau)\right]\mathrm{d}\tau$, which follows from $\int_0^\infty l(\tau)T(\tau)\,\mathrm{d}\tau = 0$ and $\int_0^\infty l(\tau)b(\tau)\,\mathrm{d}\tau = 1$, since in any monomorphic resident population, the basic reproductive number must be one (i.e., $R(\mathbf{u}_{\mathrm{r}}, \mathbf{u}_{\mathrm{r}}) = 1$ for all $\mathbf{u}_{\mathrm{r}} \in \boldsymbol{\mathcal{U}}[\mathcal{T}, \mathcal{U}]$). Hence, we have established that

$$\lambda_{\mathrm{l}}(t) = \frac{(\lambda_{\mathrm{l}}(0) - 1)}{l(t)} + \frac{1}{l(t)}\int_t^\infty l(\tau)\left[b(\tau) + \eta_{\mathrm{T}} T(\tau)\right]\mathrm{d}\tau. \tag{B.9}$$

The second summand represents the current value reproductive value, which is the expected reproduction when an individual has reached age t. This has to be finite in a population that is density-dependent regulated, since on average every individual just replaces itself in the resident population. For the same reason, the value of life cannot be infinite and hence the right-hand side of eq. (B.9) must converge as $t \to \infty$. This occurs when $\lambda_{\mathrm{l}}(0) = 1$, and thus we have shown that for biological reasons the value of life satisfies

$$\lambda_{\mathrm{l}}(t) = \frac{1}{l(t)}\int_t^\infty l(\tau)\left[b(\tau) + \eta_{\mathrm{T}} T(\tau)\right]\mathrm{d}\tau. \tag{B.10}$$

Appendix C: Age-dependent metabolic constraint on assimilation under transfers

In this Appendix, we present the key components needed to apply the maximum principle to the scenario with transfers when subject to the age-dependent metabolic constraint eq. (85), without deriving the complete set of necessary conditions, as we analyse this model only numerically. The standard optimal control theory results for inequality constraints (e.g. Caputo, 2005, Theorem 4.4. and Theorem 14.3), imply that when we have an additional inequality constraint in the form of eq. (85), we need to augment the Hamiltonian, eq. (15), to

$$H(\mathbf{u}_{\mathrm{m}}(t),\mathbf{y}_{\mathrm{m}}(t),\boldsymbol{\lambda}(t),\eta_A(t),\mathbf{u}_{\mathrm{r}}) = l_{\mathrm{m}}(t)\Big[b\left(\mathbf{u}_{\mathrm{m}}(t),\mathbf{x}_{\mathrm{m}}(t),\mathbf{u}_{\mathrm{r}}\right) - \lambda_{\mathrm{l}}(t)\mu\left(\mathbf{u}_{\mathrm{m}}(t),\mathbf{x}_{\mathrm{m}}(t),\mathbf{u}_{\mathrm{r}}\right)\Big] + \boldsymbol{\lambda}_{\mathrm{x}}(t)\cdot\boldsymbol{g}(\mathbf{u}_{\mathrm{m}}(t),\mathbf{x}_{\mathrm{m}}(t),\mathbf{u}_{\mathrm{r}}) + \eta(t)T(\mathbf{u}_{\mathrm{m}}(t),\mathbf{x}_{\mathrm{m}}(t),\mathbf{u}_{\mathrm{r}}) + \eta_A(t)\left[A_{\max}(\mathbf{x}_{\mathrm{m}}(t)) - A(\mathbf{u}_{\mathrm{m}}(t),\mathbf{x}_{\mathrm{m}}(t))\right], \quad \text{(C.1)}$$

where

$$A_{\max}(\mathbf{x}_{\mathrm{m}}(t)) - A(\mathbf{u}_{\mathrm{m}}(t),\mathbf{x}_{\mathrm{m}}(t)) \geq 0, \quad \text{(C.2)}$$

is the inequality constraint (85) of the main text where $\mathbf{x}_{\mathrm{m}}(t) = k_{\mathrm{m}}(t), q_{\mathrm{m}}(t)$, but we have re-arranged to be of the standard form (see e.g. Caputo, 2005, p. 104–105). Formally, the shadow value $\eta_A(t) \geq 0$ is a Lagrange multiplier associated with the inequality constraint (C.2) and the Hamiltonian augmented with inequality constraints is usually called a Lagrangian (see Caputo, 2005, p. 105). The necessary conditions for maximising eq. (C.1) subject to eq. (C.2) include the complementary slackness condition

$$\eta_A(t) \geq 0, \qquad \eta_A(t)\left[A_{\max}(\mathbf{x}_{\mathrm{m}}(t)) - A(\mathbf{u}_{\mathrm{m}}(t),\mathbf{x}_{\mathrm{m}}(t))\right] = 0, \quad \text{(C.3)}$$

which requires that either the constraint (C.2) be binding ($A_{\max}(\mathbf{x}_{\mathrm{m}}(t)) = A(\mathbf{u}_{\mathrm{m}}(t),\mathbf{x}_{\mathrm{m}}(t))$) or the Langrange multiplier $\eta_A(t)$ is zero. Given the augmented Hamiltonian (C.1) and the complementary slackness condition (C.3), the necessary first-order conditions follow from standard optimal control theory (see e.g. Caputo, 2005, Chapter 14).

Appendix D: Consistency of numerical solutions and analytical expressions obtained from the maximum principle

In this section, we verify that our numerically obtained uninvadable trait values $g^*(t)$, $b^*(t)$, $z^*(t)$, and $\mu^*(t)$ using the GPOPS-II optimal control solver (Fig. **1** panels (a) and (c)) satisfy the maximum principle (recall, eq. (18)–(25)). Specifically, we verify that these solutions satisfy both (i) the first-order conditions, where the selection gradients are given by eqs. (51)–(54) (with transfers) and eqs. (67)–(70) (without transfers) and (ii) the vanishing maximised Hamiltonian condition eq. (35). Fig. **S4** in S.I. displays both the numerical solutions (bullets) and analytical predictions (solid and dashed lines) for the evolving traits, demonstrating close agreement between them. We next detail how we obtained the analytical predictions displayed in Fig. **S4** in S.I..

We first derive explicit expressions for traits $z^*(t)$ and $\mu^*(t)$ from the first-order conditions of the maximum principle given by eqs. (52), (54) (with transfers) and eqs. (68), and (70) (without transfers). Since $z^*(t)$ and $\mu^*(t)$

enter nonlinearly into the Hamiltonian (eq. (50) with transfers and eq. (66) without transfers), they are expected to take interior solutions rather than boundary values. We thus obtain expressions for $z^*(t)$ and $\mu^*(t)$ by setting the first-order conditions to zero (i.e., $\partial H(t)/\partial z_{\rm m}(t)|_* = 0$ and $\partial H(t)/\partial \mu_{\rm m}(t)|_* = 0$ assuming eqs. (81)–(84)) and solve explicitly for $z^*(t)$ and $\mu^*(t)$. For our parameter values of interest, $\kappa = 2$, these interior solutions take the following forms

$$z^*(t) = \frac{\lambda_{\rm q}(t)}{2\alpha_{\rm q}\eta_{\rm T}k^*(t)l^*(t)} \text{ (with transfers)}, \tag{D.1}$$

$$\mu^*(t) = \sqrt{\frac{\alpha_\mu \eta_{\rm T}}{\lambda_{\rm l}(t)}} + \mu_0 \text{ (with transfers)}, \tag{D.2}$$

$$z^*(t) = \frac{\lambda_{\rm q}(t)}{2\alpha_{\rm q}k^*(t)\lambda_{\rm k}(t)} \text{ (without transfers)}, \tag{D.3}$$

$$\mu^*(t) = \sqrt{\frac{\alpha_\mu \lambda_{\rm k}(t)}{\alpha\lambda(t)l^*(t)}} + \mu_0 \text{ (without transfers)}. \tag{D.4}$$

These expressions for $z^*(t)$ and $\mu^*(t)$ depend on $k^*(t)$, $l^*(t)$, $\lambda_{\rm l}(t)$, $\lambda_{\rm k}(t)$, $\lambda_{\rm q}(t)$, $\eta_{\rm T}$, which we obtain numerically from the GPOPS solver. In Fig. **S4** in S.I., we show that the numerical values for $z^*(t)$ and $\mu^*(t)$ (red and pink bullets, respectively) obtained from solving the optimal control problem with GPOPS directly match closely with the analytically obtained predictions eq. (D.1)–(D.4) (red and pink solid lines, respectively).

Second, we notice that the traits $g^*(t)$ and $b^*(t)$ enter linearly in the Hamiltonian (eq. (50) with transfers and eq. (66) without transfers), and they take values at the boundaries of the feasible control space (recall, eq. (17) and section 4.1 of the main text) whereby the feasible control space for $g^*(t)$ and $b^*(t)$ for the scenario with transfers is $[0, g_{\max}]$ and $[0, b_{\max}]$, respectively. For the scenario without transfers, the controls are restricted by the budget balance constraint, eq. (65). At specific ages, these controls switch between boundary values, creating discrete switching times that we determined as follows. For growth, we determined that growth is positive $g^*(t) > 0$ from birth until the switching time $t^*_{\rm g}$, which are roots to eq. (63) (with transfers) and eq. (79) (without transfers). We also determined that there is no reproduction until $t^*_{\rm b}$, which are roots to eq. (64) (with transfers) and eq. (80) (without transfers). After age $t^*_{\rm b}$, the birth rate remains $b^*(t) > 0$ for the case without transfers, while for the case of transfers, there is a second switch time $t^*_{\rm m}$, also determined by eq. (64), after which $b^*(t) = 0$. From the boundary constraints for the two scenarios, we have that for the case of transfers, we have $g^*_{\rm pred}(t) = g_{\max}$ and $b^*(t) = b_{\max}$, whenever $g^*(t) > 0$ and $b^*(t) > 0$. For the scenario without transfers, we assumed that reproduction follows growth and thus from eq. (65) we have that

$$g^*(t) = \frac{P(k^*(t), q^*(t)) - e(\mu^*(t)) - d(k^*(t), z^*(t))}{\alpha} \tag{D.5}$$

when $g^*(t) > 0$ and

$$b^*(t) = \frac{P(k^*(t), q^*(t)) - e(\mu^*(t)) - d(k^*(t), z^*(t))}{G(P(k^*(t), q^*(t)))} \tag{D.6}$$

whenever $b^*(t) > 0$.

Third, we also verified the consistency of the results with the vanishing maximised Hamiltonian condition, which yields an explicit expression for the mortality rate (recall eq. (35)). For this consistency check, we derived the explicit

formula for the uninvadible mortality schedule μ^* for our worked-out example, by substituting eqs. (40)–(43) into (35) to obtain

$$\mu^*(t) = \begin{cases} \dfrac{b^*(t) + \lambda_{\mathrm{k}}^c(t) g^*(t) + \lambda_{\mathrm{q}}^c(t)(z^*(t) - \epsilon) + \eta_{\mathrm{T}}(t) T\left(\mathbf{u}^*(t), \mathbf{x}^*(t), \mathbf{u}^*\right)}{\lambda_{\mathrm{l}}(t)} - \mu_{\mathrm{e}} & \text{with transfers} \\ \dfrac{b^*(t) + \lambda_{\mathrm{k}}^c(t) g^*(t) + \lambda_{\mathrm{q}}^c(t)(z^*(t) - \epsilon)}{\lambda_{\mathrm{l}}(t)} - \mu_{\mathrm{e}} & \text{without transfers.} \end{cases} \tag{D.7}$$

In summary, we first determined the expressions for $z^*(t)$ and $\mu^*(t)$ consistent with the first-order condition. Then, using these results, we determined the switching times and boundary conditions for g^* and b^*. Finally, we also obtained an expression for $\mu^*(t)$ from the vanishing maximised Hamiltonian condition. Fig. **S4** in S.I. we show that the numerically obtained evolving traits (bullets) match with the prediction based on the maximum principle (solid lines) and for the expression of mortality $\mu^*(t)$ on the uninvadable path (shown in dashed pink line in Fig. **S4** in S.I.).

CRediT authorship contribution statement: Conceptualisation (P.A. & L.L.), methodology (P.A. & L.L.), resources (L.L.), formal analysis (P.A. & L.L.), software and numerical analysis (P.A.), writing (P.A. & L.L.), visualisation (P.A.).

Declaration of competing interest: The authors declare that they have no known competing financial interests or personal relationships that could have influenced the work reported in this paper.

Funding: P.A. was supported by the Research Council of Finland (grant number 360570).

Data availability: The MATLAB code for numerical optimisation will be made available in a public repository upon publication.

References

Alger, I., S. Dridi, J. Stieglitz, and M. L. Wilson. 2023. The evolution of early hominin food production and sharing. *Proceedings of the National Academy of Sciences* 120:e2218096120.

Alger, I., P. L. Hooper, D. Cox, J. Stieglitz, and H. S. Kaplan. 2020. Paternal provisioning results from ecological change. *Proceedings of the National Academy of Sciences* 117:10746–10754.

André, J.-B. and F. Rousset. 2020. Does extrinsic mortality accelerate the pace of life? A bare-bones approach. *Evolution and Human Behavior* 41:486–492.

Aseev, S. M. and A. Kryazhimskiy. 2008. Shadow prices in infinite-horizon optimal control problems with dominating discounts. *Applied Mathematics and Computation* 204:519–531.

Athans, M. and P. L. Falb. 2007. Optimal control: an introduction to the theory and its applications. Dover Publications, New York (Original work published 1966).

Avila, P. and L. Lehmann. 2023. Life history and deleterious mutation rate coevolution. *Journal of Theoretical Biology* 573:111598.

Avila, P. and C. Mullon. 2023. Evolutionary game theory and the adaptive dynamics approach: adaptation where individuals interact. *Philosophical Transactions of the Royal Society B* 378:615255.

Avila, P., T. Priklopil, and L. Lehmann. 2021. Hamilton's rule, gradual evolution, and the optimal (feedback) control of phenotypically plastic traits. *Journal of Theoretical Biology* 526:110602.

Bryson, A. E. and Y.-C. Ho. 1975. Applied optimal control: optimization, estimation and control. CRC Press, New York.

Bulmer, M. G. 1994. Theoretical evolutionary ecology. Sinauer Associates, Massachusetts.

Caputo, M. R. 2005. Foundations of dynamic economic analysis. Cambridge University Press, Cambridge, UK.

Caswell, H. 2000. Matrix population models. Sinauer Associates, Massachusetts.

Charlesworth, B. 1994. Evolution in age-structured populations. Cambridge University Press, Cambridge, 2th edn.

Chu, C. C., H.-K. Chien, and R. D. Lee. 2008. Explaining the optimality of U-shaped age-specific mortality. *Theoretical Population Biology* 73:171–180.

Chu, C. C. and R. D. Lee. 2006. The co-evolution of intergenerational transfers and longevity: an optimal life history approach. *Theoretical Population Biology* 69:193–201.

Cichoń, M. and J. Kozłowski. 2000. Ageing and typical survivorship curves result from optimal resource allocation. *Evolutionary Ecology Research* 2:857–870.

Clutton-Brock, T. H. 1991. The evolution of parental care, vol. 10. Princeton University Press.

Crump, S. C. and C. J. Mode. 1968. A general age-dependent branching process. 1. *Journal of Mathematical Analysis and Applications* 24:494–508.

Davison, R. and M. Gurven. 2022. The importance of elders: extending Hamilton's force of selection to include intergenerational transfers. *Proceedings of the National Academy of Sciences* 119:e2200073119.

Day, T. and P. D. Taylor. 1997. Von Bertalanffy's growth equation should not be used to model age and size at maturity. *The American Naturalist* 149:381–393.

Day, T. and P. D. Taylor. 2000. A generalization of Pontryagin's maximum principle for dynamic evolutionary games among relatives. *Theoretical Population Biology* 57:339–356.

Dockner, E., S. Jorgensen, N. V. Long, and G. Sorger. 2000. Differential games in economics and management science. Cambridge University Press, Cambridge.

Dorfman, R. 1969. An economic interpretation of optimal control theory. *American Economic Review* 59:817–831.

Ellis, S., D. W. Franks, M. L. K. Nielsen, M. N. Weiss, and D. P. Croft. 2024. The evolution of menopause in toothed whales. *Nature* 627:579–585.

Eshel, I., M. Feldman, and A. Bergman. 1998. Long-term evolution, short-term evolution, and population genetic theory. *Journal of Theoretical Biology* 191:391–396.

Eshel, I. and M. W. Feldman. 1984. Initial increase of new mutants and some continuity properties of ESS in two-locus systems. *The American Naturalist* 124:631–640.

Ewald, C. O., J. McNamara, and A. Houston. 2007. Parental care as a differential game: A dynamic extension of the Houston–Davies game. *Applied Mathematics and Computation* 190:1450–1465.

Ferrière, R. and M. Gatto. 1995. Lyapunov exponents and the mathematics of invasion in oscillatory or chaotic populations. *Theoretical Population Biology* 48:126–171.

Fisher, R. A. 1930. The Genetical Theory of Natural Selection. Clarendon Press, Oxford.

Gavrilets, S. 2012. Human origins and the transition from promiscuity to pair-bonding. *Proceedings of the National Academy of Sciences* 109:9923–9928.

Geritz, S. A. H., E. Kisdi, G. Meszéna, and J. A. J. Metz. 1998. Evolutionarily singular strategies and the adaptive growth and branching of the evolutionary tree. *Evolutionary Ecology* 12:35–57.

Glazier, D. S. 2005. Beyond the '3/4-power law': variation in the intra-and interspecific scaling of metabolic rate in animals. *Biological Reviews* 80:611–662.

González-Forero, M., T. Faulwasser, and L. Lehmann. 2017. A model for brain life history evolution. *PLOS Computational Biology* 13:e1005380.

Gurven, M., H. S. Kaplan, and M. Gutierrez. 2006. How long does it take to become a proficient hunter? Implications for the evolution of extended development and long life span. *Journal of Human Evolution* 51:454–470.

Gurven, M., J. Stieglitz, P. L. Hooper, C. Gomes, and H. Kaplan. 2012. From the womb to the tomb: the role of transfers in shaping the evolved human life history. *Experimental Gerontology* 47:807–813.

Gurven, M. D. 2024. Life History. In Koster, J., B. Scelza, and M. K. Shenk (eds.), *Human Behavioral Ecology*, pp. 20–47. Cambridge University Press, Cambridge.

Hartl, R. F., S. P. Sethi, and R. G. Vickson. 1995. A survey of the maximum principles for optimal control problems with state constraints. *SIAM Review* 37:181–218.

Hawkes, K., J. F. O'Connell, N. B. Jones, H. Alvarez, and E. L. Charnov. 1998. Grandmothering, menopause, and the evolution of human life histories. *Proceedings of the National Academy of Sciences* 95:1336–1339.

Hou, C., W. Zuo, M. E. Moses, W. H. Woodruff, J. H. Brown, and G. B. West. 2008. Energy uptake and allocation during ontogeny. *Science* 322:736–739.

Houston, A. I. and J. M. McNamara. 1999. Models of adaptive behaviour: an approach based on state. Cambridge University Press, Cambridge, UK.

Hrdy, S. B. 2009. Mothers and others. Cambridge, MA: Harvard University Press.

Irie, T. and Y. Iwasa. 2005. Optimal growth pattern of defensive organs: The diversity of shell growth among mollusks. *The American Naturalist* 165:238–249.

Iwasa, Y. and J. Roughgarden. 1984. Shoot/root balance of plants: optimal growth of a system with many vegetative organs. *Theoretical Population Biology* 25:78–105.

Kamien, M. I. and N. L. Schwartz. 2012. Dynamic optimization: the calculus of variations and optimal control in economics and management. Dover Publications, New York, 1th edn.

Kaplan, H., K. Hill, A. M. Hurtado, and J. Lancaster. 2001. The embodied capital theory of human evolution. In Ellison, P. T. (ed.), *Reproductive ecology and human evolution*, pp. 293–317. Aldine de Gruyter, New York.

Kaplan, H. S. 1994. Evolutionary and wealth flows theories of fertility: Empirical tests and new models. *Population and Development Review* 20:753–791.

Kaplan, H. S., M. Gurven, J. Winking, P. L. Hooper, and J. Stieglitz. 2010. Learning, menopause, and the human adaptive complex. *Annals of the New York Academy of sciences* 1204:30–42.

Kaplan, H. S., K. Hill, J. Lancaster, and A. M. Hurtado. 2000. A theory of human life history evolution: diet, intelligence, and longevity. *Evolutionary Anthropology* 9:156–185.

Kaplan, H. S., P. L. Hooper, and M. Gurven. 2009. The evolutionary and ecological roots of human social organization. *Philosophical Transactions of the Royal Society B-Biological Sciences* 364:3289–3299.

Kaplan, H. S. and A. J. Robson. 2002. The emergence of humans: the coevolution of intelligence and longevity with intergenerational transfers. *Proceedings of the National Academy of Sciences of the United States of America* 99:10221–10226.

Kaplan, H. S. and A. J. Robson. 2009. We age because we grow. *Proceedings of the Royal Society B-Biological Sciences* 276:1837–1844.

Karlin, S. and H. M. Taylor. 1981. A second course in stochastic processes. Academic Press, San Diego.

Kopp, R. E. and H. G. Moyer. 1965. Necessary conditions for singular extremals. *AIAA Journal* 3:1439–1444.

Kozłowski, J. 1992. Optimal allocation of resources to growth and reproduction: implications for age and size at maturity. *Trends Ecol Evol* 7:15–9.

Lee, R. 2020. Population aging and the historical development of intergenerational transfer systems. *Genus* 76:31.

Lee, R. D. 2003. Rethinking the evolutionary theory of aging: transfers, not births, shape senescence in social species. *Proceedings of the National Academy of Sciences of the United States of America* 100:9637–9642.

Lehmann, L., C. Mullon, E. Akçay, and J. Van Cleve. 2016. Invasion fitness, inclusive fitness, and reproductive numbers in heterogeneous populations. *Evolution* 70:1689–1702.

León, J. A. 1976. Life histories as adaptive strategies. *Journal of Theoretical Biology* 60:301–335.

Lessard, S. 1990. Evolutionary stability: one concept, several meanings. *Theoretical Population Biology* 37:159–170.

Liberzon, D. 2011. Calculus of variations and optimal control theory: a concise introduction. Princeton University Press, Princeton.

Loo, S. L., D. Rose, M. Weight, K. Hawkes, and P. S. Kim. 2020. Why males compete rather than care, with an application to supplying collective goods. *Bulletin of Mathematical Biology* 82:1–20.

Mace, R. 2000. Evolutionary ecology of human life history. *Animal Behaviour* 59:1–10.

Mangel, M. and C. W. Clark. 1988. Dynamic modeling in behavioral ecology. Princeton University Press.

Mas-Colell, A., M. D. Whinston, and J. R. Green. 1995. Microeconomic theory. Oxford Unversity Press, Oxford.

Metz, J. A. J. 2011. Thoughts on the geometry of meso-evolution: collecting mathematical elements for a post-modern synthesis. In Chalub, F. A. C. C. and J. Rodrigues (eds.), *The mathematics of Darwin's legacy*, Mathematics and biosciences in interaction, pp. 193–231. Birkhäuser, Basel.

Metz, J. A. J., S. D. Mylius, and O. Diekmann. 2008. When does evolution optimize? *Evolutionary Ecology Research* 10:629–654.

Metz, J. A. J., R. M. Nisbet, and S. A. H. Geritz. 1992. How should we define fitness for general ecological scenarios? *Trends in Ecology and Evolution* 7:198–202.

Metz, J. A. J., K. Staňková, and J. Johansson. 2016. The canonical equation of adaptive dynamics for life histories: from fitness-returns to selection gradients and Pontryagin's maximum principle. *Journal of Mathematical Biology* 72:1125–1152.

Michel, P. 1982. On the transversality condition in infinite horizon optimal problems. *Econometrica* 50:975–985.

Michod, R. E. 1979. Evolution of life histories in response to age-specific mortality factors. *The American Naturalist* 113:531–550.

Mode, C. J. 1971. Multitype branching processes: theory and applications. Elsevier, New York.

Mullon, C. and L. Lehmann. 2017. Invasion fitness for gene-culture co-evolution in family-structured populations and an application to cumulative culture under vertical transmission. *Theoretical Population Biology* 116:33–46.

Nakamura, M. and H. Ohtsuki. 2016. Optimal decision rules in repeated games where players infer an opponent's mind via simplified belief calculation. *Games* 7:1–23.

Oster, G. and E. O. Wilson. 1977. Caste and ecology in the social insects. Princetion University Press, Princeton, NJ.

Patterson, M. A. and A. V. Rao. 2014. GPOPS-II: A MATLAB software for solving multiple-phase optimal control problems using hp-adaptive Gaussian quadrature collocation methods and sparse nonlinear programming. *ACM Transactions on Mathematical Software (TOMS)* 41:1–37.

Perrin, N. 1992. Optimal resource allocation and the marginal value of organs. *American Naturalist* 139:1344–1369.

Perrin, N., R. Sibly, and N. Nichols. 1993. Optimal growth strategies when mortality and production rates are size-dependent. *Evolutionary Ecology* 7:576–592.

Perrin, N. and R. M. Sibly. 1993. Dynamic models of energy allocation and investment. *Annual Review of Ecology and Systematics* 24.

Pontzer, H. 2015. Energy expenditure in humans and other primates: a new synthesis. *Annual Review of Anthropology* 44:169–187.

Pontzer, H., M. H. Brown, D. A. Raichlen, H. Dunsworth, B. Hare, K. Walker, A. Luke, L. R. Dugas, R. Durazo-Arvizu, D. Schoeller, J. Plange-Rhule, P. Bovet, T. E. Forrester, E. V. Lambert, M. E. Thompson, R. W. Shumaker, and S. R. Ross. 2016. Metabolic acceleration and the evolution of human brain size and life history. *Nature* 533:390–392.

Rand, D. A., H. B. Wilson, and J. M. McGlade. 1994. Dynamics and evolution: evolutionarily stable attractors, in-

vasion exponents and phenotype dynamics. *Philosophical Transactions of the Royal Society B-Biological Sciences* 343:261–83.

Rebhuhn, D. 1978. On the stability of the existence of singular controls under perturbation of the control system. *SIAM Journal on Control and Optimization* 16:463–472.

Robson, S. L., C. P. Van Schaik, and K. Hawkes. 2006. The derived features of human life history. *The evolution of human life history* 17:17–44.

Roper, M., J. P. Green, R. Salguero-Gómez, and M. B. Bonsall. 2023. Inclusive fitness forces of selection in an age-structured population. *Communications Biology* 6:909.

Rousset, F. 2004. Genetic structure and selection in subdivided populations. Princeton University Press, Princeton, NJ.

Schaffer, W. M. 1982. The application of optimal control theory to the general life history problem. *American Naturalist* 121:418–431.

Schaffer, W. M. 1983. The application of optimal control theory to the general life history problem. *The American Naturalist* 121:418–431.

Stearns, S. 1992. The Evolution of Life Histories. Oxford University Press, Oxford.

Sydsaeter, K., P. Hammond, A. Seierstad, and A. Strøm. 2008. Further Mathematics for Economic Analysis. Prentice Hall, Essex, 2th edn.

Tirole, J. 1988. The theory of industrial organization. MIT press.

van Schaik, C. P. 2016. The primate origin of human behavior. Wiley-Blackwell, New Jersey.

Vaupel, J. W., A. Baudisch, M. Dolling, D. A. Roach, and J. Gampe. 2004. The case for negative senescence. *Theoretical Population Biology* 65:339–351.

Weber, T. A. 2011. Optimal Control Theory with Applications in Economics. MIT press Cambridge, Cambridge, MA.

West, G. B., J. H. Brown, and B. J. Enquist. 1997. A general model for the origin of allometric scaling laws in biology. *Science* 276:122–126.

Wood, B. and I. Gilby. 2017. From *Pan* to man the hunter: hunting and meat sharing by chimpanzees, humans, and our common ancestor. In Muller, M. N., R. W. Wrangham, and D. R. Pilbeam (eds.), *Chimpanzees and Human Evolution*, pp. 339–382. The Belknap Press of Harvard University Press.

Wrangham, R. 2009. Catching fire: how cooking made us human. Basic books.

Yegian, A. K., S. B. Heymsfield, E. R. Castillo, M. J. Müller, L. M. Redman, and D. E. Lieberman. 2024. Metabolic scaling, energy allocation tradeoffs, and the evolution of humans' unique metabolism. *Proceedings of the National Academy of Sciences* 121:e2409674121.

Table 1: Summary of key variables in Sections 2 and 3 and their biological meanings

Variable	Symbol	Biological Meaning
Fitness proxy, control, and state variables		
Age	$t \in \mathcal{T} = [0, \infty)$	Age of an individual throughout its lifespan.
Control schedule	$\mathbf{u} = \{\mathbf{u}(t)\}_{t\in\mathcal{T}}$	Genetically evolving multidimensional life history trait with trait expression at age t being $\mathbf{u}(t) \in \mathcal{U} \subset \mathbb{R}^{n_\mathrm{u}}$. Mutant, resident, and uninvadable controls are noted as $\mathbf{u}_\mathrm{m}(t)$, $\mathbf{u}_\mathrm{r}(t)$, $\mathbf{u}^*(t) \in \mathcal{U} \subset \mathbb{R}^{n_\mathrm{u}}$, respectively.
State schedule	$\mathbf{x} = \{\mathbf{x}(t)\}_{t\in\mathcal{T}}$	Multidimensional quantitative state (e.g. body size, brain size, fat reserve) with state expressed at age t being $\mathbf{x}(t) \in \mathbb{R}^{n_\mathrm{x}}$. Mutant, resident, and uninvadable state variables $\mathbf{x}_\mathrm{m}(t)$, $\mathbf{x}_\mathrm{r}(t)$, $\mathbf{x}^*(t) \in \mathbb{R}^{n_\mathrm{x}}$, respectively.
Survival probability	$l_\mathrm{m}(t)$, $l_\mathrm{r}(t)$	Probability of surviving to age t of mutant and resident individuals, respectively.
Basic reproductive number	$R(\mathbf{u}_\mathrm{m}, \mathbf{u}_\mathrm{r})$	Expected lifetime offspring production of an individual with trait $\mathbf{u}_\mathrm{m}$ in a population of resident individuals expressing trait $\mathbf{u}_\mathrm{r}$.
Vital rates and energy rates. All rates are for an individual expressing trait $\mathbf{u}_\mathrm{m}(t)$ in state $\mathbf{x}_\mathrm{m}(t)$ at age t; dependence on $\mathbf{u}_\mathrm{r}$ indicates dependence on the resident population schedule.		
Birth rate	$b(\mathbf{u}_\mathrm{m}(t), \mathbf{x}_\mathrm{m}(t), \mathbf{u}_\mathrm{r})$	Effective fecundity at age t.
Mortality rate	$\mu(\mathbf{u}_\mathrm{m}(t), \mathbf{x}_\mathrm{m}(t), \mathbf{u}_\mathrm{r})$	Mortality rate at age t.
State dynamics	$\boldsymbol{g}(\mathbf{u}_\mathrm{m}(t), \mathbf{x}_\mathrm{m}(t), \mathbf{u}_\mathrm{r})$	Rate of change of states at age t.
Production rate	$P(\mathbf{u}_\mathrm{m}(t), \mathbf{x}_\mathrm{m}(t), \mathbf{u}_\mathrm{r})$	Gross rate of energy produced/collected at age t.
Assimilation rate	$A(\mathbf{u}_\mathrm{m}(t), \mathbf{x}_\mathrm{m}(t))$	Rate of energy consumed by the organism at age t.
Transfer rate	$T(\mathbf{u}_\mathrm{m}(t), \mathbf{x}_\mathrm{m}(t), \mathbf{u}_\mathrm{r})$	Net energy transfer rate (production minus assimilation) at age t.
Reproduction cost	$E_\mathrm{b}(\mathbf{u}_\mathrm{m}(t), \mathbf{x}_\mathrm{m}(t))$	Rate of energy allocated to reproduction at age t.
Survival cost	$E_\mu(\mathbf{u}_\mathrm{m}(t), \mathbf{x}_\mathrm{m}(t))$	Rate of energy allocated to survival at age t.
Growth cost	$E_\mathrm{x}(\mathbf{u}_\mathrm{m}(t), \mathbf{x}_\mathrm{m}(t))$	Rate of energy allocated to physiological state growth at age t.
Maintenance cost	$E_\mathrm{M}(\mathbf{u}_\mathrm{m}(t), \mathbf{x}_\mathrm{m}(t))$	Rate of energy allocated to maintenance at age t.
Fitness increase rate and shadow values		
Hamiltonian	$H(t)$	The rate of fitness increase of a mutant individual at age t through reproduction, survival, and changes in somatic physiological state. Formally, $H(t) = H(\mathbf{u}_\mathrm{m}(t), \mathbf{y}_\mathrm{m}(t), \boldsymbol{\lambda}(t), \mathbf{u}_\mathrm{r})$, where $\mathbf{y}_\mathrm{m}(t) = (\mathbf{x}_\mathrm{m}(t), l_\mathrm{m}(t))$.
Shadow value of energy	$\eta(t)$	Marginal effect of transferring energy on remaining fitness evaluated in the resident population.
Shadow value of metabolic capacity	$\eta_A(t)$	Marginal fitness benefit of increasing metabolic capacity at age t. When $\eta_A(t) > 0$, the organism is operating at its maximal metabolic capacity $A_\mathrm{max}(t)$ and would benefit from higher capacity. When $\eta_A(t) = 0$, the organism assimilates less energy than its maximal metabolic capacity.
Value of life	$\lambda_\mathrm{l}(t)$	Marginal effect of increasing survival $l_\mathrm{m}(t)$ on remaining fitness evaluated in the resident population.
Shadow value of state	$\boldsymbol{\lambda}_\mathrm{x}(t)$	Vector of marginal effects of increasing the multidimensional physiological state on remaining fitness evaluated in the resident population.
Fisher's reproductive value	$v_\mathrm{F}(t)$	Expected future reproduction from age t onward evaluated in the resident population.
Transfer value	$v_\mathrm{T}(t)$	Remaining net energy transfer from age t onward evaluated in the resident population.

Table 2: Summary of variables in Section 4 and their biological meanings

Variable	Symbol	Biological Meaning
Control variables (evolving traits)		
Birth rate allocation	$b_{\mathrm{m}}(t)$	Rate of resource allocation to reproduction. Without transfers $b_{\mathrm{m}}(t) \in \mathbb{R}_+$ and with transfers $b_{\mathrm{m}}(t) \in [0, b_{\max}]$, where $b_{\max}$ is the maximal birth rate from the scenario without transfers (see section 4.1 for more details).
Growth rate	$g_{\mathrm{m}}(t)$	Rate of somatic capital growth. Without transfers $g_{\mathrm{m}}(t) \in \mathbb{R}_+$ and with transfers $g_{\mathrm{m}}(t) \in [0, g_{\max}]$, where $g_{\max}$ is the maximal growth rate from the scenario without transfers.
Mortality rate	$\mu_{\mathrm{m}}(t) \in \mathbb{R}_+$	Mortality conceived as a trait.
Quality investment	$z_{\mathrm{m}}(t) \in \mathbb{R}_+$	Rate of investment in somatic quality maintenance.
State and costate variables		
Somatic quantity	$k_{\mathrm{m}}(t)$	Amount/size of somatic capital (e.g., body mass, brain size) at age t.
Somatic quality	$q_{\mathrm{m}}(t)$	Quality/efficiency of somatic capital at age t.
Survival probability	$l_{\mathrm{m}}(t)$	Probability of surviving to age t.
Shadow value of somatic quantity	$\lambda_{\mathrm{k}}(t)$	Marginal effect of increasing somatic quantity on remaining fitness evaluated in the resident population.
Shadow value of somatic quality	$\lambda_{\mathrm{q}}(t)$	Marginal effect of increasing somatic quality on remaining fitness evaluated in the resident population.
Value of life	$\lambda_{\mathrm{l}}(t)$	Marginal effect of increasing survival $l_{\mathrm{m}}(t)$ on remaining fitness evaluated in the resident population.
Energy variables		
Production rate	$P(k_{\mathrm{m}}(t), q_{\mathrm{m}}(t))$	Gross rate of total energy produced/collected. In the worked-out example, we assume $P(k_{\mathrm{m}}(t), q_{\mathrm{m}}(t)) = a[k_{\mathrm{m}}(t)]^c q_{\mathrm{m}}(t)$.
Reproduction energy	$E_{\mathrm{b}}(b_{\mathrm{m}}(t), k_{\mathrm{m}}(t), q_{\mathrm{m}}(t))$	Energy allocated to reproduction, $E_{\mathrm{b}}(b_{\mathrm{m}}(t), k_{\mathrm{m}}(t), q_{\mathrm{m}}(t)) = G(P(k_{\mathrm{m}}(t), q_{\mathrm{m}}(t)))b_{\mathrm{m}}(t)$. In the worked-out example, we assume $G(P(k_{\mathrm{m}}(t), q_{\mathrm{m}}(t))) = \alpha_{\mathrm{b}} \exp(-r_{\mathrm{b}} P(k_{\mathrm{m}}(t), q_{\mathrm{m}}(t)))$.
Somatic quantity energy	$E_{\mathrm{k}}(g_{\mathrm{m}}(t))$	Energy allocated to increase the somatic quantity, $E_{\mathrm{k}}(g_{\mathrm{m}}(t)) = \alpha g_{\mathrm{m}}(t)$.
Survival energy	$E_{\mu}(u(t))$	Energy allocated to survival. In the worked-out example, we assume $E_{\mu}(u(t)) = e(u(t)) = \alpha_{\mu}/(\mu_{\mathrm{m}}(t) - \mu_0)$.
Maintenance energy	$E_{\mathrm{q}}(k_{\mathrm{m}}(t), z_{\mathrm{m}}(t))$	Energy allocated to quality maintenance. In the worked-out example, we assume $E_{\mathrm{q}}(k_{\mathrm{m}}(t), z_{\mathrm{m}}(t)) = d(k_{\mathrm{m}}(t), z_{\mathrm{m}}(t)) = \alpha_{\mathrm{q}}[z_{\mathrm{m}}(t)]^{\kappa} k_{\mathrm{m}}(t)$.
Parameters		
Reproduction cost	α_{b}	Parameter adjusting the energy cost per unit of reproduction.
Growth cost	α	Energy cost per unit of increasing somatic capital.
Survival cost	α_{μ}	Parameter adjusting the energy cost per unit of allocating resources to increase survival.
Maintenance cost	α_{q}	Parameter adjusting the energy cost per unit of increasing the quality of somatic capital.
Quality depreciation	ϵ	Baseline degradation rate of somatic quality.
External mortality	μ_{e}	External mortality

Table 3: Key results on parameter variation analysis

Finding	**Without transfers**	**With transfers**	**Biological Relevance**
Energy productivity	Limited early investment	Enhanced early somatic investment yields higher lifetime productivity	High productivity and high energy expenditure over lifespan, extended human juvenile dependency
Life phases	2-phase: growth, reproduction	4-phase: growth ($T < 0$), mixed growth and reproduction ($T < 0$), reproduction ($T > 0$), post-reproductive ($T > 0$)	Post-reproductive lifespan is an outcome of life history optimisation under transfers
Mortality schedule	U-shaped (lowest at the end of growth)	U-shaped (lowest at the end of growth), but overall lower mortality	Transfers lead to higher longevity
Maintenance schedule	U-shaped (low early, spike late)	Dome-shaped (peaks before reproduction), but overall higher quality maintenance	Transfers lead to higher quality maintenance
Shadow value of energy ($\eta(t)$)	Highest in young (very strong), decreases throughout life	Highest in young (moderate), decreases throughout life	Evolution of parental care
Maintenance cost (α_{q})	Scenarios converge under lower α_{q}, no ageing	Scenarios converge, no ageing	Negligible senescence can occur when α_{q} is low enough
External mortality (m_{e})	Increased m_{e} leads to "faster" life history strategy	Increased m_{e} leads to "faster" life history strategy, but the effect is smaller compared to the case without transfers	Transfers mitigate some of the effect of high external mortality.
Quality depreciation rate (ϵ)	Lower ϵ increases investment into soma, longer lifepan	Lower ϵ increases more investment into soma, longer lifepan. Amplifies the effects of transfers, creating stronger divergence between the case without transfers.	Transfer and longevity mutually reinforce when the somatic depreciation rate ϵ is low.

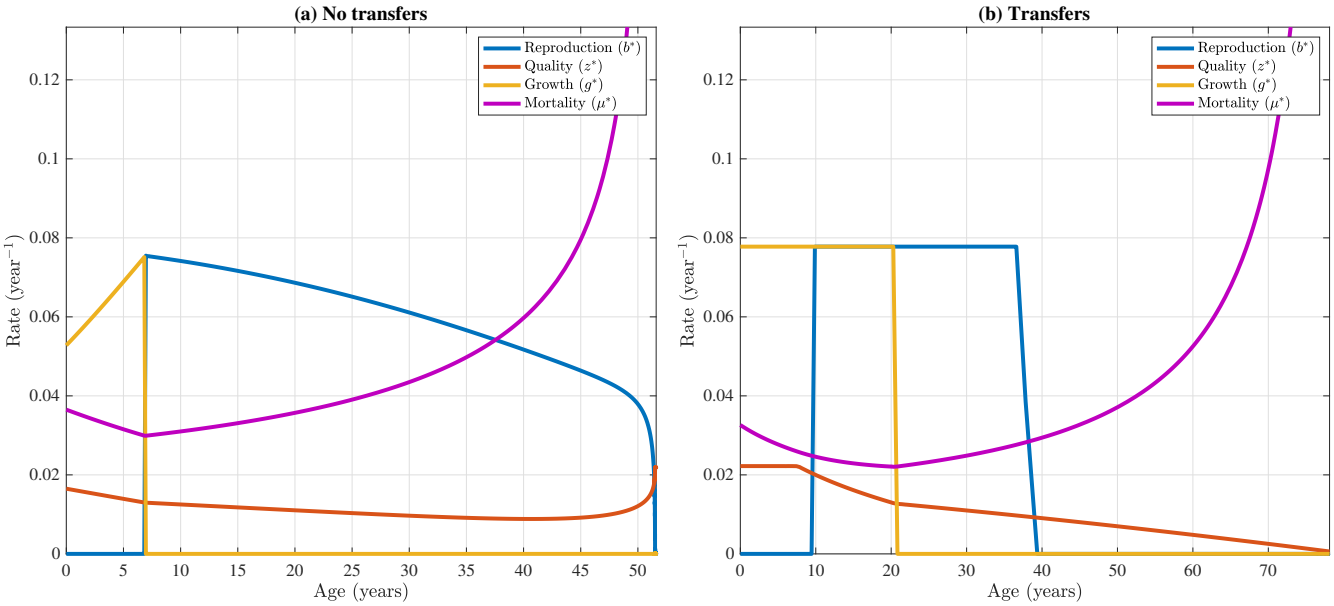

Figure 1: Uninvadable life history rates (evolving traits) with and without intergenerational transfers. Panels show age-specific reproduction (b^*, blue), somatic quality maintenance (z^*, red), growth (g^*, yellow), and mortality (μ^*, purple) for scenarios (a) without and (b) with transfers. Model outputs are rescaled to a human-like timeframe for ease of interpretation, $t_{years} = t_{model} \times 4.5$, and the plotted rates are $\mathbf{u}^*_{years} = \mathbf{u}^*_{model}/4.5$. This scaling is illustrative rather than a calibration to empirical human data. See S.I. for the unscaled numerical solutions. Parameter values: $\alpha_\mathrm{b} = 2$, $\alpha = 2$, $\alpha_\mathrm{q} = 40$, $\alpha_\mu = 0.05$, $m_\mathrm{e} = 0.01$, $m_0 = 0.00001$, $r_\mathrm{b} = 0.001$, $a = 1$, $c = 0.75$, $x_0 = 1$, $q_0 = 1$, $\epsilon = 0.1$, $\kappa = 2$, $\xi = 1$. Results plotted for survival $l^*(t) > 0.01$.

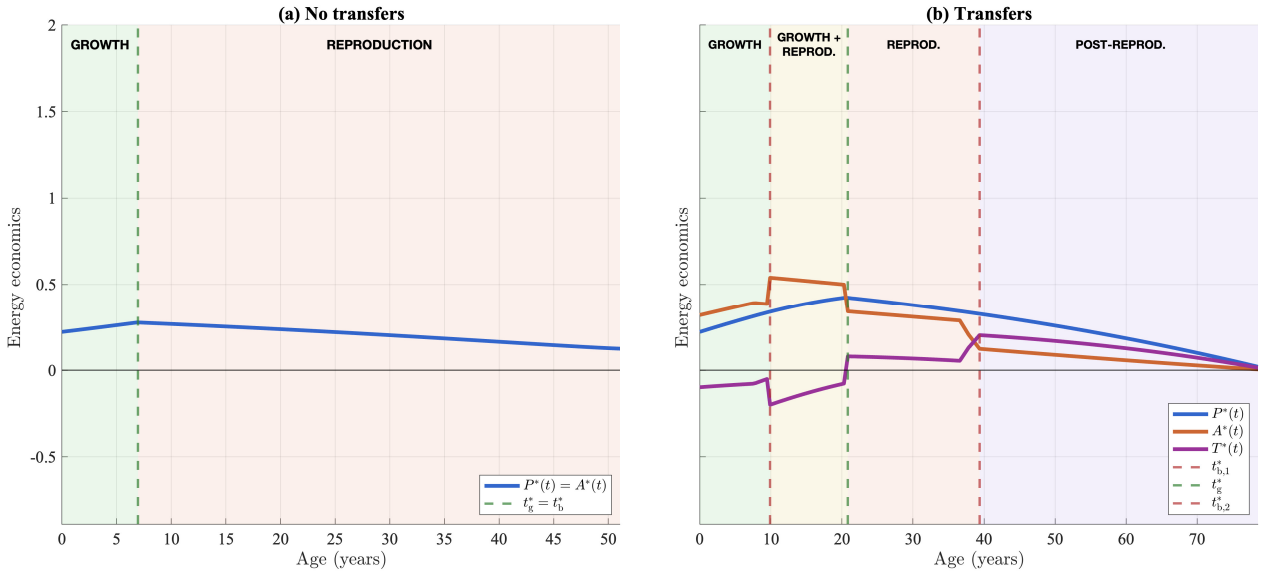

Figure 2: Uninvadable life history phases and energy economics under the two budget constraints. Panel (a): without transfers: two phases, juvenile growth (green area) followed by reproduction (red area), with production equal to assimilation throughout ($P^*(t) = A^*(t)$, blue line). Panel (b): with transfers without age-specific energy balance ($P^*(t) \neq A^*(t)$, blue and red lines), two new phases emerge: continued growth after reproduction (yellow area) and post-reproductive phase (purple area). Individuals are net-energy consumers until growth stops ($T^*(t) < 0$, negative, purple line). Parameter values and scaling details are given as in Figure 1.

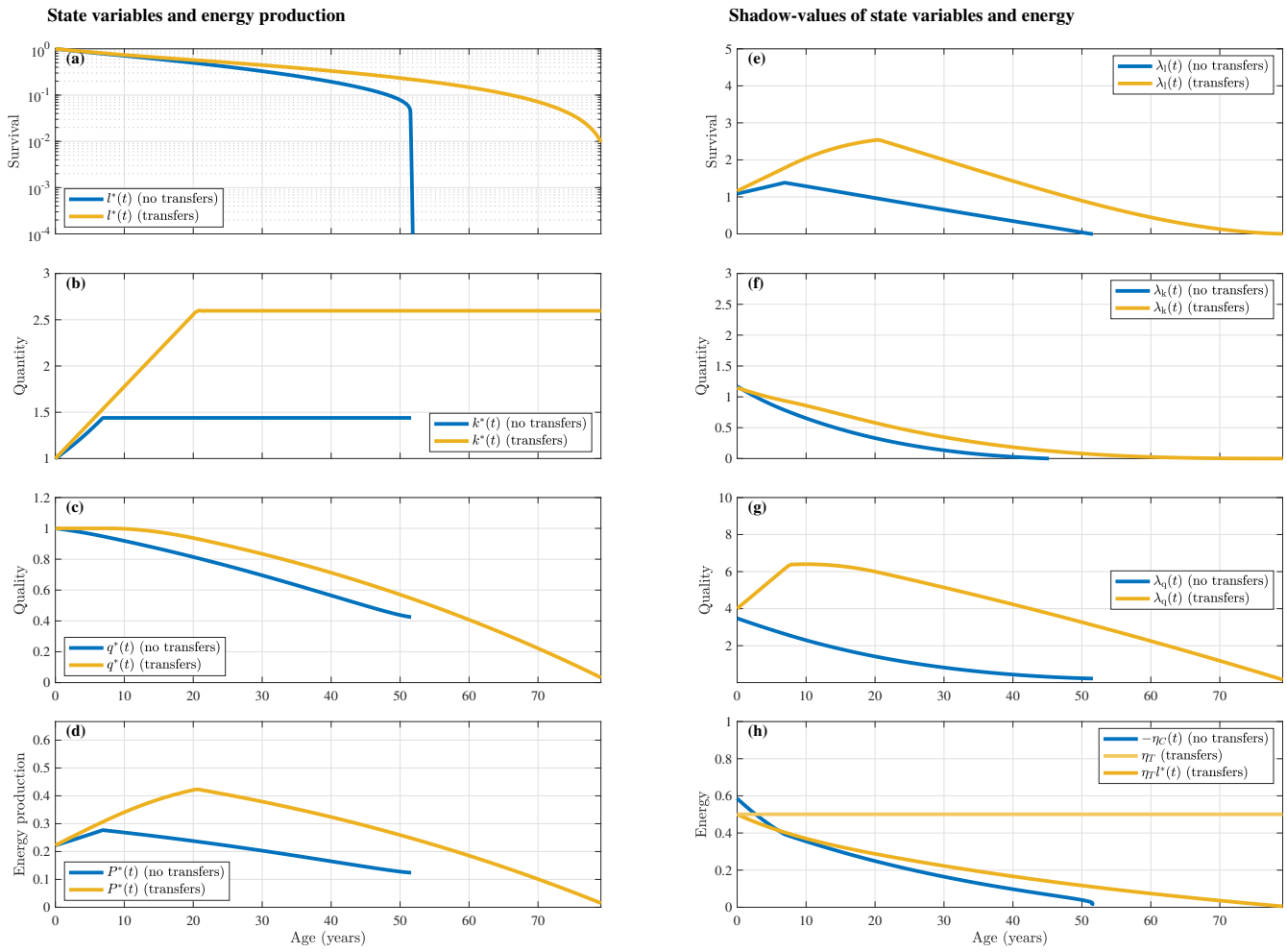

Figure 3: Uninvadable state variables, energy production, and corresponding shadow values across lifespan with and without transfers. The values without transfers (blue), with transfers (yellow). Left column: survival probability $l^*(t)$ (a), somatic capital $k^*(t)$ (b), somatic quality $q^*(t)$ (c), and energy production $P^*(t)$ (d). Right column: value of life $\lambda_l(t)$ (e), shadow value of somatic capital $\lambda_k(t)$ (f), shadow value of somatic quality $q^*(t)$ (g), shadow value of energy: $\eta(t) = \eta_T l^*(t)$ (transfers), $\eta(t) = \eta_C(t)$ (without transfers) (h). Parameter values and scaling details are given as in Figure 1.

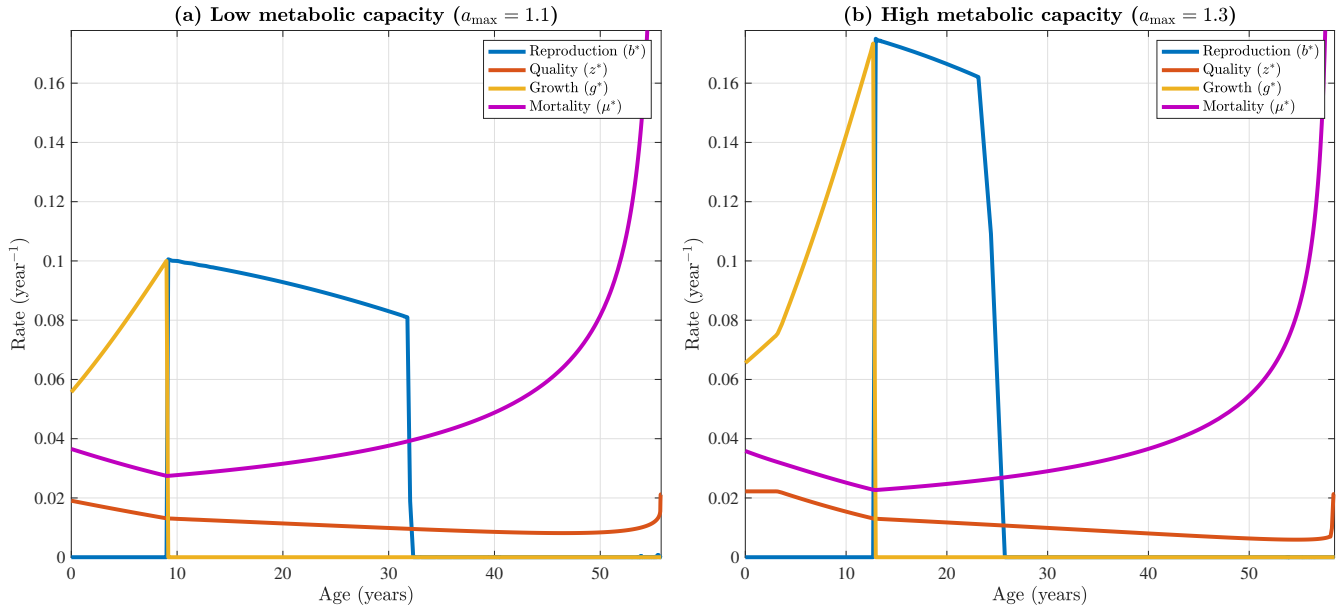

Figure 4: Uninvadable life history rates (evolving traits) with intergenerational transfers assuming Kleiber's law in assimilated metabolic capacity. Panels show age-specific reproduction (b^*, blue), somatic quality maintenance (z^*, red), growth (g^*, yellow), and mortality (μ^*, purple). Panel (a) low metabolic capacity $a_{\max} = 1.1$ and panel (b) high metabolic capacity $a_{\max} = 1.3$. For comparison, the model outputs are rescaled: $t_{years} = t_{model} \times 4.5$, and the plotted rates are $\mathbf{u}^*_{years} = \mathbf{u}^*_{model}/4.5$. Parameter values for the unscaled model: $\alpha_{\rm b} = 2$, $\alpha = 2$, $\alpha_{\rm q} = 40$, $\alpha_\mu = 2$, $\zeta = 40$, $m_{\rm e} = 0.01$, $m_0 = 0.00001$, $r_{\rm b} = 0.001$, $a = 1$, $c = 0.75$, $x_0 = 1$, $q_0 = 1$, $\epsilon = 0.1$, $\kappa = 2$, $\xi = 1$. Results plotted for survival $l^*(t) > 0.01$.

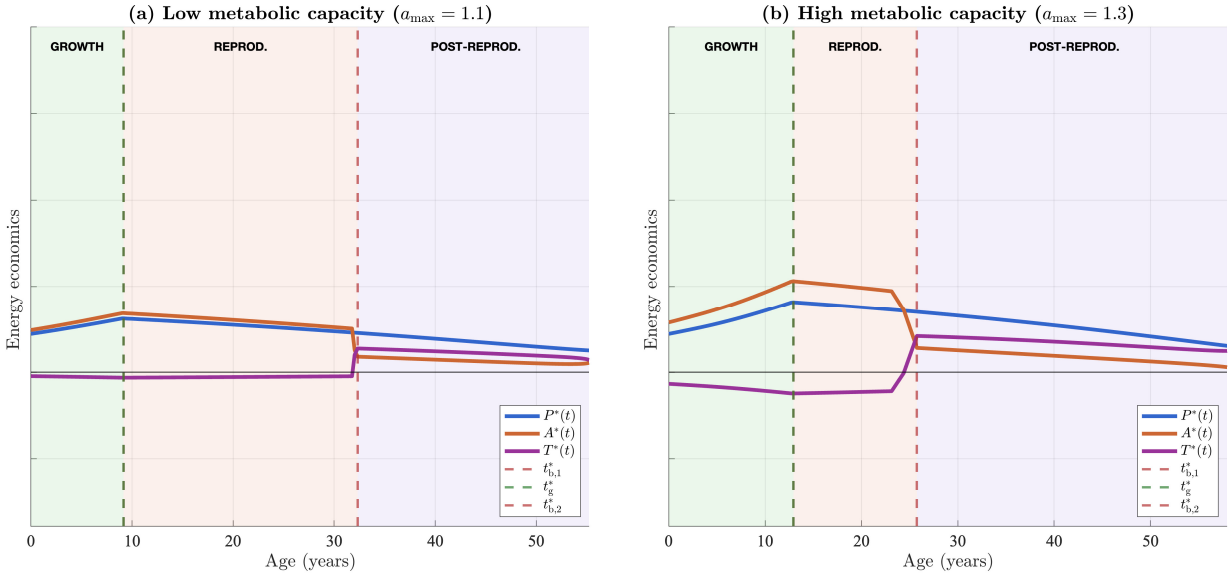

Figure 5: Uninvadable life history phases and energy economics with intergenerational transfers assuming Kleiber's law in assimilated metabolic capacity. Panel (a) low metabolic capacity $a_{\max} = 1.1$ and panel (b) high metabolic capacity $a_{\max} = 1.3$. Here, there are three life-history phases: juvenile growth (green area), adult reproduction (red area), a post-reproductive phase (purple area). Transfers become positive at the end of the reproductive phase. Parameter values and scaling details are given as in Figure 4.

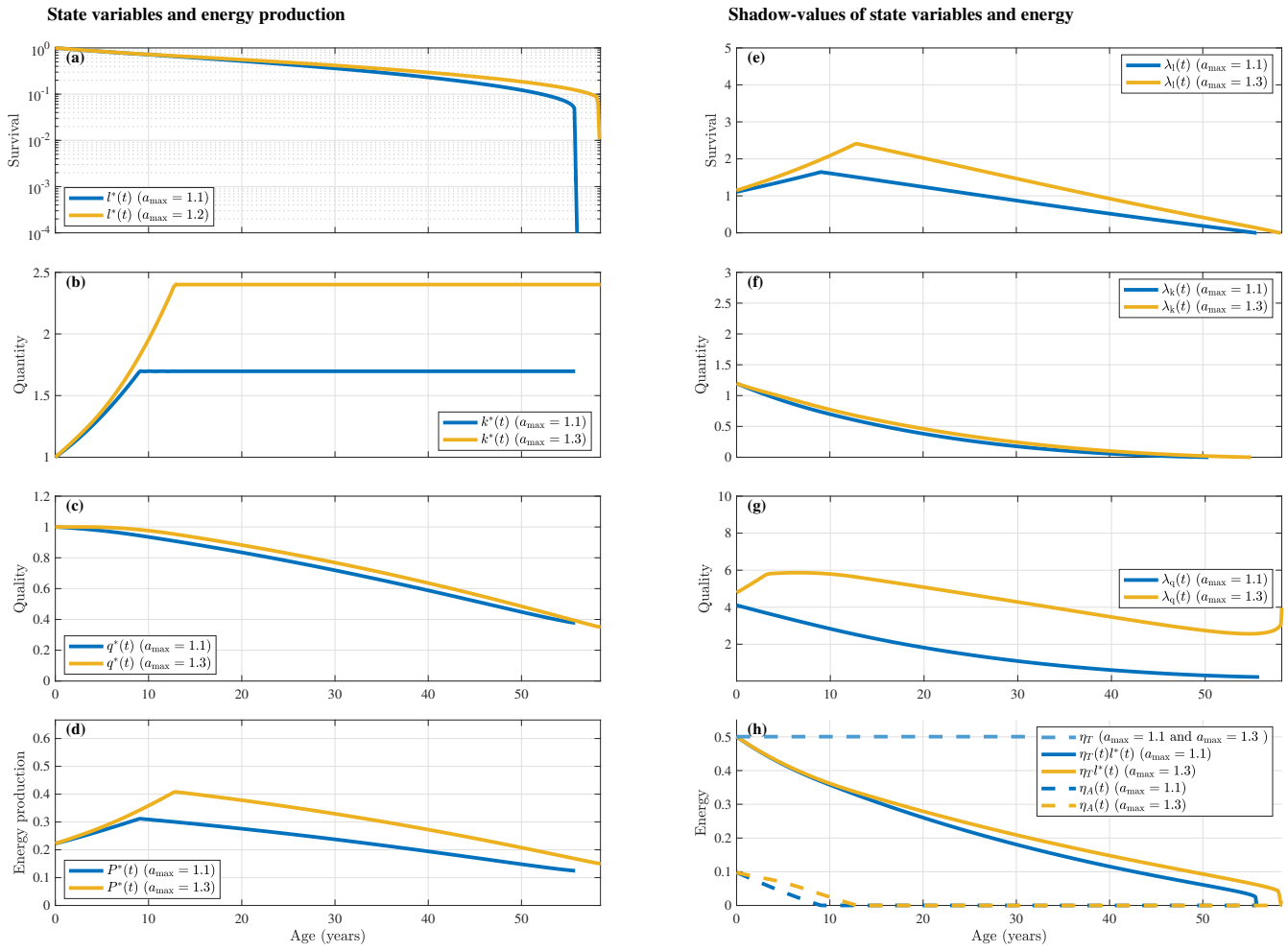

Figure 6: Uninvadable state variables, energy production, and corresponding shadow values across lifespan with intergenerational transfers assuming Kleiber's law in assimilated metabolic capacity. The values low metabolic capacity $a_{\max} = 1.1$ (blue) and high metabolic capacity $a_{\max} = 1.3$ (yellow). Left column: survival probability $l^*(t)$ (a), somatic capital $k^*(t)$ (b), somatic quality $q^*(t)$ (c), and energy production $P^*(t)$ (d). Right column: value of life $\lambda_l(t)$ (e), shadow value of somatic capital $\lambda_k(t)$ (f), shadow value of somatic quality $q^*(t)$ (g), shadow value of energy $\eta(t) = \eta_T l^*(t)$ (transfers) and $\eta(t) = \eta_C(t)$ (without transfers), shadow value $\eta_A(t)$ associated with the metabolic constraint $A_{\max}(t)$ (h). Parameter values and scaling details are given as in Figure 4.

Supplementary Information:

"Life-history evolution and uninvadable mortality schedules with an without intergenerational energy transfers"

In this Supplementary Information (S.I.), we provide additional details on our numerical results. For ease of comparison and reproducibility, all figures here use the unscaled time units. The baseline model from the main text, given in Figs. **1**–**3**, is reproduced in unscaled form in Figs. **S2**–**S4**. We first present a validation of the numerical solutions against analytical predictions (Section S1), followed by sensitivity analyses examining how key parameters affect our results (Section S2).

S1 Numerical validation of analytical predictions

To verify the accuracy of our numerical solutions, we compare the results obtained using the GPOPS-II optimal control solver against the analytical predictions derived from the first-order conditions of Pontryagin's maximum principle (see Appendix D of the main text for details). Fig. **S1** illustrates this comparison for the baseline parameter values. These baseline results appear as Figs. **1**–**3** in the main text (Figs. **S2**–**S4** presented in this S.I. show the same results in unscaled time units). The close agreement between numerical results (shown as bullets) and analytical predictions (solid lines) in Fig. **S1** shows the agreement between analytical and numerical results. The dashed pink line displays the mortality rate when the Hamiltonian equals zero, providing an additional consistency check between analytics and numerics. Similar figures illustrating the agreement between numerical results and analytical predictions are provided at the end of each sensitivity analysis in Section S2.

S2 Parameter variation analyses

We now examine how variations in key model parameters affect our main results. Each subsection below explores the effect of changing a single parameter relative to the baseline case (Figs. **S2**–**S4**).

S2.1 The effect of the marginal cost of maintenance

Our analysis reveals that ageing, characterised by increasing mortality and declining fertility, is not an inevitable outcome of the life history model presented in Section 4 of the main text, but rather emerges from the assumption that the somatic maintenance costs are high enough. We demonstrate this by reducing the marginal cost of

quality maintenance by 25% (from $\alpha_q = 40$ in our baseline case Figs. **S2**–**S4** to $\alpha_q = 30$ in Figs. **S5**–**S7**), which produces dramatically different life histories. We observe from Fig. **S5** panels (a) and (c) that actuarial and reproductive ageing appears negligible under both budget-constraint scenarios ($\mu^*(t) \approx const.$ and $b^*(t) \approx const.$ after reproductive maturity has been reached, from age $t \approx 25$ onward). Note that the results here are plotted for survival $l^*(t) > 0.001$, which is a period of life, when natural selection can meaningfully optimise life history traits and that the expected lifespan based on external mortality alone for this parameter combination is 100 years. We recall that the mortality rate $\mu^*(t)$ appearing constant is composed of an external mortality $\mu_e = 0.001$ component and some additional component because energy devoted to lowering mortality is bounded ($E_\mu(t) < \infty$, recall our assumptions eqs. (40), (46) and (83)). Furthermore, we find that the energetic advantages conferred by intergenerational transfers largely disappear. Although the transfer scenario allows slightly faster juvenile growth (Fig. **S7** panel (b)), both scenarios converge to nearly identical somatic capital and production levels (Fig. **S7** panel (d)). The quality of the somatic quantity is maintained throughout the lifespan (Fig. **S7** panel (c)). The transfer scenario produces a unique three-phase life history (Fig. **S6** panel (b)), which differs from the baseline scenario, where senescence occurs (Fig. **S3** panel (b)). Here, we can observe from Fig. **S6** panel (b) that the life history follows three phases: (i) a *juvenile growth phase* with juveniles being energy consumers, (ii) a pre-reproductive producer phase where individuals generate energy surpluses for transfers while neither growing nor reproducing, and (iii) a reproductive phase during which energy balance is maintained. Thus, we find that the no-transfer scenario maintains the classic two-phase pattern of juvenile growth followed by adult reproduction. In contrast, the transfer scenario creates a unique life cycle in which resource transfers occur in a narrow window after growth ceases but before reproduction begins. This temporal specialisation enables faster juvenile growth and slightly extended lifespans, although both scenarios ultimately achieve similar levels of adult somatic capital and maintain quality throughout life.

An important question is whether the approximately constant mortality observed in Fig. **S5** represents a true stationary state or whether senescence eventually emerges at later ages, as we do observe the value of life declining at later ages (Fig. **S7** panel (f)). Since we have external mortality causing survival $l^*(t) \to 0$ as $t \to \infty$, this means that traits that affect vital rates beyond some age $t > t'$ when $l^*(t') \approx 0$ will have a negligible contribution to fitness (this is the so-called "selection shadow"). This means that the optimal control solvers like GPOPS-II are not able to optimise traits affecting vital rates for ages $t > t'$. However, we are also not able to analyse the systems without external mortality. In fact, optimal control solvers like GPOPS-II are not well suited for steady-state problems where control variables reach constant values, as such problems become numerically degenerate. Therefore, we do not interpret solutions at late ages where $l^*(t') \approx 0$. Importantly, this numerical limitation aligns with the fundamental biological constraint brought forth by external mortality. Natural selection operates only on phenotypes expressed in organisms with non-negligible survival probability. Thus, the presence of external mortality renders the distinction between true asymptotic stationarity and eventual senescence beyond some negligible survival threshold biologically immaterial. Characterising life history solutions within the window before for ages $t < t'$ when $l^*(t') \approx 0$, as we do here, is practically sufficient for understanding evolutionary outcomes and making predictions that can be empirically verified.

These results suggest that intergenerational transfers produce more pronounced differences in life history out-

comes when somatic maintenance costs are high enough to induce ageing within the expected lifespan before death due to external mortality. Under such conditions, when ageing occurs, the benefits of transfers in terms of total energy produced over a lifespan become more substantial, potentially creating stronger selection for compensatory resource flows across generations. When somatic maintenance is relatively inexpensive and ageing is absent, the impact of transfers on life history evolution is more modest, resulting in relatively similar outcomes in terms of somatic capital accumulation and lifespan. Fig. **S8** confirms the consistency between analytical and numerical results for this parameter combination.

S2.2 The effect of external mortality

Our analysis reveals that higher external mortality rates (fourfold increase from $m_{\mathrm{e}} = 0.01$ in Figs. **S2**–**S4** to $m_{\mathrm{e}} = 0.04$ in Figs. **S9**–**S11**) produce results consistent with standard results on external mortality in classical life history theory. In particular, we observe that increased external mortality induces shorter growth phases, decreased investment into somatic quantity, earlier onset of reproduction, decreased investment in maintenance and survival, and higher fecundity rate. However, our novel finding here is that higher external mortality causes a life history strategy to be more "front loaded", with greater assimilation of resources during the earlier stages of life and a steeper decline in the value of energy over time. Fig. **S12** confirms the consistency between analytical and numerical results for this parameter combination.

S2.3 The effect of quality depreciation rate

The baseline quality depreciation rate ϵ (recall eq. (43) of the main text) can be interpreted as the natural rate at which the soma degrades (e.g. via natural cellular damage, oxidative stress, external assaults) if there is no investment into somatic maintenance. In Figs. **S13**–**S15** we illustrate the results, where the quality depreciation rate has been decreased from $\epsilon = 0.1$ to $\epsilon = 0.09$ (compared to the baseline scenario Figs. **S2**–**S4**). Unsurprisingly, we observe that quality depreciation begins in later phases of development when the baseline depreciation rate is lower, particularly in the transfers scenario. In the no-transfers scenario, we observe a "growth spurt" phenomenon during which somatic quality begins to degrade. This lower depreciation rate enables a longer period of growth and greater investment into somatic quantity, ultimately allowing for extended lifespans. Thus, a lower baseline depreciation rate enhances the benefits from transitioning from no transfers to transfers. Fig. **S16** confirms the consistency between analytical and numerical results for this parameter combination.

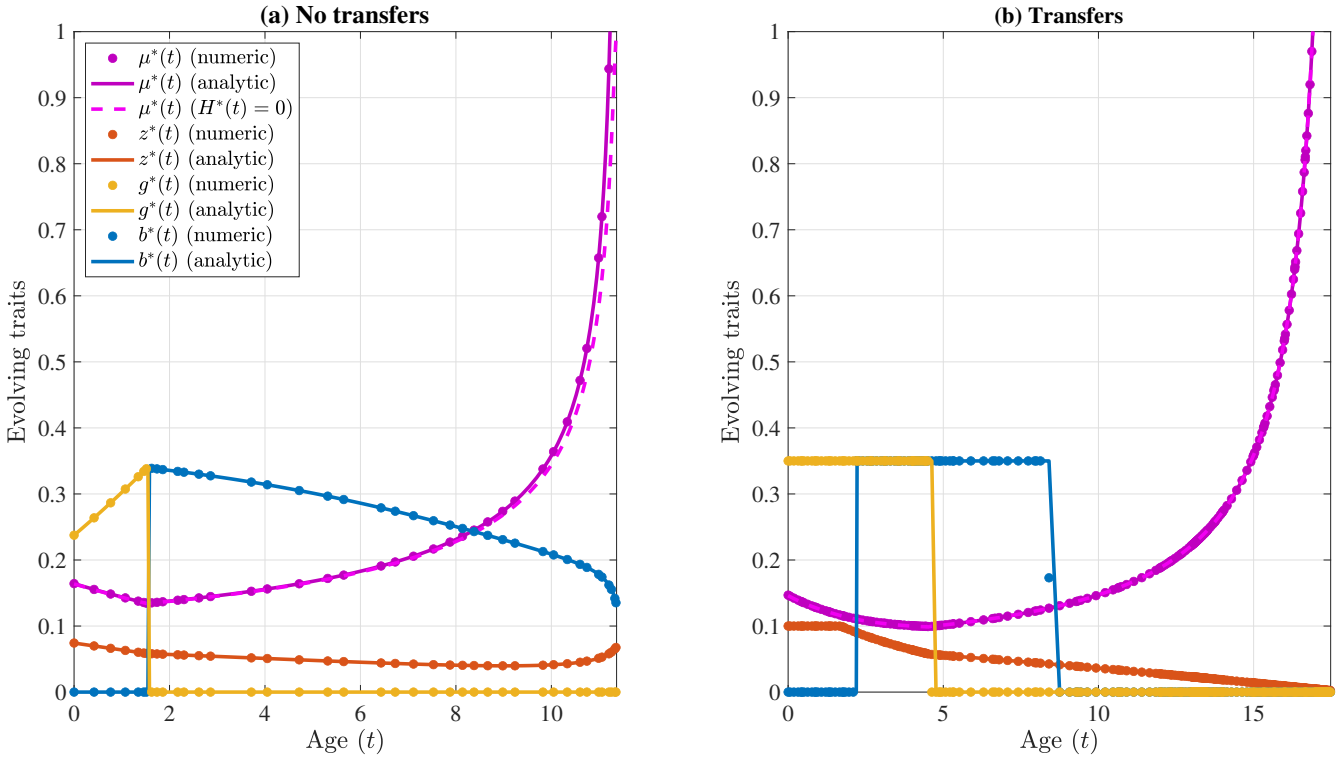

Figure S1: Numerical validation for the unscaled baseline model for scenarios without transfers (panel a) and transfers (panel b). Age-specific reproduction (b^*, blue), somatic quality maintenance (z^*, red), growth (g^*, yellow), and mortality (μ^*, purple) for scenarios without transfers (panel a) and with transfers (panel c). Numerical results (bullets) with the predicted values for the evolving traits obtained from the first-order conditions for the maximum principle (solid lines) and the mortality on the uninvadable path (dashed pink line). See Appendix D for further details. Parameter values: $\alpha_\mathrm{b} = 2$, $\alpha_\mathrm{x} = 2$, $\alpha_\mathrm{q} = 40$, $\alpha_\mu = 2$, $\zeta = 40$, $m_\mathrm{e} = 0.04$, $m_0 = 0.00001$, $r_\mathrm{b} = 0.001$, $a = 1$, $c = 0.75$, $x_0 = 1$, $q_0 = 1$, $\epsilon = 0.1$, $\kappa = 2$. Results plotted for survival $l^*(t) > 0.001$. Under the case with transfers, growth and reproduction rate are capped by $b_\mathrm{max} = g_\mathrm{max} = 0.3$, which corresponds to the highest growth/reproduction rate under the case without transfers.

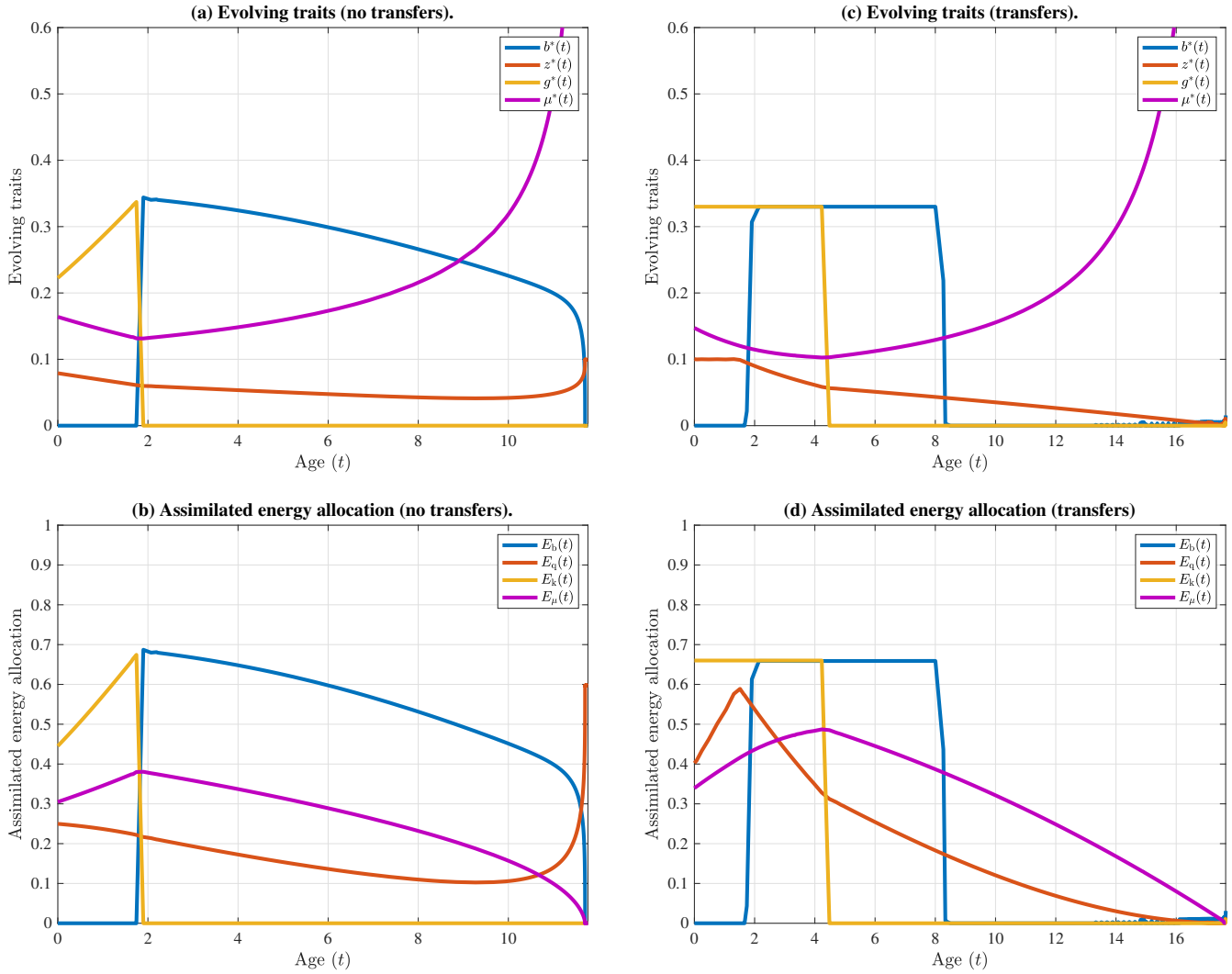

Figure S2: Unscaled baseline model. Uninvadable life history rates and assimilated energy with and without intergenerational transfers. Age-specific reproduction (b^*, blue), somatic quality maintenance (z^*, red), growth (g^*, yellow), and mortality (μ^*, purple) for scenarios without transfers (panel a) and with transfers (panel c). Corresponding assimilated energy allocation rate to reproduction ($E_\mathrm{b}(t)$, blue), somatic maintenance ($E_\mathrm{q}(t)$, red), growth ($E_\mathrm{k}(t)$, yellow), and survival ($E_\mu(t)$, purple) for scenarios without transfers (panel b) and with transfers (panel d). Parameter values: $\alpha_\mathrm{b} = 2$, $\alpha_\mathrm{x} = 2$, $\alpha_\mathrm{q} = 40$, $\alpha_\mu = 2$, $\zeta = 40$, $m_\mathrm{e} = 0.04$, $m_0 = 0.00001$, $r_\mathrm{b} = 0.001$, $a = 1$, $c = 0.75$, $x_0 = 1$, $q_0 = 1$, $\epsilon = 0.1$, $\kappa = 2$. Results plotted for survival $l^*(t) > 0.001$. Under the case with transfers, growth and reproduction rate are capped by $b_\mathrm{max} = g_\mathrm{max} = 0.3$, which corresponds to the highest growth/reproduction rate under the case without transfers.

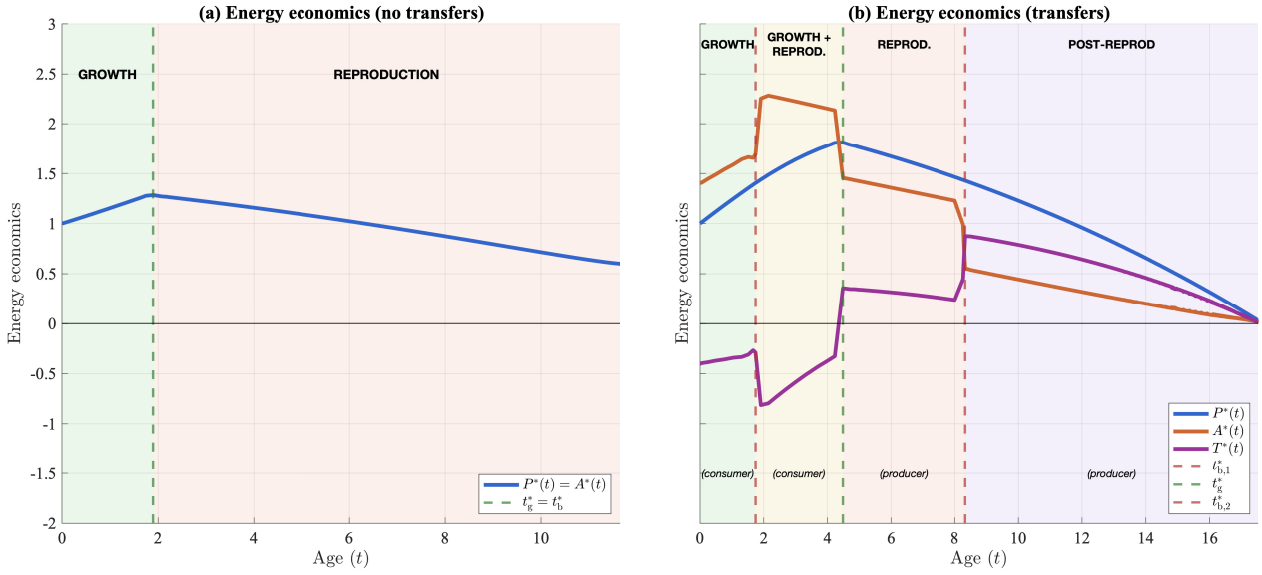

Figure S3: Unscaled baseline model. Uninvadable life history phases and energy economics; comparison between life history without transfers (panel a) and with transfers (panel b). Under the classical life history scenario (no transfers, panel a), there are two distinct phases: (i) a juvenile growth phase and (ii) a reproductive phase. Intergenerational transfers (panel b) create four distinct life history phases: (i) growth phase, during which individuals are net energy consumers (ii) mixed growth and reproduction, during which individuals are mostly at net energy balance; (iii) reproduction phase, during which individuals are net energy producers; (iv) reproductive phase, during which individuals become net energy balance. Parameter values are the same as in Figure S2.

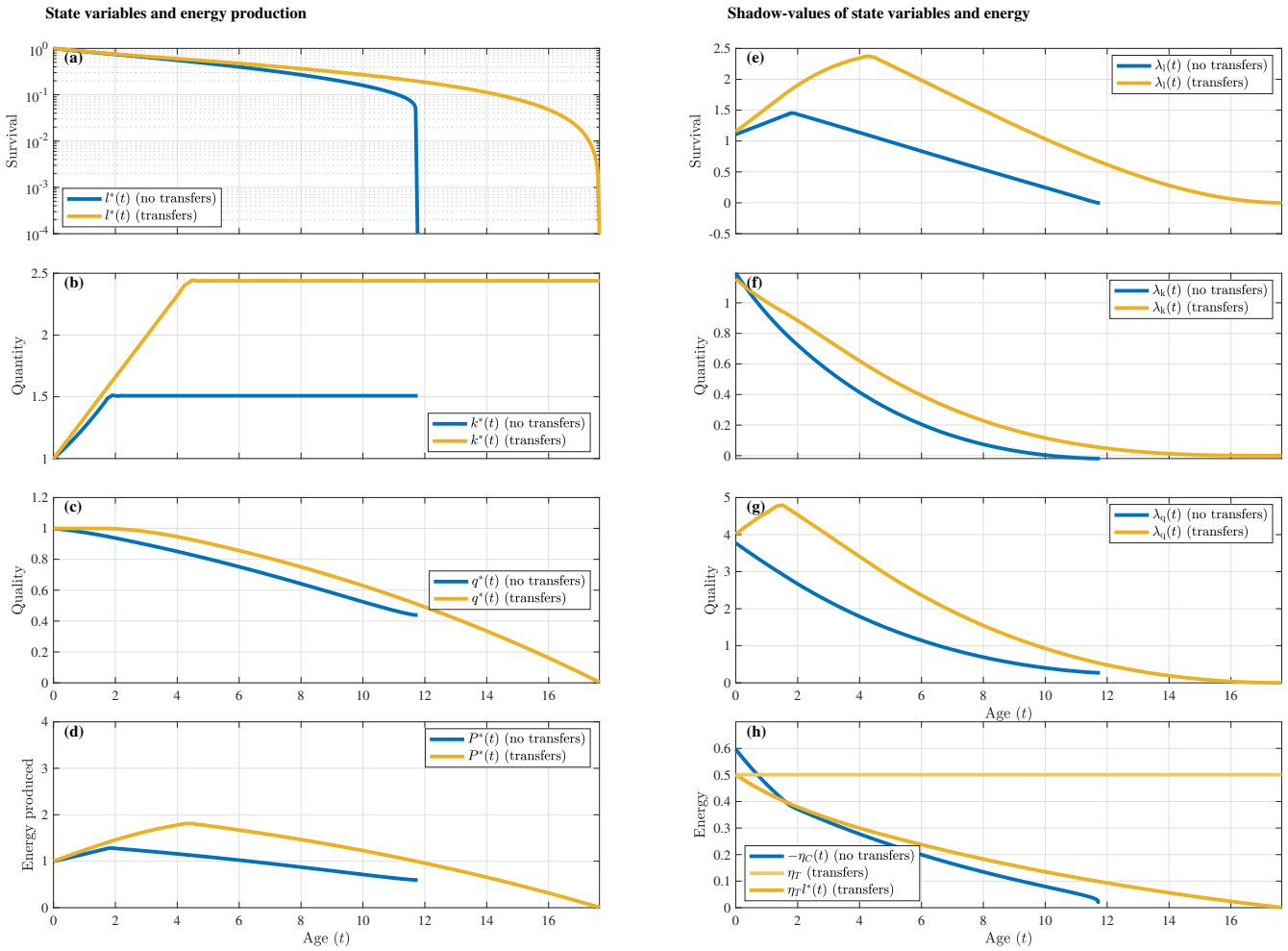

Figure S4: Unscaled baseline model. Uninvadable state and costate variables (shadow-values). The values without transfers (blue), with transfers (yellow). Left column: survival probability $l^*(t)$ (a), somatic capital $k^*(t)$ (b), somatic quality $q^*(t)$ (c), and energy production $P^*(t)$ (d). Right column: value of life $\lambda_l(t)$ (e), shadow value of somatic capital $\lambda_k(t)$ (f), shadow value of somatic quality $q^*(t)$ (g), shadow value of energy: $\eta(t) = \eta_T l^*(t)$ (transfers), $\eta(t) = \eta_C(t)$ (without transfers) (h). Parameter values and scaling details are given as in Figure S2.

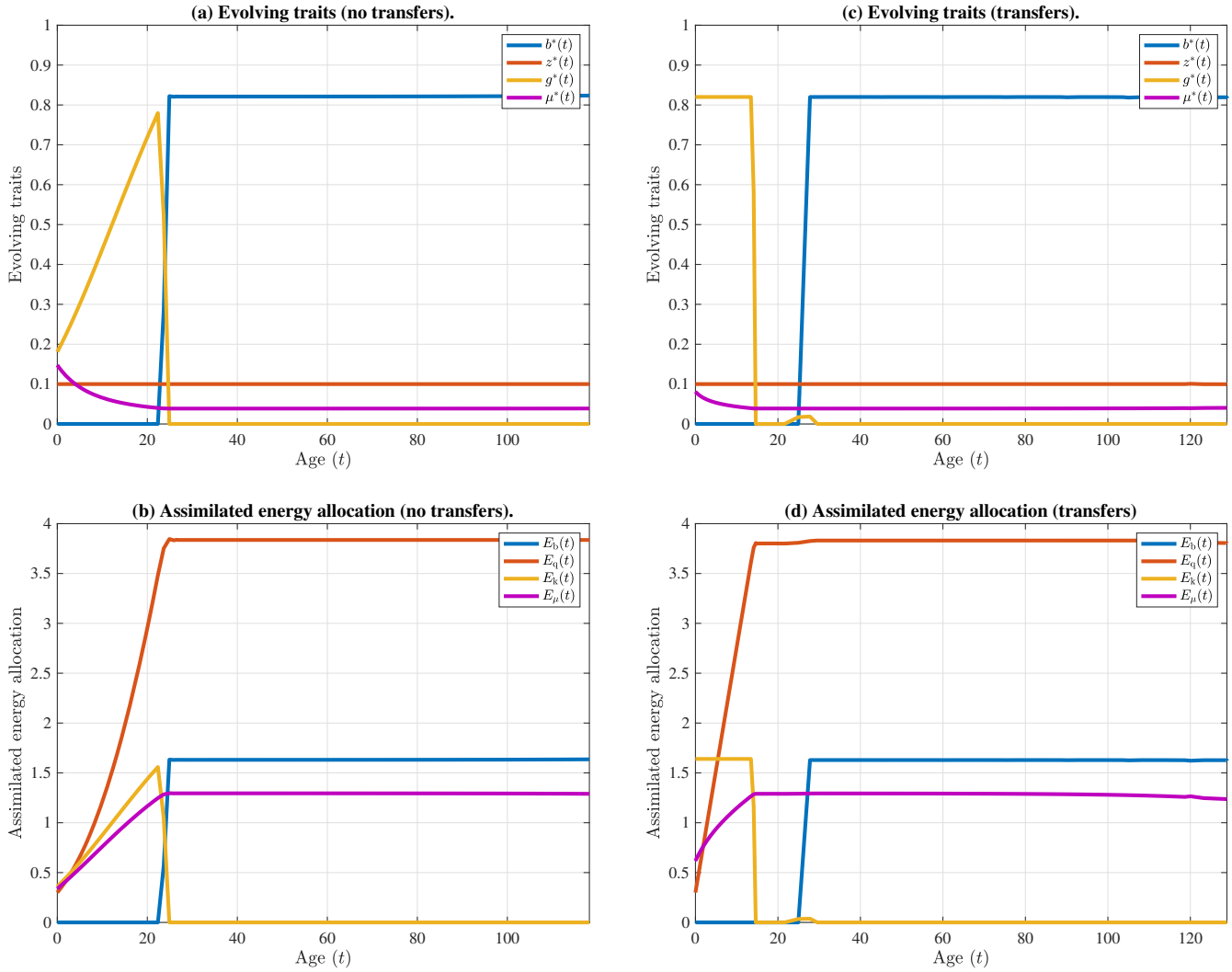

Figure S5: Negligible senescence after reaching reproductive maturity. Uninvadable life history rates and assimilated energy with and without intergenerational transfers. Age-specific reproduction (b^*, blue), somatic quality maintenance (z^*, red), growth (g^*, yellow), and mortality (μ^*, purple) for scenarios without transfers (panel a) and with transfers (panel c). Corresponding assimilated energy allocation rate to reproduction ($E_\mathrm{b}(t)$, blue), somatic maintenance ($E_\mathrm{q}(t)$, red), growth ($E_\mathrm{k}(t)$, yellow), and survival ($E_\mu(t)$, purple) for scenarios without transfers (panel b) and with transfers (panel d). Parameter values: same as in Fig. S2, except $\alpha_\mathrm{q} = 30$, i.e. the marginal cost of maintenance of somatic capital is 25% smaller compared to the baseline case. Under the transfer scenario, growth and reproduction rates are capped at $b_\mathrm{max} = g_\mathrm{max} = 0.82$, corresponding to the maximum rates observed without transfers.

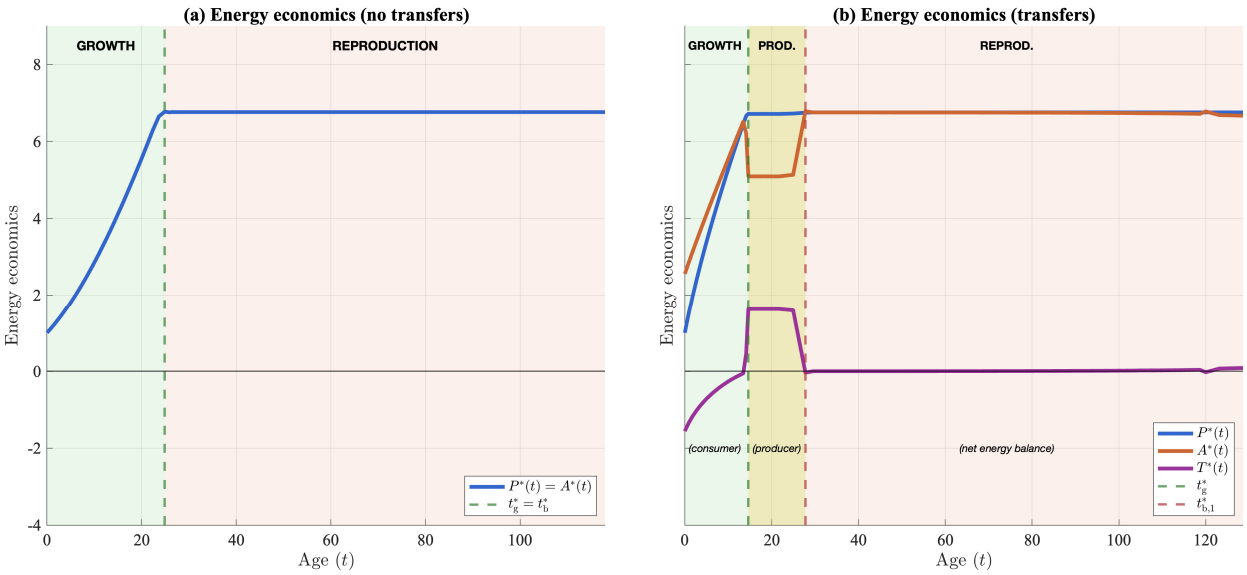

Figure S6: Negligible senescence after reaching reproductive maturity. Uninvadable life history phases and energy economics: comparison between life history without transfers (panel a) and with transfers (panel b). Under the classical life history scenario (no transfers, panel a), there are two distinct phases: (i) a juvenile growth phase and (ii) a reproductive phase. Here, intergenerational transfers (panel b) create three distinct life history phases: (i) juvenile growth, during which individuals are net energy consumers; (ii) simultaneous growth and reproduction, during which individuals are net energy producers; (iii) reproductive phase, during which individuals are in net energy balance. Parameter values are as in Figure S5.

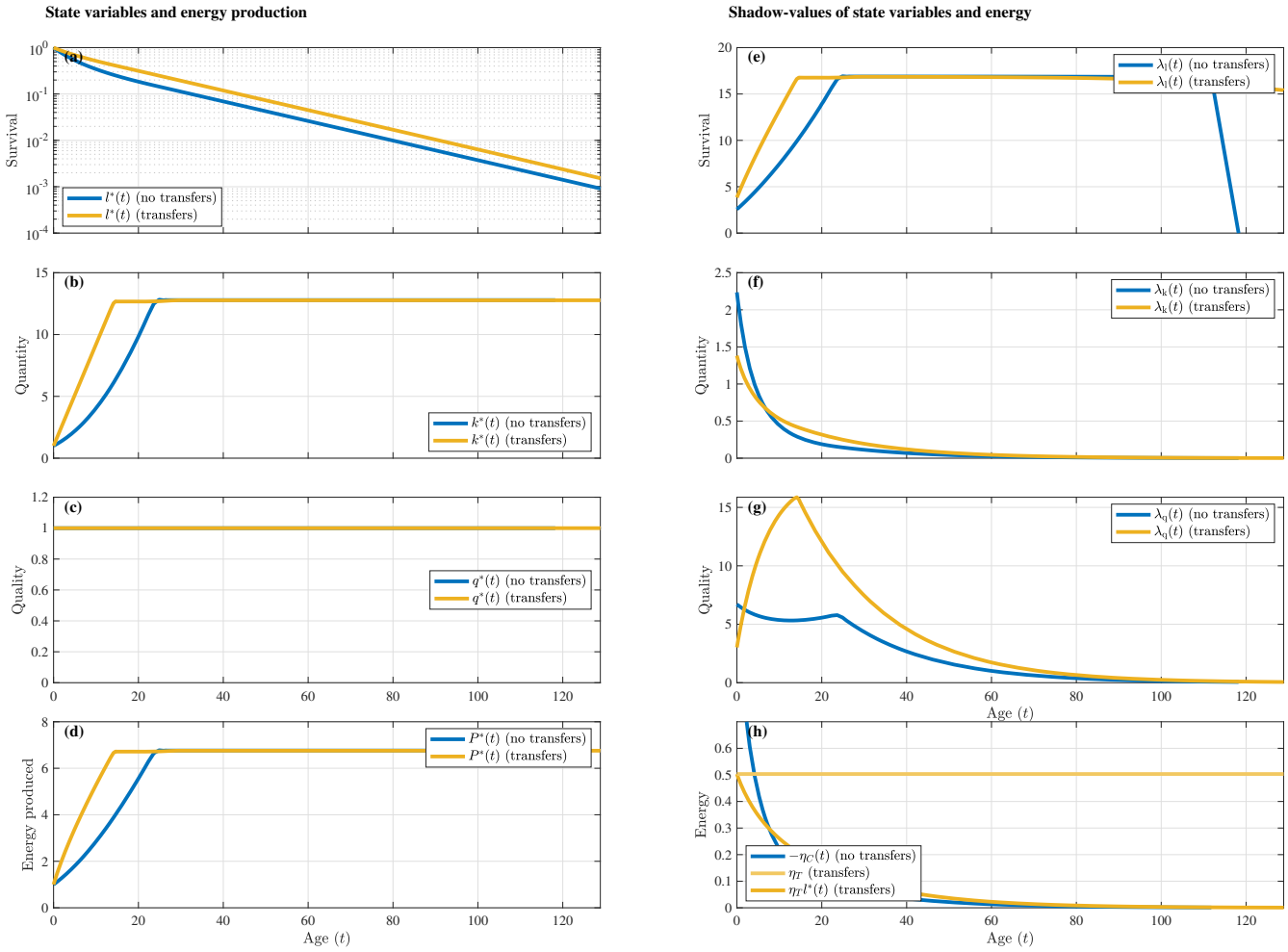

Figure S7: Negligible senescence after reaching reproductive maturity. Uninvadable state and costate variables (shadow-values). The values without transfers (blue), with transfers (yellow). Left column: survival probability $l^*(t)$ (a), somatic capital $k^*(t)$ (b), somatic quality $q^*(t)$ (c), and energy production $P^*(t)$ (d). Right column: value of life $\lambda_{\mathrm{l}}(t)$ (e), shadow value of somatic capital $\lambda_{\mathrm{k}}(t)$ (f), shadow value of somatic quality $q^*(t)$ (g), shadow value of energy: $\eta(t) = \eta_{\mathrm{T}} l^*(t)$ (transfers), $\eta(t) = \eta_{\mathrm{C}}(t)$ (without transfers) (h). Note that here we observe that survival $l^*(t)$ in panel (a) appears as a linearly declining function (in log scale), in contrast to Fig. S4 panel (a). Parameter values are as in Figure S5.

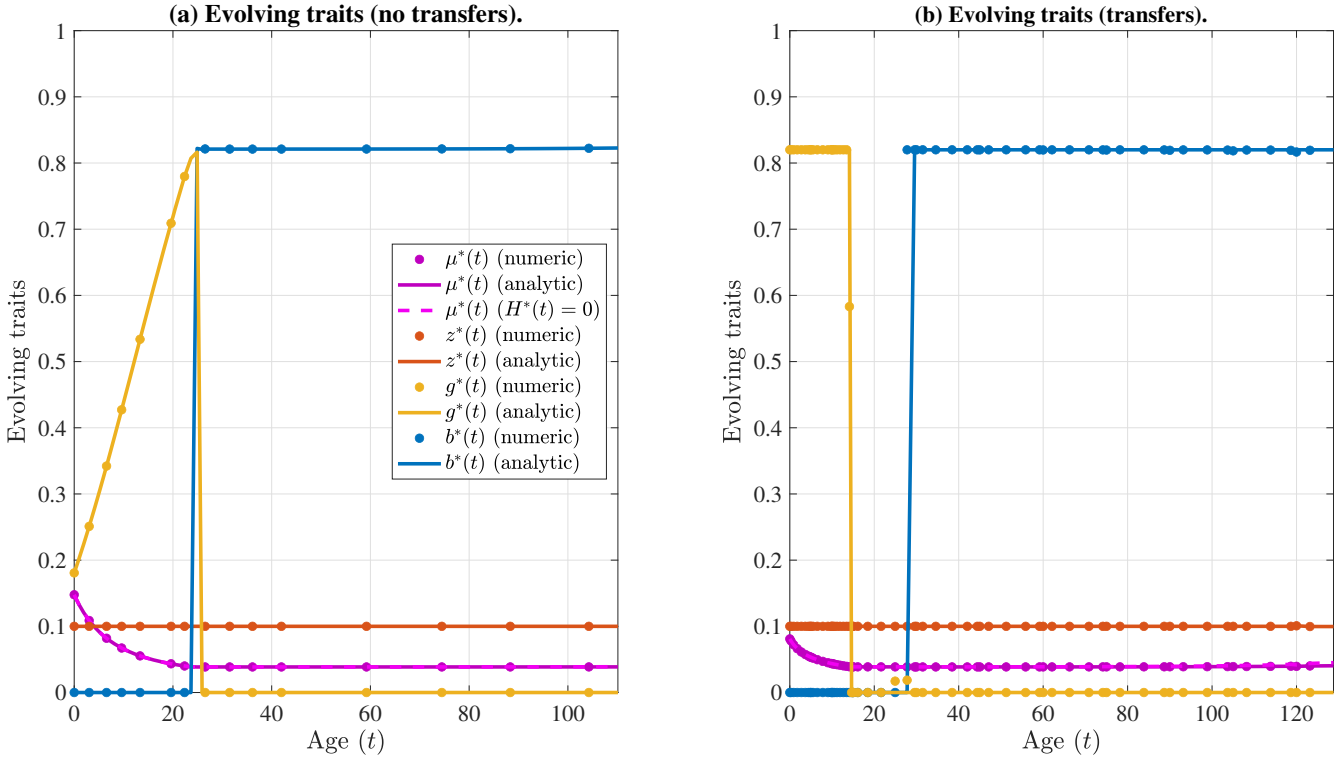

Figure S8: Negligible senescence after reaching reproductive maturity. Numerical validation for scenarios without transfers (panel a) and transfers (panel b). Numerical results (bullets) with the predicted values for the evolving traits obtained from the first-order conditions for the maximum principle (solid lines) and the mortality on the uninvadable path (dashed pink line). See Appendix D for further details. Parameter values as in Figure S5.

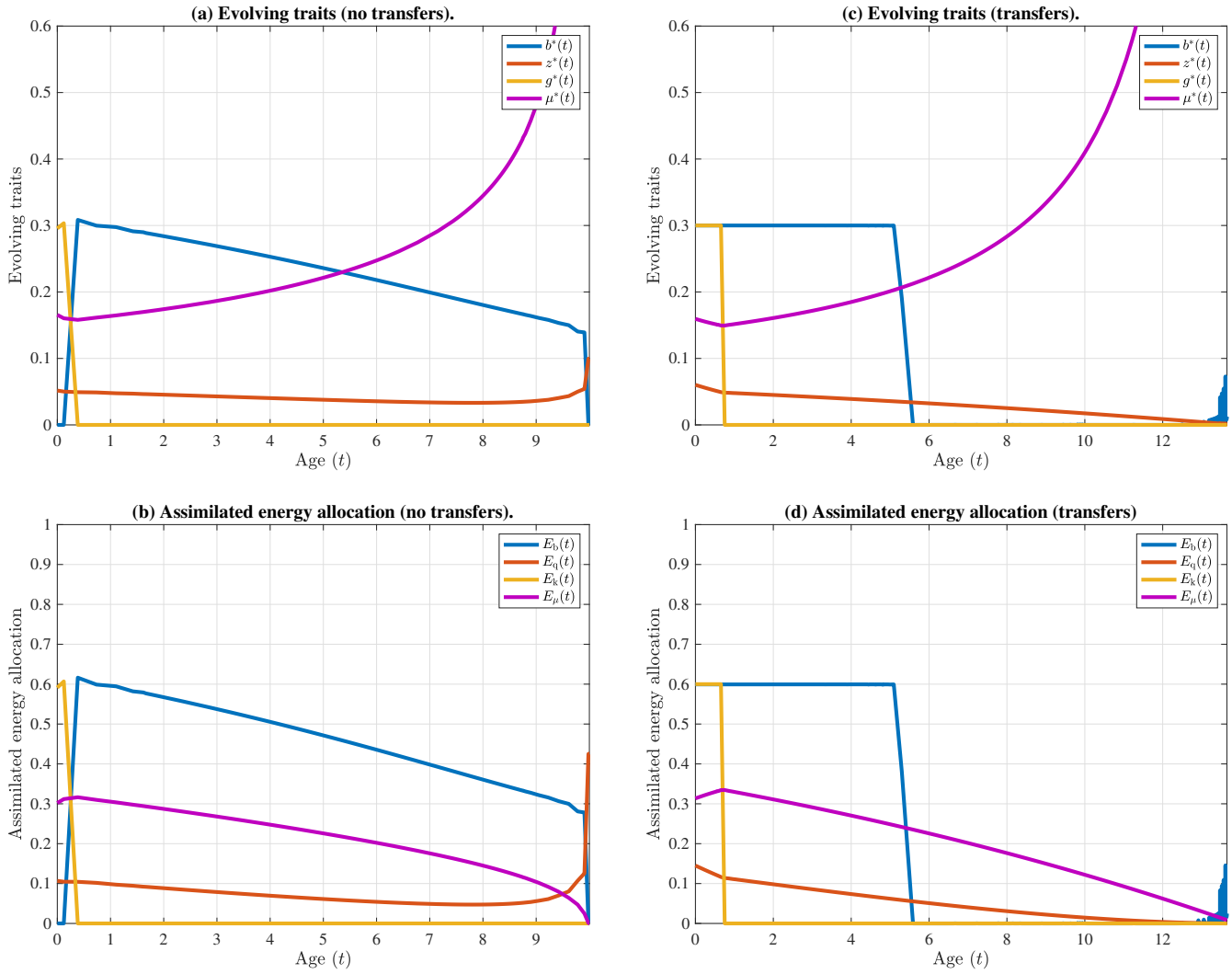

Figure S9: The effect of increased external mortality. Uninvadable life history rates and assimilated energy with and without intergenerational transfers. Age-specific reproduction (b^*, blue), somatic quality maintenance (z^*, red), growth (g^*, yellow), and mortality (μ^*, purple) for scenarios without transfers (panel a) and with transfers (panel c). Corresponding assimilated energy allocation rate to reproduction ($E_\mathrm{b}(t)$, blue), somatic maintenance ($E_\mathrm{q}(t)$, red), growth ($E_\mathrm{k}(t)$, yellow), and survival ($E_\mu(t)$, purple) for scenarios without transfers (panel b) and with transfers (panel d). Parameter values: same as in Fig. S2, except $m_\mathrm{e} = 0.04$. Results plotted for survival $l^*(t) > 0.001$. Under the case with transfers, the rates of growth and reproduction are capped by $b_\mathrm{max} = g_\mathrm{max} = 0.3$, which corresponds to the highest growth/reproduction rate under the case without transfers.

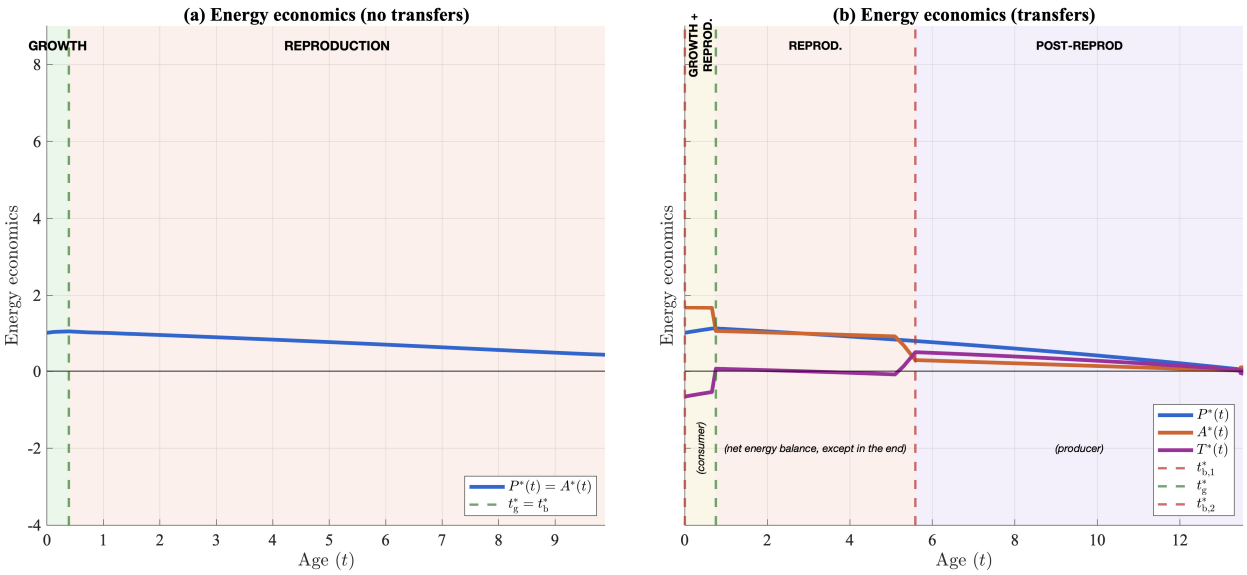

Figure S10: The effect of increased external mortality. Uninvadable life history phases and energy economics; comparison between life history without transfers (panel a) and with transfers (panel b). Under the classical life history scenario (no transfers, panel a), there are two distinct phases: (i) a juvenile growth phase and (ii) a reproductive phase. Here, intergenerational transfers (panel b) create three distinct life history phases: (i) mixed growth and reproduction, during which individuals are in energy deficit; (ii) reproduction phase, during which individuals are in net energy balance; (iii) reproductive phase, during which individuals transfer resources. Parameter values are as in Figure S9.

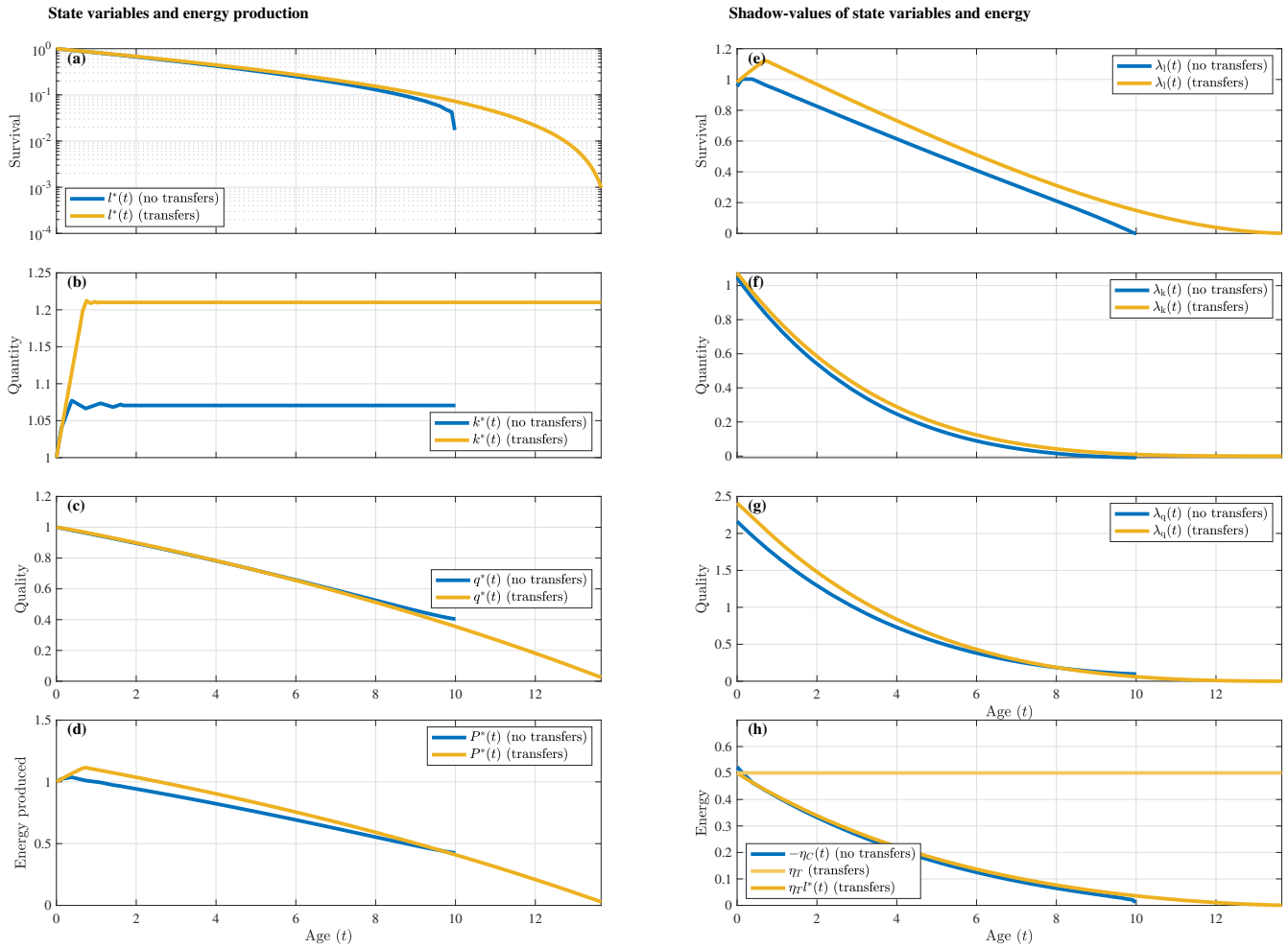

Figure S11: The effect of increased external mortality. Uninvadable state and costate variables (shadow-values). The values without transfers (blue), with transfers (yellow). Left column: survival probability $l^*(t)$ (a), somatic capital $k^*(t)$ (b), somatic quality $q^*(t)$ (c), and energy production $P^*(t)$ (d). Right column: value of life $\lambda_l(t)$ (e), shadow value of somatic capital $\lambda_k(t)$ (f), shadow value of somatic quality $q^*(t)$ (g), shadow value of energy: $\eta(t) = \eta_T l^*(t)$ (transfers), $\eta(t) = \eta_C(t)$ (without transfers) (h). Parameter values are as in Figure S9.

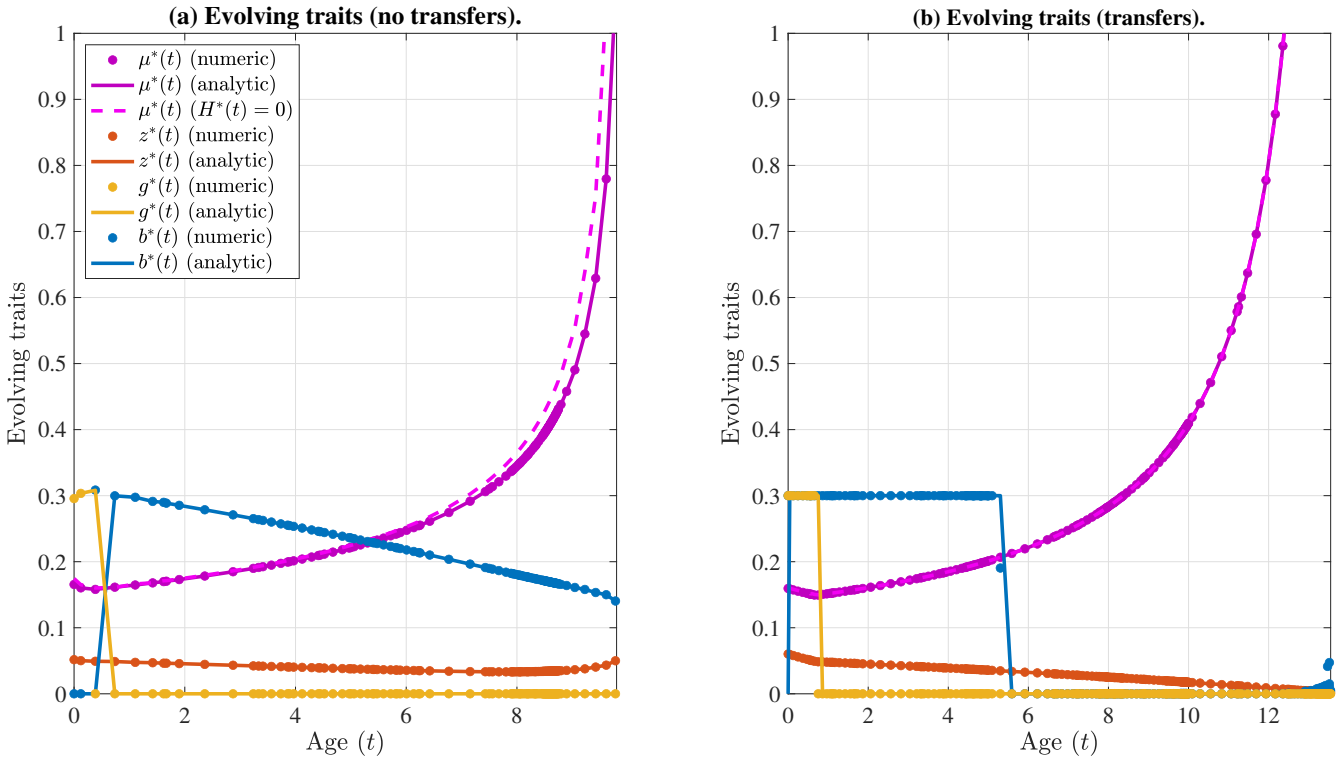

Figure S12: The effect of increased external mortality. Numerical validation for scenarios without transfers (panel a) and transfers (panel b). Numerical results (bullets) with the predicted values for the evolving traits obtained from the first-order conditions for the maximum principle (solid lines) and the mortality on the uninvadable path (dashed pink line). See Appendix D for further details. Parameter values as in Figure S9.

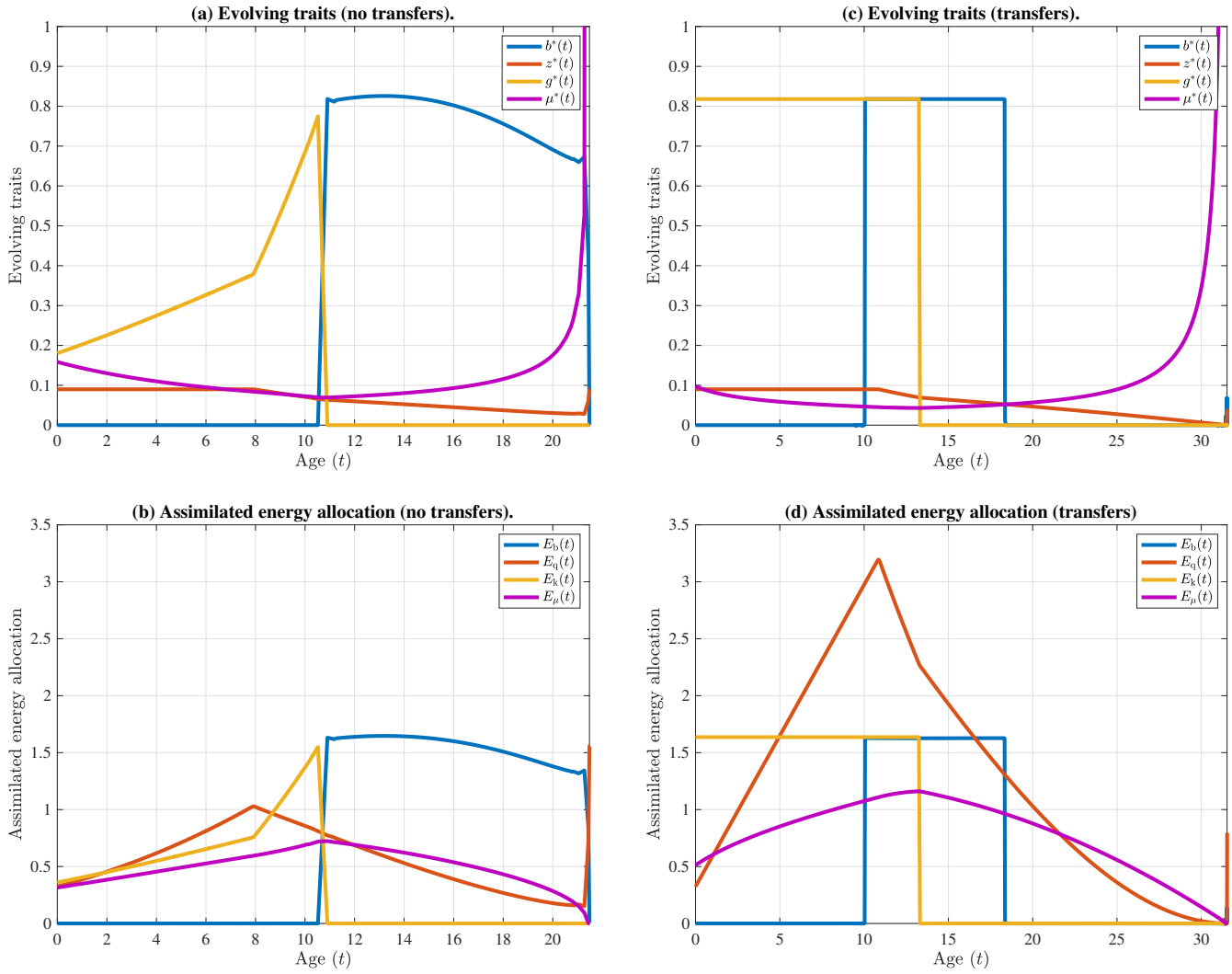

Figure S13: The effect of a lower baseline depreciation rate of the somatic capital. Uninvadable life history rates and assimilated energy with and without intergenerational transfers. Age-specific reproduction (b^*, blue), somatic quality maintenance (z^*, red), growth (g^*, yellow), and mortality (μ^*, purple) for scenarios without transfers (panel a) and with transfers (panel c). Corresponding assimilated energy allocation rate to reproduction ($E_b(t)$, blue), somatic maintenance ($E_q(t)$, red), growth ($E_k(t)$, yellow), and survival ($E_\mu(t)$, purple) for scenarios without transfers (panel b) and with transfers (panel d). Parameter values: same as in Fig. S2, except $\epsilon = 0.09$. Results plotted for survival $l^*(t) > 0.001$. Under the case with transfers, the rates of growth and reproduction are capped by $b_{max} = g_{max} = 0.82$.

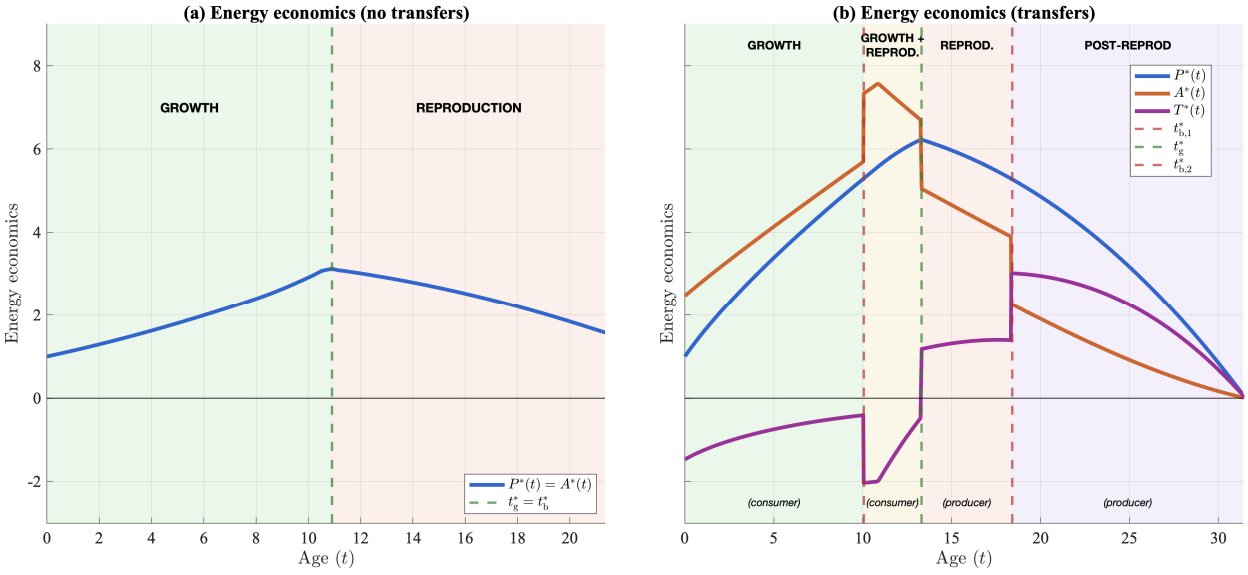

Figure S14: The effect of a lower baseline depreciation rate of the somatic capital. Uninvadable life history phases and energy economics; comparison between life history without transfers (panel a) and with transfers (panel b). Under the classical life history scenario (no transfers, panel a), there are two distinct phases: (i) a juvenile growth phase and (ii) a reproductive phase. Intergenerational transfers (panel b) create four distinct life history phases: (i) growth phase, during which individuals are net energy consumers (ii) mixed growth and reproduction, during which individuals are mostly at net energy balance; (iii) reproduction phase, during which individuals are net energy producers; (iv) reproductive phase, during which individuals become net energy balance. Parameter values are the same as in Figure S13.

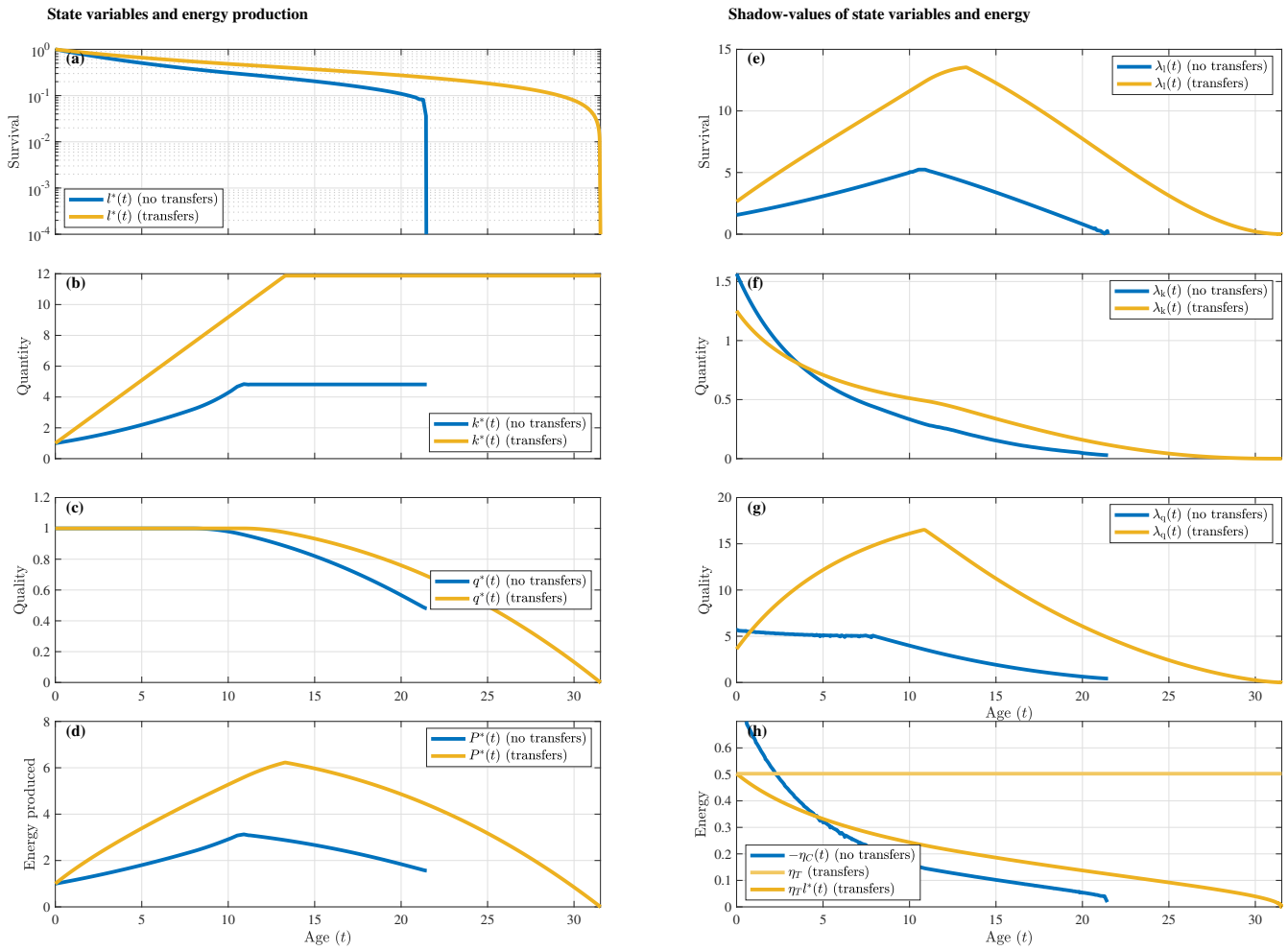

Figure S15: The effect of a lower baseline depreciation rate of the somatic capital. Uninvadable state and costate variables (shadow-values). The values without transfers (blue), with transfers (yellow). Left column: survival probability $l^*(t)$ (a), somatic capital $k^*(t)$ (b), somatic quality $q^*(t)$ (c), and energy production $P^*(t)$ (d). Right column: value of life $\lambda_l(t)$ (e), shadow value of somatic capital $\lambda_k(t)$ (f), shadow value of somatic quality $q^*(t)$ (g), shadow value of energy: $\eta(t) = \eta_T l^*(t)$ (transfers), $\eta(t) = \eta_C(t)$ (without transfers) (h). Parameter values as in Figure S13.

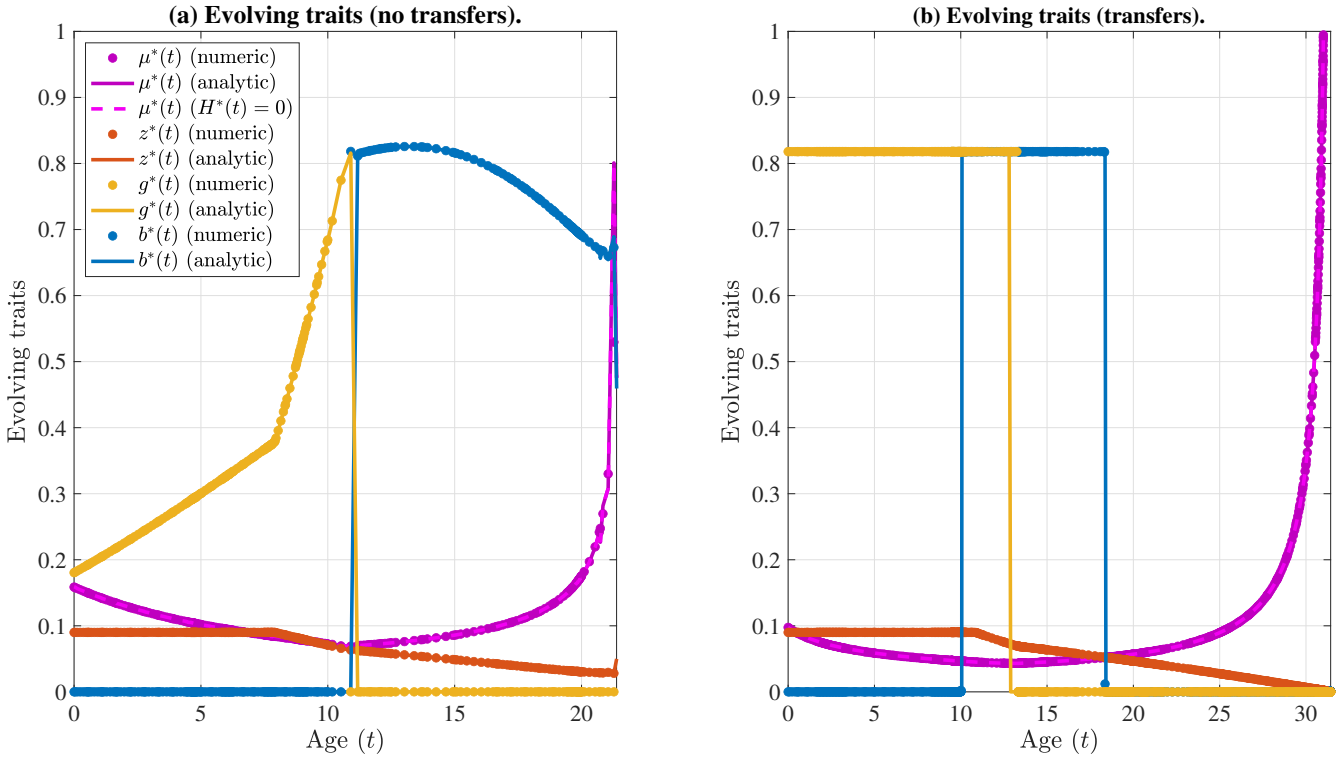

Figure S16: The effect of a lower baseline depreciation rate of the somatic capital. Numerical validation for scenarios without transfers (panel a) and transfers (panel b). Numerical results (bullets) with the predicted values for the evolving traits obtained from the first-order conditions for the maximum principle (solid lines) and the mortality on the uninvadable path (dashed pink line). See Appendix D for further details. Parameter values as in Figure S13.